
LAPPEENRANNAN TEKNILLINEN KORKEAKOULU
LAPPEENRANTA UNIVERSITY OF TECHNOLOGY

TIETEELLISIÄ JULKAISUJA 15
RESEARCH PAPERS

TIMO HYPPÄNEN

AN EXPERIMENTAL AND THEORETICAL STUDY OF MULTIPHASE FLOW IN A CIRCULATING FLUIDIZED BED

ISBN 978-952-214-874-2 (PDF)

LAPPEENRANNAN TEKNILLINEN KORKEAKOULU
LAPPEENRANTA UNIVERSITY OF TECHNOLOGY

UDK 532.529
662.9
66.096.5

TIETEELLISIÄ JULKAISUJA
RESEARCH PAPERS

15

TIMO HYPPÄNEN

AN EXPERIMENTAL AND THEORETICAL STUDY OF MULTIPHASE FLOW IN A CIRCULATING FLUIDIZED BED

Thesis for the degree of Doctor of Technology to be presented with due permission for public examination and criticism in the Auditorium 3.10 at Lappeenranta University of Technology (Lappeenranta, Finland) on the 11th of August 1989, at noon.

LAPPEENRANTA
1989

ISBN 951-763-589-3

ISSN 0356-8210

ERRATUM

Nomenclature : the unit mole of the stoichiometric coefficient ν must be replaced by -

page 15 line 6 : divided by density must be replaced by divided by mass

page 18 equation (2.26): dV must be replaced by dA

page 31 line 2 : terms of equation (3.49) must be replaced by terms on the right hand side of equation (2.51)

page 31 equation (2.54): n_ω must be replaced by n_R

page 31 equation (2.55): dA in the first term on the right hand side must be dV

page 31 equation (2.55) and page 33 equation (2.60) : all V_r:s must be replaced by V_c:s

page 32 equation (2.56): $+ \int_{V_B} \theta \, dV$ must be $- \int_{V_B} \theta \, dV$

page 32 equation (2.56): $\overset{\circ}{\phi}$ must be $\overset{\circ}{\phi}_c$

page 33 equation (2.59): in the last term ϕ_c must be $\overset{\circ}{\phi}_c$

page 33 equation (2.60) and page 34 line 4 : $(\overset{\circ}{\phi}_c)$ must be $\langle \overset{\circ}{\phi}_c \rangle$

page 36 equation (2.64): in the third term A_{RR} must be A_{RS}

page 37 equation (2.65): sign - in the third term must be +

page 40 equation (2.71): dV a_{rs}dV must be dV

page 44 equation (2.85): $(\overset{\circ}{\phi}_c)$ must be $\langle \overset{\circ}{\phi}_c \rangle$

page 50 line 9 : (2.93) must be (2.91)

page 52 equations
(2.105) and (2.106) : the first sign = must be +

page 58 line 20 : equation 2.80 must be replaced by equation 2.83

page 60 equation (2.125): $(\overset{\circ}{\mathbf{T}}_g)$ must be $\langle\overset{\circ}{\mathbf{T}}_g\rangle$

page 70 equation (2.153): all subscripts c must be replaced by g

page 71 line 7 : on the left must be replaced by on the right

page 83 line 12 : $\varrho_r \underline{v}_r$ must be $\varrho_r^{\epsilon} \underline{v}_r$

page 85 equations (3.22) and (3.23) and
page 87 equations (3.26) and (3.27) : all A_T:s must be A_{Ti}

page 89 line 5 : m/s must be m/s^2

page 91 equation (3.32) and
page 93 equation (3.39) and
page 94 equation (3.43) : I_r^w must be $\underline{I}_r^w$

page 94 equation (3.42) and
page 100 equation (3.58) and
page 102 equation (3.64) : $\underline{T}_{cr}^I$ must be $\underline{T}_{cs}^I$

page 100 equation (3.57) : $\underline{n}_{ri}$ must be $\underline{n}_{Ti}$

page 101 equation (3.63) : subscripts c must be replaced by r

page 106 equation (3.74) : $\underline{T}_{cr,d}^I$ must be $\underline{T}_{cs,d}^I$

page 107 equation (3.75) : $\underline{T}_{cr,e}^I$ must be $\underline{T}_{cs,e}^I$

page 118 equation (3.107): both of the letters β must have subscripts cr and subscripts g must be replaced by subscripts c

page 171 equation (5.4) : $I_r^w(v)$ must be $\underline{I}_r^w(v)$

ABSTRACT

A systematic averaging procedure has been derived in order to obtain an integral form of conservation equations for dispersed multiphase flow, especially applicable to fluidized beds. A similar averaging method is applied further to formulate macroscopic integral equations, which can be used in one-dimensional and macroscopic multi-dimensional models. Circulating fluid bed hydrodynamics has been studied experimentally and both macroscopic and microscopic flow profiles have been measured in a cold model. As an application of the theory, the one-dimensional model has been used to study mass and momentum conservation of gas and solid in a circulating fluid bed. Axial solid mixing has also been modelled by the one-dimensional model and mixing parameters have been evaluated.

ACKNOWLEDGEMENTS

This study has been carried out in 1985-1986 at the Lappeenranta University of Technology and at the Domestic Fuel Laboratory at the Technical Research Centre of Finland and in 1986-1988 at the A. Ahlstrom Research Center in Karhula. The support of all of them is gratefully acknowledged as well as the research grant by Tekniikan Edistämissäätiö.

I thank all the persons who have helped me with this study, especially Tech. Lic. Esa Vakkilainen and Mr Visa Poikolainen for reviewing the manuscript and M.Sc. Harri Vilokki for his contribution during the experimental work.

Special acknowledgement is given to my wife, Anita, and two sons, Tommi and Teemu, for their full support and understanding throughout this work.

Karhula, June 1989

Timo Hyppänen

TABLE OF CONTENTS

NOMENCLATURE

A	area, m^2; parameter in equation (2.149), $(N/m^2)^{0.5}$
A_{rs}	boundary area between the fields r and s in small scale, m^2
A_{RS}	boundary area between the fields R and S in macroscopic scale, m^2
a	parameter in equation (4.1)
a'	parameter in equation (4.3)
a_1	parameter in equation (3.111)
a_2	parameter in equation (3.111)
a_{rs}	specific surface area between fields r and s (equation 2.1), m^2/m^3
b	parameter in equation (4.1)
b'	parameter in equation (4.3)
C_1	parameter in equation (3.113)
C_2	parameter in equation (3.113)
C_3	parameter in equation (3.113)
C_{Dr}	drag coefficient (equation 2.127), -
$C_r(\psi)$	microscopic dispersion of a property ψ
$C_r^T(\psi)$	macroscopic dispersion of a property ψ
c'	parameter in equation (4.3)
D	dispersion coefficient, m^2/s
d	microscopic characteristic length, m
$\dot{d}_p$	rate of change of particle diameter, m/s

d_p	diameter of a particle, m
e	coefficient of restitution , -
F	non-convective flux of a conservative property
$F(\epsilon_g)$	aggregation function, equation (3.113)
f	field fraction (equations 3.78 and 3.79), -
$f(\epsilon_r)$	function (equation 2.134)
G	modulus of elasticity, N/m^2
g_1	constant in equation 2.148, N/m^2
g_2	constant in equation 2.148
g	gravitation constant, m/s^2
h	enthalpy, J/kg
I	intensity of radiation, -
$\underline{I}_r^s(\psi)$	convection of a property ψ through field interfaces
$I_{i,j}^{i,k}(\psi)$	transfer of a property ψ from region j to region k of field i
$\underline{I}_{i,j}^{w}(\psi)$	transfer of property through the walls in region j
i_r^s	mass transfer of field r to field s divided by area, kg/m^2s
$i_{r\alpha}^s$	mass transfer of species α of field r to field s divided by area, kg/m^2s
J	transfer of a property through field definition limits
K_v	interphase heat transfer coefficient in equation 2.155, $\frac{W}{m^3K}$
k	attenuation coefficient, m^2/kg

L	macroscopic characteristic length, m
l	Chapter 2: averaging characteristic length, m
	Chapter 4: beam length in reactor, m
l_v	distance between optic fiber probes, m
M	molecular weight, kg/mol
m	mass, kg
$\dot{m}$	mass flow rate, kg/s
$\mathbf{n}$	unit normal vector, -
p	Chapter 2: derivative partial volume fraction (equation 2.96), 1/m; Chapters 3, 4 and 5: pressure, N/m^2
P	partial volume fraction (equation 2.97)
q	heat flux, W/m^2s
$R_{xy}(\tau)$	cross-correlation function
$\dot{R}'''$	reaction rate divided by volume, mol/m^3s
Re_p	Reynolds number (equation 2.129), -
Re_{rm}	Reynolds number (equation 2.135), -
t	time, s
$\mathbf{T}$	stress tensor, N/m^2
T	temperature, K
$\underline{T}^{s,e}_{r,d}$	momentum flux from field r in region d into field s in region e divided by volume, $\frac{kg}{s^2m^2}$
$\mathbf{v}$	velocity, m/s
v_{brs}	velocity of a field boundary, m/s
$\bar{v}^*_{i,j}$	average velocity for momentum transfer from field i in region j to the other region, m/s
v_{sl}	gas-particle slip velocity, m/s

v_t terminal velocity, m/s

v_T^* effective cluster velocity, m/s

$\mathbf{x}$ space vector, m

x height variable, m

Greek symbols

α tracer concentration, -

β drag coefficient, 1/s

γ field function, -

ϵ volume fraction, -

ε turbulent diffusion coefficient, m^2/s

$\boldsymbol{\theta}$ source term for a conservative property

λ thermal conductivity, W/mK

μ dynamic viscosity, kg/ms

ν stoichiometric coefficient, mole

ρ material density, kg/m^3

ρ^{ϵ} (intrinsic) density (equation 2.80), kg/m^3

τ average time delay, s

$\boldsymbol{\phi}$ flux of a conservative property

$\boldsymbol{\phi}_{cr}^{I}$ continuum-solid field interaction term (equation 2.85)

$\boldsymbol{\phi}_{cr}$ non-convective continuum flux (equations 2.86 and 2.87)

$\boldsymbol{\phi}_{rs}^{V}$ solid-solid interaction term (equation 2.88)

$\boldsymbol{\psi}$ conservative property

Ω any function in equations (2.32) and (2.33)

ω shape factor of a particle, -

superscripts

c	continuum
d	flow region
e	flow region
r	any field, solid field
s	solid field
v	momentum equation
w	wall
+	upper limit
-	lower limit
°	rapidly varying component
~	fluctuating
*	tracer

subscripts

B	common control volume and solid boundaries
C	macroscopic scale continuum
c	continuum
d	flow region
e	flow region
I	boundaries inside control volume
m	mixture
max	maximum
min	minimum

p	particle
R	any macroscopic scale field
r	any field
S	macroscopic scale solid
s	solid field
sys	system quantity in equations (2.61) and (2.62)
T	macroscopic scale total control space
t	microscopic scale total control space
w	wall
α	species
1	lower boundary in 1-dimensional models
2	upper boundary in 1-dimensional models
+	upper limit
-	lower limit, microscopic average
$\bar{}$	macroscopic average
=	momentum average

1. INTRODUCTION

Gas fluidized beds have been used for commercial processes since the 1920's, when powdered coal was gasified in fluidized bed. The method has been applied after that to processes in the chemical and petroleum industry, metallurgy and also to coal carbonization or combustion. The development of solid fuel combustion in fluidized beds was started heavily in the mid 1970's, when the rise of oil prices forced the industry to look for substitutes for it. Then it was found that fluidized bed combustion is one of the most promising ways of burning coal efficiently and adaptively. Increasing attention to emission figures of sulphur and nitrogen oxides in the 1980's has made the combustion method even more competitive because of its low NO_x values and ability of absorption SO_2 with limestone addition.

During the development of fluidized beds for coal combustion it was found that also higher gas flow rate fluidization could be applied for coal combustion. This fluidization mode was termed circulating fluid bed (CFB) or fast fluid bed. First commercial CFB boilers for coal combustion started operation in the beginning of the 1980's. It has been found, that CFBs operate at higher combustion efficiencies and lower excess-air levels than the more familiar bubbling-bed combustors [Schwieger 1985]. In addition

they are more easily adaptable for staged combustion for NO_x control and require less limestone for SO_2 capture than bubbling beds. Thus CFB's are achieving more and more significant position in combustion of solid fuels.

Although commercial practice of CFB has shown its efficiency in solid fuel combustion, fundamental research on it has been considerably smaller than e.g. on bubbling fluidized beds so that only a few research groups have been studying CFBs before 1980. Main emphasis has been on experimental research of small, less than 15 cm diameter reactors, which are far from the big commercial unit size of several meters. Experimental methods for gas-solid flow studies have also been poor making the research difficult. Thus scaling of the research data for commercial units has been unreliable especially because theoretical and modeling research of the process has been scanty. There is also lack of comprehensive flow studies, in which all the main flow properties are determined and presented for one single device.

In this work continuum flow equations are first derived for non-continuous multiphase gas-solid flow applying integrated balance equations and definitions of space- and time-averaged quantities. The physical meaning of different terms and the closure of the flow equation set will be also discussed.

The continuum equation set is difficult to solve in 3-dimen-

sional case especially for multiphase case, because of the requirement for large amount of grid cells and non-linearity of equations. Thus also engineering balance equations are derived from continuum equations applying macroscopic space averaging. These equations are applied to 1-dimensional multiphase flow.

Due to lack of comprehensive experimental data set for CFB devices, cold model flow experiments are done applying a few most promising experimental techniques for fluidized beds. Macroscopic flow properties, local flow values, as well as some solid mixing profiles are measured.

Macroscopic 1-dimensional equations are applied to flow models, the parameters of which are evaluated using experimental data from the cold model and from literature. Numerical results of model simulations are presented.

2. THEORY OF MULTIPHASE FLOW

Mathematical model for gas-solid-fluidization can be formulated by using single-phase Navier-Stokes equations for the fluid flow and Newtonian equations of motion for the particle flow and by considering suitable gas-solid boundary conditions.A solution for such a model is, however, impossible to get in practice. Thus, there is a need to formulate simplified models for which solutions can be obtained. The same way as the single-phase flow is modeled by continuum mechanics instead of statistical mechanics, discontinuities in multiphase flow field can be avoided by modeling all phases as continuum fields. When speaking of gas-solid-fluidization, different parts of the same phase may behave quite differently. For example, if there are two different particle sizes of the same phase in the flow, the constitutive equations for them may differ totally from each other and modeling them as one phase may not give satisfactory results.

So instead of terms multiphase or multicomponent, the term multifield is occasionally used in the following to stress the fact that within one phase or one component there may be parts which behave differently and these parts must be modeled as their own continuum fields. The multifield continuum model may be considered as an extension of multiphase or multicomponent continuum models. Thus theories for multiphase flow can be applied also to

multifield flow, in the connection of modeling interactions and shift between fields within one phase.

2.1 REVIEW OF TWO-PHASE FLOW THEORIES

Principally there has been three different ways of obtaining equations for multiphase continuum models: intuitive models, models based on continuum theory of mixtures and models based on averaging procedure.

Intuitive models have been based on intuitive and empirical postulations. These models have mainly been presented in earlier papers for gas-particle flows [Soo 1967, Murray 1965, Pigford and Baron 1965, Jackson 1963] and for dispersed flows [van Deemter and van der Laan 1960, Wallis 1969]. These intuitive models are generally limited in application to specific systems and they result in equation set, which is not usually very applicable in practice.

Another way of postulating the multiphase equations relies on the continuum theory of mixtures [Eringen and Ingram 1965, Truesdell and Toupin 1960, Truesdell 1969, Bowen 1976] extended to multiphase flow [Passman et al. 1983, Drumheller and Bedford 1980, Goodman and Covin 1972]. However, these generalized continuum formulations result in quite complex constitutive equations and numerical values of most of the coefficients are not yet available.

In the late 60's the foundations of the averaging approach were laid in the articles by Slattery (1967), Whitaker (1969) and

Anderson and Jackson (1967). The first two were for porous media and the last one was for fluidized bed application. They first derived volume-average theorems for gradient of time and space, which theorems have been treated after that in many articles [Gray and Lee 1977, Cushman 1982, Veverka 1981, Howes and Whitaker 1985, Gray 1983, Tosun and Willis 1980 and 1981].

The main assumptions in volume-averaging are that characteristic length l for averaging volume satisfies the condition d << l << L (where d is the microscopic scale of the medium and L is the scale of gross inhomogeneities) and that averaged quantities and their derivatives are continuous. In order to make derivatives continuous, averaging can be done in space and time twice [Drew 1971, Drew and Segel 1971a, 1971b]. Thus it is not necessary to assume smoothness in averaged variables. Some authors [Ishii 1975, Dobran 1985] have doubted the necessity to do double averagings. However, in the review by Bedford and Drumheller (1983) it was stated, that reasoning behind Drew's averaging procedure seems well-motivated.

The difference between these points of view is that mathematically double averaging makes derivatives continuous in general, but also in single averaging smoothness can in practice be obtained as an assumption. Howes and Whitaker (1985) have shown, that for the layered two-phase system rectangular or cylindrical averaging volumes do not lead to continuous derivatives, but spherical volume does. They also expect, that spherical averaging volume yields continuous averaged functions in general. Howes and Whitaker do not

have any arguments for their generalization and it seems, that when flow consists of phase boundaries, which are at least partly similar in shape with averaging volume boundary, the averaged variables have discontinuities for derivatives. In practice, fortunately, the fraction of phase boundaries having the same curvature as in the averaging volume boundary may be considered small and so smoothness assumption seems to be reasonable.

Since the work in the 60's, different averaging formulations have been used to obtain multiphase flow equations for various applications [Bachmat and Bear 1986a, 1986b, Banerjee and Chan 1980, Bouré 1979a, Chawla and Ishii 1980, Crapiste et al. 1986, Delhaye 1977, Drew and Lahey 1979, Drew and Segel 1971a, 1971b, Dobran 1981, 1984 and 1985, Gray 1975, Gray and Lee 1977, Hassanizadeh and Gray 1979a and 1979b, Hughes 1979, Hughes et al. 1976, Ishii 1975, Jiang et al. 1987, Muzyka 1985, Nigmatulin 1979, Peters and Prybylowski 1983, Sha and Slattery 1980, Soo et al. 1983, 1984, Trapp 1976, Whitaker 1973]. Different averagings used are space averaging (volume, area or line averaging), time averaging and probabilistic averaging.

A common feature with different averaging methods is that when closing the equation set, averages of functions depending on averaged variables have to be expressed by functions, which depend on averaged variables. That leads to different kinds of correlation terms, which are either assumed to be negligible or are meant to be determined empirically. At this time propositions for correla-

tion terms rely on quite loose arguments or totally on intuition. One difficulty has been that different formulations lead to various correlation terms, which are not comparable. So, uniform development between researchers for closing the equation system is not simple. There are also differences in interpretation of certain essential terms in equations. E.g. different forms for pressure and drag terms in momentum equation have been the main subject in many articles [Bouré 1979, Sha and Soo 1979, Rietema and Akker 1983, Prosperetti and Jones 1984].

2.2 OBJECTIVES FOR THEORY FORMULATION

In the following theoretical work the aim has been to formulate general multifield equations, which are physically reasonable and in which variables and correlations have clear physical interpretations. The form for pressure terms in momentum equation (as well as any flux term in any conservation term) has been obtained by systematic handling of general integral flux term. Averaging is done in space and time in such way that pure space averaged form may be obtained as an reduction from the general case.

In conventional averaging procedures the formulation lies on the differential equations for each phase, which are then averaged in a proper way. In the following work formulation is based on integral balances for different fields and then averaging definitions are used to get integral forms presented by averaged quan-

tities. Differential equations may then be obtained as an application of the integral equations.

2.3 NOTATION, DEFINITIONS AND THEOREMS

During the development of continuum flow equations different notations and definitions are needed for presentation of equations. Also some known general and averaging theorems have been applied in this chapter. These are all listed below before the actual theory formulation begins.

2.3.1 Control spaces

In the following formulations total control volume is fixed in space. Its volume is denoted by V_T and surface by A_T . Unit normal vector n_T for the volume boundary is defined to point outward from volume considered (Figure 2.1).

Control volume for a field r is the volume inside the total volume occupied by field r, the volume of which is denoted by V_R and boundary area by A_R.

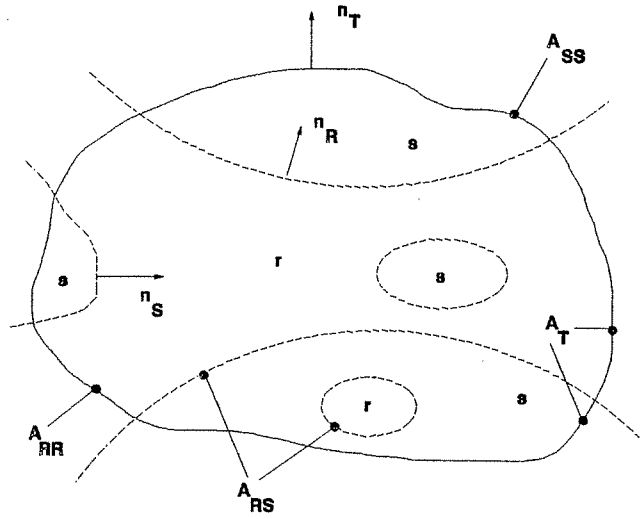

Figure 2.1 Control spaces

Capital letters T,S and R in subscripts relate to macroscopic space quantities and small letters t,s and r relate to space-averaging scale. Thus, e.g. V_r means averaging volume and A_r averaging area in the field r and V_R and A_R are total control volume and surface for the field r.

Other fields than r are represented by the symbol s so that $\sum_{s\neq r}$ means summation over all other fields than r and $\sum_{s}$ means summation including the field r.

The boundary between the fields r and s is denoted by A_{RS} and common boundary for the total and field control volume by A_{RR}. So boundary area for the field volume (field r) can be split

into boundaries A_{RR} and $\sum_{S\neq R} A_{RS}$

$$A_R = A_{RR} + \sum_{S\neq R} A_{RS} = \sum_{S} A_{RS}$$

Boundary A_{RR} is fixed and boundaries A_{RS} move with boundary velocity v_{bRS}. Boundary A_T may be expressed respectively

$$A_T = A_{RR} + \sum_{S\neq R} A_{SS} = \sum_{S} A_{SS}$$

where A_{SS} is the boundary for field s common with the total control volume. Total control volume consists of all the field control volumes

$$V_T = V_R + \sum_{S\neq R} V_S = \sum_{S} V_S$$

Macroscopic characteristic length L is the length for large scale changes in flow field, averaging characteristic length l relates to space-averaged quantities and microscopic characteristic length d is the microscopic scale of the medium. So the main assumption usually made in averaging formulation can be expressed in the form $L >> l >> d$.

Specific surface of the r and s field boundary per unit volume a_{rs} is defined

$$a_{rs} = \frac{1}{V_t} \int_{A_{rs}(V_t)} dA = \frac{A_{rs}}{V_t} \tag{2.1}$$

2.3.2 Definitions relating to averaging

Many integral forms will be used in the formulation of averaged conservation equations. In order to make presentation clearer, suitable definitions are required for integrals which are used in averaging procedure. Definitions are summarized in this chapter. Some of these definitions have been presented in the literature cited in section 2.1 and some additional definitions have been introduced.

Field function $\gamma_r(\mathbf{x})$ is used to represent space, which is occupied by the field r and is defined as follows [Drew 1971]

$$\gamma_r(\mathbf{x}) = \begin{cases} 1 \text{ , if } \mathbf{x} \text{ belongs to } V_R \\ 0 \text{ , if } \mathbf{x} \text{ does not belong to } V_R \end{cases} \tag{2.2}$$

Local space averaging definitions are needed for field volume and area averages, for intrinsic volume and area averages and for field boundary area averages

Field volume and area averages ${}^{V_t}\langle\psi\rangle_r$, ${}^{A_t}\langle\psi\rangle_r$, [Whitaker 1969]

$$ {}^{V_t}\langle\psi\rangle_r = \frac{1}{V_t}\int_{V_t} \psi\gamma_r dV \tag{2.3} $$

$$ {}^{A_t}\langle\psi\rangle_r = \frac{1}{A_t}\int_{A_t} \psi\gamma_r dA \tag{2.4} $$

Field intrinsic volume and area averages ${}^{V_r}\langle\psi\rangle_r$, ${}^{A_r}\langle\psi\rangle_r$, [Gray 1975]

$$ {}^{V_r}\langle\psi\rangle_r = \frac{1}{V_r}\int_{V_t} \psi\gamma_r dV \tag{2.5} $$

$$ {}^{A_r}\langle\psi\rangle_r = \frac{1}{A_r}\int_{A_t} \psi\gamma_r \, dA \tag{2.6} $$

Field interphase area average ${}^{A_{rs}}\langle\psi\rangle_r$

$$ \int_{A_{rs}} \psi\cdot n_r dA = \int_{V_t} {}^{A_{rs}}\langle\psi\rangle_r \cdot a_{rs} dV \tag{2.7} $$

Volume fraction ϵ_r for the field r is defined to be field volume average of unit value [Hassanizadeh and Gray 1979]

$$ \epsilon_r = {}^{V_t}\langle 1\rangle_r = \frac{1}{V_t}\int_{V_t} \gamma_r \, dV = \frac{V_r}{V_t} \tag{2.8} $$

Time average ${}^{t}\langle\phi\rangle$ definition is needed, when conservation equations are averaged in time. The length of the averaging time is assumed large enough for filtering small scale time fluctuations out and small enough not to disturb macroscopic transient analysis.

$$ {}^{t}\langle\phi\rangle = \frac{1}{t}\int_{t} \phi \, dt \tag{2.9} $$

When time and space averagings are combined, there are integrals both in space and time and following definitions are used for space/time averages ${}^{t,V_t}\langle\phi\rangle_r$, ${}^{t,A_t}\langle\phi\rangle_r$

$$ {}^{t,V_t}\langle\phi\rangle_r = {}^{t}\langle {}^{V_t}\langle\phi\rangle_r\rangle = \frac{1}{t\, V_t}\int_{t}\int_{V_t} \phi\gamma_r \, dV \, dt \tag{2.10} $$

$$ {}^{t,A_t}\langle\phi\rangle_r = {}^{t}\langle {}^{A_t}\langle\phi\rangle_r\rangle = \frac{1}{t\, A_t}\int_{t}\int_{A_t} \phi\gamma_r \, dA \, dt \tag{2.11} $$

and respectively intrinsic space/time averages

$$ {}^{t,V_r}\langle\psi\rangle_r \quad , \quad {}^{t,A_r}\langle\psi\rangle_r $$

$$ {}^{t,V_r}\langle\psi\rangle_r = {}^{t}\langle {}^{V_r}\langle\psi\rangle_r \rangle = \frac{1}{t} \int_t \frac{1}{V_r} \int_{V_t} \psi\gamma_r \, dV \, dt \qquad (2.12) $$

$$ {}^{t,A_r}\langle\psi\rangle_r = {}^{t}\langle {}^{A_r}\langle\psi\rangle_r \rangle = \frac{1}{t} \int_t \frac{1}{A_r} \int_{A_t} \psi\gamma_r \, dA \, dt \qquad (2.13) $$

In addition to space and time averaging, general quantities are presented as specific values, i.e. values divided by density. This definition leads to a considerable simplification and reduction in length of the equations, as Favre[1] has presented for one-phase time-averaged equations. Mass-weighted averaging is especially convenient for the treatment of flows of non-constant density. If density fluctuations are negligible, mass-weighted and Reynolds averaging formulations become identical.

For mass-weighted variables we use definition

---

[1] cited e.g. in [Hinze 1975]

specific space/time average $^{\rho,t,S_t}_{\quad <\psi>_r}$

$$\rho,t,S_{t_{<\psi>_r}} = \frac{t,S_{t_{<\rho\psi>_r}}}{t,S_{t_{<\rho>_r}}} = \frac{\int_t \int_{S_t} \gamma_r \rho\psi \; dSdt}{\int_t \int_{S_t} \gamma_r \rho \; dSdt} \quad , \tag{2.14}$$

where S_t is space quantity V_t or A_t

Space/time averages for volume fractions $^{t,V_t}_{\quad <\epsilon_r>}$, $^{t,A_t}_{\quad <\epsilon_r>}$ are defined with respective density averages

$$t,V_{t_{<\epsilon_r>}} = \frac{t,V_{t_{<\rho>_r}}}{t,V_{r_{<\rho>_r}}} \tag{2.15}$$

$$t,A_{t_{<\epsilon_r>}} = \frac{t,A_{t_{<\rho>_r}}}{t,A_{r_{<\rho>_r}}} \tag{2.16}$$

Presenting averages of products of variables with products of averaged variables gives rise to additional dispersion terms and there is need for the following fluctuating value definitions

Fluctuating density $\tilde{\rho}_r$

$$\tilde{\rho}_r = \rho_r - {}^{t,S_t}\langle\rho\rangle_r \tag{2.17}$$

Fluctuating general property $\tilde{\psi}_r$

$$\tilde{\psi}_r = \psi_r - {}^{\rho,t,S_t}\langle\psi\rangle_r \tag{2.18}$$

Fluctuating volume fraction $\tilde{\epsilon}_r$

$$\tilde{\epsilon}_r = \epsilon_r - {}^{t,S_t}\langle\epsilon\rangle_r \tag{2.19}$$

2.3.3 Relations

In addition to definitions, there are some basic relationships between defined quantities which will be used later in formulation of balance equations.

The sum of all volume fractions ϵ_s is unity

$$\sum_s \epsilon_s = \frac{\Sigma_s V_s}{V_t} = \frac{V_t}{V_t} = 1 \tag{2.20}$$

It is agreed [Whitaker 1969, Nigmatulin 1979, Bachmat and Bear 1986a] that volume and area averages can be considered equal

$$^{V_r}\langle\psi\rangle_r = {}^{A_r}\langle\psi\rangle_r \tag{2.21}$$

$$^{V_t}\langle\psi\rangle_r = {}^{A_t}\langle\psi\rangle_r \tag{2.22}$$

From definitions (2.3), (2.5) and (2.8) comes equality

$$^{V_t}\langle\psi\rangle_r = \epsilon_r \, {}^{V_r}\langle\psi\rangle_r \tag{2.23}$$

and from equations (2.21), (2.22) and (2.23)

$$^{A_t}\langle\psi\rangle_r = \epsilon_r \, {}^{A_r}\langle\psi\rangle_r \tag{2.24}$$

From the definition of field function (2.2) we may write also [Hassanizadeh and Gray 1979]

$$\int_{V_R} \psi \, dV = \int_{V_T} \gamma_r \psi \, dV \tag{2.25}$$

$$\int_{A_{RR}} \psi \cdot n_R dA = \int_{A_T} \gamma_r \psi \cdot n_T dV \tag{2.26}$$

Equation (2.27) may be obtained from definition (2.7) for integral in boundary of fields r and s

$$\int_{A_{RS}} \psi \cdot n_R dA = \int_{V_T} A_{rs} \langle \psi \rangle_r \cdot a_{rs} dV \qquad (2.27)$$

2.3.4 Theorems

The literature of averaging theory presents some averaging theorems, which have been applied also in this chapter. In addition, general theorems, such as transport theorem and Gauss theorem have been applied.

Averaging theorem [Slattery 1967, Whitaker 1969, Gray 1975]

$$\int_{A_{rr}} \psi \cdot n_r dA = \nabla \cdot \int_{V_r} \psi \, dV \text{ , if } l << L \qquad (2.28)$$

Transport theorem gives a means of transferring general principles for a system to principles for a control volume, which is convenient when dealing with moving continua. [Slattery 1981, Arpaci 1984]

$$\frac{D}{Dt}_{sys} \int_{V_{r,sys}} \psi \, dV = \frac{d}{dt} \int_{V_r} \psi \, dV + \int_{\sum_s A_{rs}} \psi (v_r - v_{rs}) \cdot n_r dA \qquad (2.29)$$

Theorems for integrals of averages [Whitaker 1969, Slattery 1981] are needed especially in integral formulation of averaging equations

$$\int_{V_T} \psi\gamma_r dV = \int_{V_T} {}^{V_t}\langle\psi\rangle_r dV \ , \ \text{if } l << L \tag{2.30}$$

$$\int_{A_T} \psi\gamma_r \cdot \mathbf{n}_T \, dA = \int_{A_T} {}^{A_t}\langle\psi\rangle_r \cdot \mathbf{n}_T dA \ , \ \text{if } l << L \tag{2.31}$$

A local space/time averaged variable may be taken out of local space/time averaging procedure, because according to averaging preconditions it can be considered constant within local averaging space and time. This has also been assumed in one way or the other in many references cited in this work. Assumption can be proved when average value is written in a Taylor series and averaging preconditions, $l << L$ and $t << T$, where T is macroscopic time length, are applied [Whitaker 1969]. Assumption may be written as follows

$${}^{t,S_t}\langle\Omega\rangle \, {}^{t,S_t}\langle\langle\psi\rangle_r\rangle_r = {}^{t,S_t}\langle\Omega\rangle_r \, {}^{t,S_t}\langle\psi\rangle_r \tag{2.32}$$

$${}^{t,S_t}\langle\Omega\rangle \, {}^{\rho,t,S_t}\langle\langle\psi\rangle_r\rangle_r = {}^{t,S_t}\langle\Omega\rangle_r \, {}^{\rho,t,S_t}\langle\psi\rangle_r \tag{2.33}$$

where Ω is any function.

Gauss theorem is also needed for changing area integrals into volume integrals. For a general quantity

$$\int_{A_T} \boldsymbol{\phi} \cdot \mathbf{n}_T dA = \int_{V_T} \nabla \cdot \boldsymbol{\phi} \, dV \qquad (2.34)$$

2.4 NON-CONVECTIVE FLUX TERMS

As presented in section 2.1, pressure terms in multiphase momentum equation have been the subject of many articles. In general, similar problem confronts with all non-convective flux terms in general conservation equations. In this chapter these terms are formulated and certain physical meanings are given for them in multifield equations of continuum-solid particles flow. Approach will be similar to pressure term derivation presented by Prosperetti and Jones (1984). This is by no means the one and only way of expressing different terms. The division depends e.g. on how terms are going to be determined experimentally, what kind of equation closure is to be used and on how minimum amount of parameters is obtained in the model for the flow case considered.

For a general quantity, effect of a non-convective flux in conservation balance may be written with surface integral term

$$\int_{\substack{\Sigma \\ S}} \boldsymbol{\phi} \cdot \mathbf{n}_R dA_{RS}$$

Respectively to pressure term division of Prosperetti and Jones (1984), flux ϕ_r is divided into two parts; slowly in space varying component $<\phi_r>$ and rapidly varying component $\overset{\circ}{\phi}_r$

$$\phi_r = <\phi_r> + \overset{\circ}{\phi}_r \tag{2.35}$$

where $<\phi_r>$ is defined to be equal to volume averaged flux

$$V_r <\phi_r>_r$$

2.4.1 Continuum

Indexes C and c are used here for continuum field and S and s for solid field.

For a control volume (Figure 2.2) term

$\int_{\Sigma_S} \phi_c \cdot n_C dA$ can be written into three parts F_{1C}, F_{2C} and F_{3C} A_{CS}

F_{1C} : Flux through free boundaries of control volume V_C,

$A_{CC} = A_C \cap A_T$

F_{2C} : Flux through boundaries of particles totally inside V_T,

surface A_I

F_{3C} : Flux through boundaries of particles partly inside V_T, surface A_B

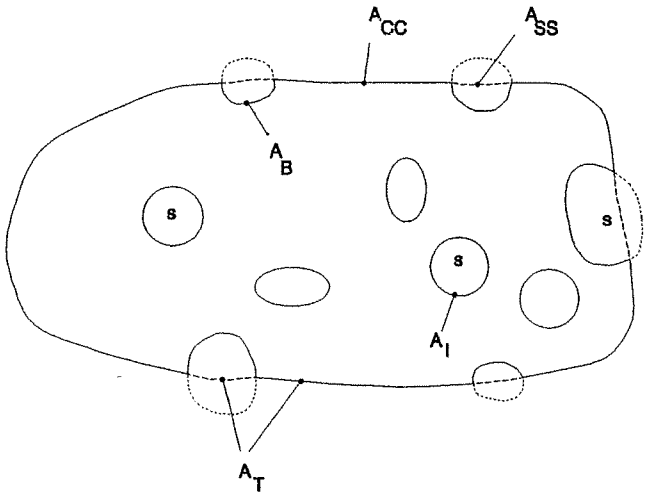

Figure 2.2 Control volume and field boundaries

Suitable forms can be derived for different parts F_{1C}, F_{2C} and F_{3C} by applying equations (2.26), (2.31) and (2.35) as follows

$$F_{1C} = \int_{A_{CC}} \phi_C \cdot n_C dA = \int_{A_T} \gamma_C \phi_C \cdot n_T dA = \int_{A_T} \epsilon_C {}^{V_C}\langle \phi_C \rangle_C \cdot n_T dA \qquad (2.36)$$

$$F_{2C} = \int_{A_I} \phi_C \cdot n_C dA = \int_{A_I} {}^{V_C}\langle \phi_C \rangle_C \cdot n_C dA + \int_{A_I} \overset{\circ}{\phi}_C \cdot n_C dA \qquad (2.37)$$

For a single particle the first term of the right side of the equation (2.37) can be written

$$\int_{A_{Ip}} {}^{V_C}\langle\phi_C\rangle_C \cdot n_C dA = -\int_{V_{Ip}} \nabla\cdot {}^{V_C}\langle\phi_C\rangle \, dV \approx -\nabla\cdot {}^{V_C}\langle\phi_C\rangle_C V_{Ip} \qquad (2.38)$$

Sign changes because n_C is opposite to particle unit vector. The last equality holds because particle dimension is much smaller than space averaging length, and thus $\nabla\cdot {}^{V_C}\langle\phi_C\rangle$ may be assumed constant in particle scale.

The third term ϕ_c may be divided into two components

$$F_{3C} = \int_{A_B} \phi_C \cdot n_C dA = \int_{A_B} {}^{V_C}\langle\phi_C\rangle_C \cdot n_C dA + \int_{A_B} \mathring{\phi}_C \cdot n_C dA \qquad (2.39)$$

For a single particle (additional subscript p is used), which is lying on the control volume boundary we may write

$$\int_{A_{Bp}} {}^{V_C}\langle\phi_C\rangle_C \cdot n_C dA = \int_{A_{Bp}} {}^{V_C}\langle\phi_C\rangle_C \cdot n_C dA - \int_{A_{SSp}} {}^{V_C}\langle\phi_C\rangle_C \cdot n_T dA$$

$$+ \int_{A_{SSp}} {}^{V_C}\langle\phi_C\rangle_C \cdot n_T dA = -\nabla\cdot {}^{V_C}\langle\phi_C\rangle_C V_{Bp} + \int_{A_{SSp}} {}^{V_C}\langle\phi_C\rangle_C \cdot n_T dA \qquad (2.40)$$

where V_{Bp} is the part of particle volume, which is bounded by surfaces A_{Bp} and A_T.

Combining terms F_{1C}, F_{2C} and F_{3C} gives

$$F_{1C}+ F_{2C}+ F_{3C}= \int_{A_T} \epsilon_c {}^{V_c}\langle \phi_c \rangle_c \cdot n_c dA - \sum_{Ip} V_{Ip} \nabla \cdot {}^{V_c}\langle \phi_c \rangle_c$$

$$- \sum_{Bp} V_{Bp} \nabla \cdot {}^{V_c}\langle \phi_c \rangle_c + \sum_{s\neq c} \int_{A_{SS}} {}^{V_c}\langle \phi_c \rangle_c \cdot n_T dA + \sum_{s\neq c} \int_{A_{CS}} \mathring{\phi}_c \cdot n_C dA \qquad (2.41)$$

Summation index Ip takes into consideration all the particles, which are totally inside the volume and index Bp particles on the boundary.

Adding the second and the third terms and also the first and the fourth terms together we may write the flux term

$$\sum_{s} \int_{A_{CS}} \phi_c \cdot n_c dA = \int_{A_T} {}^{V_c}\langle \phi_c \rangle_c \cdot n_T dA - \int_{V_T} (1-\epsilon_c) \nabla \cdot {}^{V_c}\langle \phi_c \rangle_c dV + \sum_{s\neq c} \int_{A_{CS}} \mathring{\phi}_c \cdot n_C dA \qquad (2.42)$$

Another form may be obtained, if the Gauss theorem (2.34) is

applied to the first term on the right hand side of equation (2.42) by adding the first and the second terms together and using equation (2.27)

$$\int_{\substack{\Sigma \\ S}} \phi_c \cdot n_c dA_{CS} = \int_{V_T} \epsilon_c \nabla \cdot {}^{V_c}\langle \phi_c \rangle_c dV + \int_{V_T} \sum_{S \neq C} {}^{A_{cs}}\langle \overset{\circ}{\phi}_c \rangle_c a_{cs} dV \qquad (2.43)$$

2.4.2 Particles

Indexes R and r are used in this section for the solid considered, S and s for other solid fields and indexes C and c for the continuum field. In order to formulate the total flux for the solid field r, the flux acting on one particle lying on the control volume boundary is examined first, Figure 2.3.

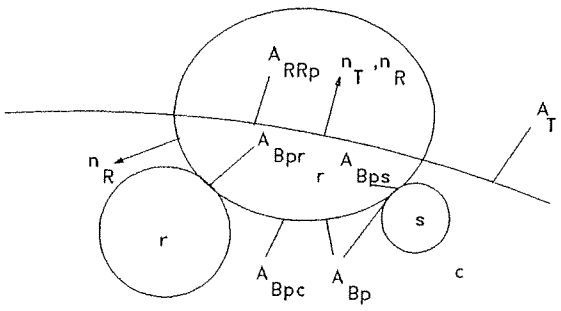

Figure 2.3 Particle on the control volume boundary

General quantity balance equation may be written for that part of the particle, which is inside the total control volume

$$\int_{A_{RRp}} \phi_r \cdot n_T dA + \int_{A_{Bp}} \phi_r \cdot n_R dA = \frac{D}{Dt} \int_{V_{Bp,sys}} \rho\phi \, dV - \int_{V_{Bp}} \theta_r dV \quad , \tag{2.44}$$

where $V_{Bp,sys}$ is system volume and V_{Bp} is control volume. Their size at the moment considered is equal.

Flux term on A_{Bp} consists of continuum - solid field r interaction and interactions between field r and all solid fields, i.e. collisions and contacts (includes also interactions between particles within field r)

$$\int_{A_{Bp}} \phi_r \cdot n_R dA = \int_{A_{Bpc}} \phi_c \cdot n_R dA + \int_{\substack{\Sigma \\ s \neq c}} \phi_s \cdot n_R dA \quad , \tag{2.45}$$

where

$A_{Bpc} = A_{Bp} \cap A_{RC}$ and $A_{Bps} = A_{Bp} \cap A_{RS}$

Summing the flux term $\int_{A_{RRp}} \phi_r \cdot n_T dA$ for all particles, which belong to the field r and are on the boundary A_T and applying equation (2.45) to equation (2.44) gives

$$\int_{A_{RR}} \boldsymbol{\phi}_r \cdot n_T dA = - \int_{A_{Bc}} \boldsymbol{\phi}_c \cdot n_R dA - \sum_{s \neq c} \int_{A_{Bs}} \boldsymbol{\phi}_s \cdot n_R dA + \frac{D}{Dt} \int_{V_{B,sys}} \rho \boldsymbol{\psi} \, dV$$

$$- \int_{V_B} \theta_r dV \qquad (2.46)$$

Next the flux term for particle field r is written into three parts, respectively as was done for the gas flux term

$$\sum_S \int_{A_{RS}} \boldsymbol{\phi}_r \cdot n_R dA = F_{1S} + F_{2S} + F_{3S} \quad , \qquad (2.47)$$

where

$$F_{1S} = \int_{A_{RR}} \boldsymbol{\phi}_r \cdot n_T dA \qquad (2.48)$$

corresponding to the flux through the free boundary of control volume V_R, $A_{RR} = A_R \cap A_T$

F_{2S} is flux due to interaction between the continuum and the field r and F_{3S} is flux due to interactions between field r and all solid fields, Figure 2.4.

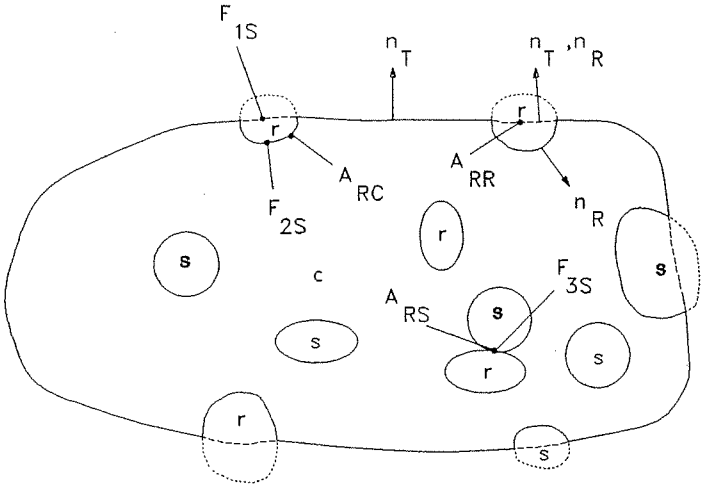

Figure 2.4 Different parts of fluxes acting on solid field r

Term F_{2S} may be obtained in the same way as continuum terms F_{2C} and F_{3C} in section 2.4.1, thus giving

$$F_{2S} = \int_{V_T} \epsilon_r \nabla \cdot {}^{V_c}\langle \phi_c \rangle_c dV - \int_{A_{RR}} {}^{V_c}\langle \phi_c \rangle_c \cdot n_T dA - \int_{A_{RC}} \mathring{\phi}_c \cdot n_R dA \qquad (2.49)$$

For term F_{3S} interactions between particles both representing field r need not to be considered, because their net effect is zero and term F_{3S} may be written

$$F_{3S} = \sum_{\substack{s \neq r,c \\ s}} \int_{A_{RS}} \phi_r \cdot n_R dA = \sum_{s \neq r,c} \int_{V_T} {}^{A_{rs}}\langle \phi_r \rangle_r a_{rs} dV \qquad (2.50)$$

Substituting the equation (2.46) into term F_{1S} and adding terms $F_{1S'}$ F_{2S} and F_{3S} together gives

$$\int_{\sum_s A_{RS}} \phi_r \cdot n_R dA = - \int_{A_{Bc}} \phi_c \cdot n_R dA - \int_{\sum_{s\neq c} A_{Bs}} \phi_s \cdot n_R dA + \frac{D}{Dt} \int_{V_{B,sys}} \rho\phi \, dV$$

$$- \int_{V_B} \theta_r dV + \int_{V_T} \epsilon_r \nabla \cdot {}^{V_c}\langle \phi_c \rangle_c dV \qquad (2.51)$$

$$- \int_{A_{RR}} {}^{V_c}\langle \phi_c \rangle_c \cdot n_T dA - \int_{A_{RC}} \mathring{\phi}_c \cdot n_R dA + \sum_{s\neq r,c} \int_{V_T} {}^{A_{rs}}\langle \phi_r \rangle_r a_{rs} dV$$

Equation (2.27) gives

$$\int_{A_{RC}} \mathring{\phi}_c \cdot n_R dA = \int_{V_T} {}^{A_{rc}}\langle \mathring{\phi}_c \rangle_r a_{rc} dV \qquad (2.52)$$

The first term on the right hand side of equation (2.51) may be written

$$- \int_{A_{Bc}} \phi_c \cdot n_R dA = - \int_{A_B} \phi_c \cdot n_R dA + \int_{\sum_{s\neq c} A_{Bs}} \phi_c \cdot n_R dA \qquad (2.53)$$

Considering definition (2.35) and equation (2.53) we may write for the first and sixth terms of equation (3.49)

$$- \int_{A_{Bc}} \phi_c \cdot n_R dA - \int_{A_{RR}} {}^{V_c}\langle \phi_c \rangle_c \cdot n_T dA = - \int_{A_B + A_{RR}} {}^{V_c}\langle \phi_c \rangle_c \cdot n_\omega dA$$

$$- \int_{A_B} \mathring{\phi}_c \cdot n_R dA + \int_{\substack{\Sigma \\ s \neq c}} \phi_c \cdot n_R dA \qquad (2.54)$$

When the Gauss theorem is applied to equation (2.54)

$$- \int_{A_{Bc}} \phi_c \cdot n_R dA - \int_{A_{RR}} {}^{V_r}\langle \phi_c \rangle_c \cdot n_T dA = - \int_{V_B} \nabla \cdot {}^{V_r}\langle \phi_c \rangle_c \, dA$$

$$(2.55)$$

$$- \int_{A_B} \mathring{\phi}_c \cdot n_R dA + \int_{\substack{\Sigma \\ s \neq c}} \phi_c \cdot n_R dA$$

Substituting equations (2.55) and (2.52) into equation (2.51) gives

$$\int_{\sum_s A_{RS}} \phi_r \cdot n_R dA = + \int_{V_T} \epsilon_r \nabla \cdot {}^{V_c}\langle \phi_c \rangle_c dV + \sum_{s \neq r,c} \int_{V_T} {}^{A_{rs}}\langle \phi_r \rangle_r a_{rs} dV$$

$$- \int_{V_B} \nabla \cdot {}^{V_c}\langle \phi_c \rangle_c dV + \int_{V_B} \theta_r \, dV + \frac{D}{Dt} \int_{V_B,sys} \rho \phi \, dV \qquad (2.56)$$

$$- \int_{A_B} \mathring{\phi} \cdot n_R dA - \int_{V_T} {}^{A_{rc}}\langle \mathring{\phi}_c \rangle_r a_{rc} dV - \int_{\sum_{s \neq c} A_{Bs}} (\phi_s - \phi_c) \cdot n_R dA = 0$$

Term $\int_{V_B} \nabla \cdot {}^{V_c} \langle \phi_c \rangle_c dV$ may be approximated as follows

$$\int_{V_B} \nabla \cdot {}^{V_c}\langle \phi_c \rangle_c dV < \int_{A_T d_r} \gamma_r \nabla \cdot {}^{V_c}\langle \phi_c \rangle_c dV \approx \int_{A_T d_r} \epsilon_r \nabla \cdot {}^{V_c}\langle \phi_c \rangle_c dV \qquad (2.57)$$

where d_r is particle's characteristic length and $A_T d_r$ is volume along total volume boundary, thickness of which is d_r.
Volume $A_T d_r << A_T l$ and when total volume is assumed to be such, that $A_T l$ is not greater in magnitude than V_T, it may be written that

$$\int_{V_T} \epsilon_r \nabla \cdot {}^{V_r}\langle \phi_c \rangle_c dV \;>>\; \int_{V_B} \nabla \cdot {}^{V_r}\langle \phi_c \rangle_c dV \qquad (2.58)$$

In the same way when applying equation (2.27) the sixth term on the r.h.s. of the equation (2.56) is smaller than the seventh term

$$\int_{A_B} \mathring{\phi}_c \cdot n_R dA \;<\; \int_{A_T d_r} {}^{A_{rc}}\langle \mathring{\phi}_c \rangle_r a_{rc}\, dV \;<<\; \int_{V_T} {}^{A_{rc}}\langle \phi_c \rangle_r a_{rc}\, dV \qquad (2.59)$$

When the flux term is later substituted into general balance equation (chapter 2.5), there are integrals over total control volume for source and rate of change terms and thus corresponding integral terms in equation (2.56) are negligible compared with them. So, the fourth and the fifth terms on the r.h.s. of the flux term equation (2.56) are dropped out.

When all the small terms are eliminated from equation (2.56) it gives

$$\sum_s \int_{A_{RS}} \phi_r \cdot n_R dA = + \int_{V_T} \epsilon_r \nabla \cdot {}^{V_r}\langle \phi_c \rangle_c dV + \sum_{s \neq r,c} \int_{V_T} {}^{A_{rs}}\langle \phi_r \rangle_r a_{rs} dV$$

$$-\int_{V_T} {}^{A_{rc}}(\mathring{\phi}_c)_r a_{rc} dV - \sum_{s \neq c} \int_{A_{Bs}} (\phi_s - \phi_c) \cdot n_R dA = 0 \qquad (2.60)$$

where terms are interpreted as follows

$\int_{V_T} \epsilon_r \nabla \cdot {}^{V_r}\langle \phi_c \rangle_c dV$; the gas average flux

$\sum_{s \neq r,c} \int_{V_T} {}^{A_{rs}}\langle \phi_r \rangle_r a_{rs} dV$; particle-particle interaction

$\int_{V_T} {}^{A_{rc}}(\mathring{\phi}_c)_r a_{rc} dV$; gas-solid interaction

$\int_{\sum_{s \neq c} A_{Bs}} (\phi_s - \phi_c) \cdot n_R dA = 0$; accounts for the flux due to solid-solid interactions on particles, which are on the boundary A_T subtracted by gas interaction on respective particles

2.5 SPACE-AVERAGED CONSERVATION EQUATIONS

Conservation balance for a general quantity ψ in field r (solid or continuum) for system volume $V_{R,sys}$ may be written

$$\frac{D}{Dt}_{sys} \int_{V_{R,sys}} \rho\psi \, dV - \int_{\substack{\Sigma \\ S}} \boldsymbol{\phi}\cdot\mathbf{n}_R dA_{RS} - \int_{V_{R,sys}} \theta_r \, dV = 0 \qquad (2.61)$$

The first term in (2.61) is the change of property in the system volume, the second term is the non-convective flux of the quantity through boundary A_R and the third represents the rate of production of quantity ψ.

According to the transport theorem (2.29), the system time derivative can be written using the time derivative for the control volume V_R

$$\frac{D}{Dt}_{sys} \int_{V_{R,sys}} \rho\psi \, dV = \frac{d}{dt} \int_{V_R} \rho\psi \, dV + \int_{\substack{\Sigma \\ S}} \rho\psi(\mathbf{v}_r-\mathbf{v}_{rs})\cdot\mathbf{n}_R dA_{RS} \qquad (2.62)$$

Surface integral in $\sum_{S} A_{RS}$ may be divided into two parts A_{RR} and $\sum_{S\neq R} A_{RS}$. In addition, the velocity for the control volume boundary is

$\mathbf{v}_{rr} = 0$ in A_{RR} and

$\mathbf{v}_{rs} = \mathbf{v}_{brs}$ in A_{RS}

so one can write

$$\sum_{S} \int_{A_{RS}} \rho\psi(\mathbf{v}_r-\mathbf{v}_{rs})\cdot\mathbf{n}_R dA = \int_{A_{RR}} \rho\psi\mathbf{v}_r\cdot\mathbf{n}_R dA + \sum_{S\neq R} \int_{A_{RS}} \rho\psi(\mathbf{v}_r-\mathbf{v}_{brs})\cdot\mathbf{n}_R dA \qquad (2.63)$$

Substituting equations (2.62) and (2.63) into equation (2.64) gives

$$\frac{d}{dt}\int_{V_R} \rho\psi\, dV + \int_{A_{RR}} \rho\psi\mathbf{v}_r\cdot\mathbf{n}_R dA + \sum_{s\neq r} \int_{A_{RR}} \rho\psi(\mathbf{v}_r-\mathbf{v}_{brs})\cdot\mathbf{n}_R dA$$
$$- \sum_{S} \int_{A_{RS}} \boldsymbol{\phi}\cdot\mathbf{n}_R dA - \int_{V_R} \theta_r dV = 0 \qquad (2.64)$$

The system volume and the control volume have been chosen to be the same at the moment considered, so in the last integral there is V_R instead of $V_{R,sys}$.

According to relations (2.25) and (2.26) equation (2.64) may also be written in the form

$$\frac{d}{dt}\int_{V_T}\gamma_r\rho\phi\ dV + \int_{A_T}\gamma_r\rho\phi\mathbf{v}_r\cdot\mathbf{n}_T dA - \int_{\substack{\Sigma\\ S\neq R}}\int_{A_{RS}}\rho\phi(\mathbf{v}_r-\mathbf{v}_{brs})\cdot\mathbf{n}_R dA \tag{2.65}$$

$$-\int_{\substack{\Sigma\\ S}}\int_{A_{RS}}\boldsymbol{\phi}_r\cdot\mathbf{n}_R dA - \int_{V_R}\theta_r dV = 0$$

At this point it should be noted, that equation (2.65) reduces to normal space-averaged differential equation, if the non-convective flux term is divided into two parts A_{RR} and $\sum_{S\neq R} A_{RS}$ and applying equations (2.22), (2.31) and (2.34)

$$\frac{\partial}{\partial t}{}^{V_t}\langle\rho\phi\rangle_r + \nabla\cdot{}^{V_t}\langle\rho\phi\mathbf{v}_r\rangle_r - \nabla\cdot{}^{V_t}\langle\boldsymbol{\phi}_r\rangle_r + \frac{1}{V_t}\int_{\substack{\Sigma\\ s\neq r}}\int_{A_{rs}}\rho\phi(\mathbf{v}_r-\mathbf{v}_{brs})\cdot\mathbf{n}_r dA \tag{2.66}$$

$$-\frac{1}{V_t}\int_{\substack{\Sigma\\ s\neq r}}\int_{A_{rs}}\boldsymbol{\phi}_r\cdot\mathbf{n}_r dA - {}^{V_t}\langle\theta_r\rangle_r = 0 \quad ,$$

which is the same form as e.g. in reference [Gray 1975].

Applying theorems (2.30) and (2.31) to equation (2.65) gives

$$\frac{d}{dt}\int_{V_T}{}^{V_t}\langle\rho\phi\rangle_r dV + \int_{A_T}{}^{A_t}\langle\rho\phi\mathbf{v}_r\rangle_r\cdot\mathbf{n}_T dA + \int_{V_T}\sum_{s\neq r}{}^{A_{rs}}\langle\rho\phi(\mathbf{v}_r-\mathbf{v}_{brs})\rangle_r a_{rs} dV$$

$$- \int_{\sum_S A_{RS}} \phi_r \cdot n_R dA - \int_{V_T} {}^{V_t}\langle \theta_r \rangle_r dV = 0 \qquad (2.67)$$

In equation (2.67), four of the five terms are integrals in the total control volume or area. The flux term is integral in area $\sum_S A_{RS}$.

The flux terms, i.e. equations (2.43) and (2.60), may now be substituted into conservation equation (2.67) to give

Continuum

$$\frac{d}{dt} \int_{V_T} {}^{V_t}\langle \rho\phi \rangle_c dV + \int_{A_T} {}^{A_t}\langle \rho\phi \mathbf{v}_c \rangle_c \cdot n_T dA + \int_{V_T} \sum_{s \neq c} {}^{A_{cs}}\langle \rho\phi (\mathbf{v}_c - \mathbf{v}_{bcs}) \rangle_c a_{cs} dV \qquad (2.68)$$

$$- \int_{V_T} \epsilon_c \nabla \cdot {}^{V_c}\langle \phi_c \rangle_c dV - \int_{V_T} \sum_{S \neq C} {}^{A_{cs}}\langle \mathring{\phi}_c \rangle_c a_{cs} dV - \int_{V_T} {}^{V_t}\langle \theta_c \rangle_c dV = 0$$

Solid field

$$\frac{d}{dt}\int_{V_T} {}^{V_t}\langle\rho\psi\rangle_r dV + \int_{A_T} {}^{A_t}\langle\rho\psi\mathbf{v}_r\rangle_r \cdot \mathbf{n}_T dA + \int_{V_T} \sum_{s\neq r} {}^{A_{rs}}\langle\rho\psi(\mathbf{v}_r-\mathbf{v}_{brs})\rangle_r a_{rs} dV$$

$$- \int_{V_T} \epsilon_r \nabla\cdot {}^{V_c}\langle\phi_c\rangle_c dV - \sum_{s\neq r,c} \int_{V_T} {}^{A_{rs}}\langle\phi_r\rangle_r a_{rs} dV \qquad (2.69)$$

$$+\int_{V_T} {}^{A_{rc}}\langle\mathring{\phi}_c\rangle_r a_{rc} dV + \int_{\sum_{s\neq c} A_{Bs}} (\phi_s-\phi_c)\cdot \mathbf{n}_R dA - \int_{V_T} {}^{V_t}\langle\theta_r\rangle_r dV = 0$$

2.6 SPACE/TIME-AVERAGED CONSERVATION EQUATIONS

Integrating equations (2.68) and (2.69) in time and applying averaging definitions, the following space/time-averaged equations may be obtained

Continuum

$$\frac{d}{dt}\int_{V_T}{}^{t,V}t_{<\rho\psi>_c}dV + \int_{A_T}{}^{t,A}t_{<\rho\psi v_c>_c}\cdot n_T dA$$

$$+ \int_{V_T}\sum_{s\neq c}{}^{t}<^{A_{cs}}<\rho\psi(v_c-v_{bcs})>_c a_{cs}> dV - \int_{V_T}\sum_{s\neq c}{}^{t}<^{A_{cs}}<\mathring{\phi}_c>_c a_{cs}> dV$$

$$- \int_{V_T}{}^{t}<\epsilon_c\nabla\cdot{}^{V_c}<\phi_c>_c> dV - \int_{V_T}{}^{t}<^{V}t_{<\theta_c>_c}> dV = 0 \qquad (2.70)$$

Solid field

$$\frac{d}{dt}\int_{V_T}{}^{t,V}t_{<\rho\psi>_r}dV + \int_{A_T}{}^{t,A}t_{<\rho\psi v_r>_r}\cdot n_T dA$$

$$+ \int_{V_T}\sum_{s\neq r}{}^{t}<^{A_{rs}}<\rho\psi(v_r-v_{brs})>_r a_{rs}>_r dV \quad a_{rs}dV - \int_{V_T}{}^{t}<\epsilon_r\nabla\cdot{}^{V_c}<\phi_c>_c> dV$$

$$\int_{V_T}\sum_{s\neq r,c}{}^{t}<^{A_{rs}}<\phi_r>_r a_{rs}> dV + \int_{V_T}{}^{t}<^{A_{rc}}<\mathring{\phi}_c>_r a_{rc}> dV + {}^{t}<\int_{\sum_{s\neq c}A_{Bs}}(\phi_s-\phi_c)\cdot n_R dA$$

$$- \int_{V_T}{}^{t,V}t_{<\theta_r>_r}dV = 0 \qquad (2.71)$$

The problem with equations (2.70) and (2.71) is that when flow properties are substituted in these equations instead of general quantity, it results in an equation system, in which there are more unknown variables than equations. To reduce the amount of unknown variables, averages of functions depending on the basic variables ρ, ψ and v should be written in the form in which there are functions depending on the averaged variables. This leads to extra dispersion terms, which are defined in the following. When choosing different forms for the definitions, the emphasis in formulation has been on obtaining averaged quantities, which are experimentally measurable and which lead to as simple an equation closure as possible.

Below we will consider first two terms in equations (2.70) and (2.71), i.e. the rate of change and convection terms, and write them as products of averaged variables instead of averages of products of variables.

From definition 2.14 we may write straight

$$t,S_{t_{<\rho\psi>_r}} = {}^{t,S_{t_{<\rho>_r}}}\,{}^{\rho,t,S_{t_{<\psi>_r}}} \qquad (2.72)$$

or applying definitions (2.15) and (2.16)

$$t,S_{t_{<\rho\phi>_r}} = {}^{t,S}t_{<\epsilon_r>}\,{}^{t,S}r_{<\rho>_r}\,{}^{\rho,T,S}t_{<\phi>_r} \tag{2.73}$$

If we apply definition (2.18), we may write

$$t,S_{t_{<\rho\phi>_r}} = {}^{t,S}t_{<\rho}\,{}^{\rho,t,S}t_{<\phi>_r>_r} + {}^{t,S}t_{<\rho\tilde{\phi}_r>_r} \tag{2.74}$$

If we take into consideration equation (2.33) and then compare equation (2.72) with (2.74), we can conclude that

$$t,S_{t_{<\rho\tilde{\phi}_r>_r}} = 0 \tag{2.75}$$

Now, for the convection term may be written applying equation (2.18)

$$\begin{aligned} t,S_{t_{<\rho v\phi>_r}} = {}& {}^{t,S}t_{<\rho>_r}\,{}^{\rho,t,S}t_{<v>_r}\,{}^{\rho,t,S}t_{<\phi>_r} \\ & + {}^{\rho,t,S}t_{<v>_r}\,{}^{t,S}t_{<\rho\tilde{\phi}_r>_r} + {}^{\rho,t,S}t_{<\phi>_r}\,{}^{t,S}t_{<\rho\tilde{v}_r>_r} \\ & + {}^{t,S}t_{<\rho\tilde{v}_r\tilde{\phi}_r>_r} \end{aligned} \tag{2.76}$$

According to equation (2.75) the second and the third terms from the equation (2.76) can be eliminated thus giving

$$^{t,S}t_{<\rho v\psi>_r} = {}^{t,S}t_{<\rho>_r}{}^{\rho,t,S}t_{<v>_r}{}^{\rho,t,S}t_{<\psi>_r} + {}^{t,S}t_{<\rho\ (\tilde{v})_r(\tilde{\psi})_r>_r} \tag{2.77}$$

Substituting equations (2.72) and (2.77) into space/time-averaged conservation equations (2.70) and (2.71) rate of change and convection terms may be written as products of averaged variables, if respective dispersion terms are added.

In order to make the notation in conservation equations simpler, new definitions are introduced as follows

$$\underline{\epsilon}_r = {}^{t,S}t_{<\epsilon_r>} \tag{2.78}$$

$$\underline{\rho}_r = {}^{t,S}r_{<\rho>_r} \tag{2.79}$$

$$\underline{\rho}_r^{\epsilon} = {}^{t,S}t_{<\rho>_r} \tag{2.80}$$

or applying equations (2.15) and (2.16)

$$\underline{\rho}_r^{\epsilon} = \underline{\epsilon}_r\ \underline{\rho}_r \tag{2.81}$$

$$\underline{\psi}_r = {}^{\rho,t,S}t_{<\psi>_r} \tag{2.82}$$

$$\underline{I}_r^s(\psi) = {}^{t}<{}^{A}rs_{<\rho\psi(v_r-v_{brs})>_r a_{rs}>} \tag{2.83}$$

$$\underline{C}_r(\psi) = {}^{t,S}t_{<\rho\ \tilde{v}_r\ \tilde{\psi}_r>_r} \tag{2.84}$$

$$\underline{\phi}^I_{cr} = {}^{t}<{}^{A_{cr}}(\mathring{\phi}_c)a_{cr}> \tag{2.85}$$

$$\nabla\cdot\underline{\phi}_{cc} = \frac{{}^{t}<\epsilon_c\nabla\cdot{}^{V_c}<\phi_c>_c>}{\underline{\epsilon}_c} \tag{2.86}$$

$$\nabla\cdot\underline{\phi}_{cr} = \frac{{}^{t}<\epsilon_r\nabla\cdot{}^{V_c}<\phi_c>_c>}{\underline{\epsilon}_r} \tag{2.87}$$

$$\underline{\phi}^V_{rs} = {}^{t}<{}^{A_{rs}}<\phi_r>_r a_{rs}> \tag{2.88}$$

$$\underline{\theta}_r(\psi) = {}^{t,V}t_{<\theta_r>_r} \tag{2.89}$$

and $\underline{\phi}^A_{rs}$ is defined with the following equation

$${}^{t}<\int_{A_{Bs}}(\phi_s-\phi_c)\cdot n_R dA> = \int_{A_T}\underline{\phi}^A_{rs}\cdot n_T dA \tag{2.90}$$

Substituting equations (2.72) and (2.78)-(2.90) into conservation equation gives

Continuum

$$\underset{(1.)}{\int_{V_T} \frac{\partial}{\partial t} (\underline{\epsilon}_c \rho_c \underline{\psi}_c) \, dV} + \underset{(2.)}{\int_{A_T} \underline{\epsilon}_c \rho_c \underline{\psi}_c \underline{v}_c \cdot n_T dA} + \underset{(3.)}{\int_{A_T} \underline{C}_c(\psi) \cdot n_T dA}$$

$$+ \underset{(4.)}{\int_{V_T} \sum_{s \neq c} \underline{I}_c^s(\psi) \, dV} - \underset{(5.)}{\int_{V_T} \sum_{s \neq c} \underline{\phi}_{cs}^I dV} - \underset{(6.)}{\int_{V_T} \underline{\epsilon}_c \nabla \cdot \underline{\phi}_{cc} dV} - \underset{(7.)}{\int_{V_T} \underline{\theta}_c(\psi) \, dV} = 0 \qquad (2.91)$$

Solid field

$$\underset{(1.)}{\int_{V_T} \frac{\partial}{\partial t} (\underline{\epsilon}_r \rho_r \underline{\psi}_r) \, dV} + \underset{(2.)}{\int_{A_T} \underline{\epsilon}_r \rho_r \underline{\psi}_r \underline{v}_r \cdot n_T dA} + \underset{(3.)}{\int_{A_T} \underline{C}_r(\psi) \cdot n_T dA}$$

$$+ \underset{(4.)}{\int_{V_T} \sum_{s \neq r} \underline{I}_r^s(\psi) \, dV} + \underset{(5.)}{\int_{V_T} \underline{\phi}_{cr}^I dV} - \underset{(6.)}{\int_{V_T} \underline{\epsilon}_r \nabla \cdot \underline{\phi}_{cr} dV} - \underset{(7.)}{\int_{V_T} \underline{\theta}_r(\psi) \, dV} \qquad (2.92)$$

$$- \underset{(8.)}{\int_{V_T} \sum_{s \neq r,c} \underline{\phi}_{rs}^V dV} + \underset{(9.)}{\int_{A_T} \sum_{s \neq c} \underline{\phi}_{rs}^A \cdot n_T dA} = 0$$

Terms in equations (2.91) and (2.92) can be interpreted as follows

(1.) : rate of change

(2.) : convection

(3.) : dispersion part of the convection

(4.) : convection of property through field interfaces

(5.) : continuum-solid field interaction

(6.) : non-convective continuum flux

(7.) : source term

(8.) : interactions between solids in volume V_T

(9.) : interaction on solids lying on surface A_T caused by solid fields subtracted by continuum interaction

When equations (2.91) and (2.92) are applied to differential volume, respective differential equations are

Continuum

$$\frac{\partial}{\partial t}\left(\underline{\epsilon}_c \rho_c \underline{\psi}_c\right) + \nabla\cdot\left(\underline{\epsilon}_c \rho_c \underline{\psi}_c \underline{v}_c\right) + \nabla\cdot\underline{C}_c(\psi) + \sum_{s\neq c} \underline{I}^s_c(\psi) - \sum_{s\neq c} \underline{\phi}^I_{cs} - \underline{\epsilon}_c \nabla\cdot\underline{\phi}_{cc} - \underline{\theta}_c(\psi) = 0 \qquad (2.93)$$

Solid field

$$\frac{\partial}{\partial t}(\underline{\epsilon}_r \rho_r \underline{\psi}_r) + \nabla\cdot(\underline{\epsilon}_r \rho_r \underline{\psi}_r \underline{v}_r) + \nabla\cdot\underline{C}_r(\psi) + \sum_{s\neq r} \underline{I}_r^s(\psi)$$

$$+ \underline{\phi}_{cr}^I - \underline{\epsilon}_r \nabla\cdot\underline{\phi}_{cr} - \underline{\theta}_c(\psi) - \sum_{s\neq r,c} \underline{\phi}_{rs}^V + \sum_{s\neq c} \nabla\cdot\underline{\phi}_{rs}^A = 0 \qquad (2.94)$$

2.7 DIFFERENT FIELDS IN CONTINUUM APPROACH

Averaging formulation may be considered as a transformation from non-continuous fields to continuous fields, where different fields are allowed to be at the same space location at the same time. As a result we can obtain similar conservation equations for different fields whether they are continuous or not.

The need for different fields within a phase or material comes from the fact that different parts of the phase may have quite different averaged values at the same point for quantities. An obvious example is differences in flow dynamics or combustion mechanism due to different particle sizes. In addition to phase properties, also different initial and boundary conditions may result in different behavior of different parts of a phase. Of course, with proper definitions all different parts of a phase can be considered as one field having common representative quantities. The problem is, however, the determination of constitutive models

to obtain the right behavior for representative quantities, especially if there is a great non-uniformity in flow. The part of non-homogeneity, which is caused by different properties or different initial and boundary conditions within a phase, may be reduced by dividing a phase into different fields defined according to the respective properties or conditions. It may then be easier to establish constitutive models for these fields .

In the following formulation a phase is divided into different fields according to particle size. In general, instead of particle size the same treatment may also be used with other quantities.

Field r is defined to represent all the particles, the size range of which is $[d_{pr-},d_{pr+}]$. Following relations [Kunii and Levenspiel 1984] and definitions may be written

$$\epsilon_{ri} = \int_{d_{pr-}}^{d_{pr+}} p_i d(d_p)\ \epsilon_i \qquad (2.95)$$

$$p_i = \frac{1}{V_i} \frac{dV_i(d_p)}{d(d_p)} \qquad (2.96)$$

$$P_i(d_p) = \int_0^{d_p} p_i d(d_p) \qquad (2.97)$$

$$P_i(\infty) = 1 \ , \qquad (2.98)$$

where

$p_i(d_p)$ is partial volume fraction of particles in phase i of size between d_p and $d_p+d(d_p)$

$P_i(d_p)$ is partial volume fraction of particles in phase i of size smaller than d_p

$dV_i(d_p)$ is volume occupied by particles in phase i size of which is between d_p and $d_p+d(d_p)$

V_i is volume occupied by all particles in phase i

Mass transfer from one field to another through field definition limits d_{p-} and d_{p+} is caused by particle size change and for property ψ transfer we may write

$$J_i(\psi) = \psi p_i \rho_i \epsilon_i \dot{d}_p \tag{2.99}$$

and net transfer in field r, $d_{pr-}<d_{pr}<d_{pr+}$ is

$$J_{ri}(\psi) = \int_{d_{pr-}}^{d_{pr+}} - \frac{\partial}{\partial d_p}(\psi p_i \epsilon_i \dot{d}_{pr})\, d(d_{pr}) \tag{2.100}$$

or in integrated form, equation (2.101)

$$J_{ri}(\psi) = - \epsilon_i \int_{d_{pr-}}^{d_{pr+}} (\psi p_i \rho_i \dot{d}_{pr}) \qquad (2.101)$$

If field limit transfer rates are defined as follows

$$J_{ri}^{+}(\psi) = - (\psi p_i \rho_i \dot{d}_{pr})|_{d_{pr+}} \cdot \epsilon_i \qquad (2.102)$$

$$J_{ri}^{-}(\psi) = - (\psi p_i \rho_i \dot{d}_{pr})|_{d_{pr-}} \cdot \epsilon_i \qquad (2.103)$$

equation (2.100) gives

$$J_{ri}(\psi) = J_{ri}^{+}(\psi) - J_{ri}^{-}(\psi) \qquad (2.104)$$

2.8 EQUATION CLOSURE

The basis for the modeling of multifield flow may be obtained by applying general equations (2.93) and (2.92) to material, momentum and energy balance. However, there are still more unknown terms in the equation system than there are equations. Thus, closing the system implies additional equations which will give relations for some of the terms so that total amount of equations

will be the same as the amount of unknown variables. At the moment the knowledge of these constitutive equations for fluidized bed applications is limited. Constitutive equations presented in literature require suitable interpretation in order to enable their application to the model frame presented herein, because many of them are connected with equations based on pure intuition or different averaging formulation. Often when an equation system has been closed, the amount of unknowns has been reduced by assuming certain terms negligible, which assumption has also been used sometimes when there has not been better knowledge of the model for the term. Various forms found in literature are introduced in the following to model unknown terms in conservation equations. Terms in literature are often written for simplified cases, e.g. in one or two dimensions. Thus in the following, some relations are presented using scalar variables instead of tensors.

2.8.1 Material balance

General conservation equations (2.91) and (2.92) may be applied for different species within a field to give similar equation form for gas and solid fields

Species equation

$$\frac{d}{dt}\int_{V_T} \underline{\epsilon}_r \underline{\rho}_{r\alpha} dV = \int_{A_T} \underline{\epsilon}_r \underline{\rho}_{r\alpha} \underline{v}_{r\alpha} \cdot n_T dA + \int_{V_T} \sum_{s\neq r} \underline{I}^s_{r\alpha}(1)\, dV$$

$$- \int_{V_T} \underline{\theta}_{r\alpha}(1)\, dV = 0 \qquad (2.105)$$

and for mass balance of field r

Mass balance

$$\frac{d}{dt}\int_{V_T} \underline{\epsilon}_r \underline{\rho}_r\, dV = \int_{A_T} \underline{\epsilon}_r \underline{\rho}_r\, \underline{v}_r \cdot n_T dA + \int_{V_T} \sum_{s\neq r} \underline{I}^s_r(1)\, dV$$

$$- \int_{V_T} \underline{\theta}_r(1)\, dV = 0 \qquad (2.106)$$

Unknown terms in equations (2.105) and (2.106) (i.e. terms, which are not functions of primary variables) are interpreted and presented as follows

Term $\underline{I}^{s}_{r\alpha}$

$\underline{I}^{s}_{r\alpha}(1)$ represents mass transfer of species α through field interfaces from field r to field s. The mathematical form for it is similar to equation (2.83)

$$\underline{I}^{s}_{r\alpha}(1) = {}^{t}< {}^{A_{rs}}<\rho_{r\alpha}(v_{r\alpha}-v_{brs})>_{r}a_{rs}> \tag{2.107}$$

or

$$\underline{I}^{s}_{r\alpha}(1) = {}^{t}< {}^{A_{rs}}<i^{s}_{r\alpha}>_{r}a_{rs}> \tag{2.108}$$

where species' mass transfer divided by area, $i^{s}_{r\alpha}$ is written as follows

$$i^{s}_{r\alpha} = \rho_{r\alpha}(v_{r\alpha}-v_{brs}) \tag{2.109}$$

If time correlation between ${}^{A_{rs}}<i^{s}_{r\alpha}>_{r}$ and a_{rs} is negligible we may write

$$\underline{I}^{s}_{r\alpha}(1) = {}^{A_{rs}}<\underline{i}^{s}_{r\alpha}>_{r}a_{rs} \tag{2.110}$$

For $\underline{i}^{s}_{r\alpha}$ suitable mass transfer model must be applied depending on the phenomena which is being studied.

Term $\underline{\theta}_{r\alpha}(1)$

$\underline{\theta}_{r\alpha}(1)$ represents source term for species α in the field r. For gas phase $\underline{\theta}_{r\alpha}(1)$ comes from homogeneous chemical reactions in the gas phase

$$\underline{\theta}_{r\alpha}(1) = \sum_i \nu_{i\alpha} M_\alpha \underline{\epsilon}_g \dot{\underline{R}}'''_{gi} \tag{2.111}$$

where i means gas phase reactions and reaction rate for reaction i in gas phase is

$$\dot{\underline{R}}'''_{gi} = \frac{t,V_t \langle \epsilon_g \dot{R}'''_{gi} \rangle}{\underline{\epsilon}_g} \tag{2.112}$$

For solid field r, $\underline{\theta}_{r\alpha}(1)$ is due to reactions in field r and due to field limit transfer rate

$$\underline{\theta}_{r\alpha}(1) = \sum_i \nu_{i\alpha} M_\alpha \underline{\epsilon}_r \dot{\underline{R}}'''_{ri} + \underline{J}^+_{ri\alpha}(1) - \underline{J}^-_{ri\alpha}(1) \tag{2.113}$$

where $\underline{J}^+_{ri\alpha}(1)$ and $\underline{J}^-_{ri\alpha}(1)$ may be obtained from equation (2.102) and (2.103)

Term $\underline{I}^s_r(1)$

$\underline{I}^s_r(1)$ represents total mass transfer through field

interface. Mathematical form for $\underline{I}^{s}_{r}(1)$ is similar to equation (2.108)

$$\underline{I}^{s}_{r}(1) = {}^{t}_{<}{}^{A}_{rs}\langle i^{s}_{r}\rangle_{r} a\rangle_{rs} \ , \tag{2.114}$$

where

$$i^{s}_{r} = \rho_{r}(v_{r}-v_{brs}) \tag{2.115}$$

If there is negligible time correlation between ${}^{A}_{rs}\langle i^{s}_{r}\rangle_{r}$ and a_{rs}, then

$$\underline{I}^{s}_{r}(1) = \underline{i}^{s}_{r} a_{rs} \tag{2.116}$$

Term $\underline{\theta}_{r}(1)$

$\underline{\theta}_{r}(1)$ is mass source for field r. For gas $\underline{\theta}_{r}(1) = 0$ and for solid fields $\underline{\theta}_{r}(1)$ takes into consideration field limit transfer rates

$$\underline{\theta}_{r}(1) = \underline{J}^{+}_{ri}(1) - \underline{J}^{-}_{ri}(1) \tag{2.117}$$

2.8.2 Momentum balance

Momentum balance is obtained when substituting $\psi = \mathbf{v}$ and $\phi = T$ into general conservation equations (2.91) and (2.92), which leads into the following forms

Gas

$$\int_{V_T} \frac{d}{dt} (\underline{\epsilon}_g \rho_g \underline{v}_g)\, dV + \int_{A_T} \underline{\epsilon}_g \rho_g \underline{v}_g \underline{v}_g \cdot n_T dA + \int_{A_T} \underline{C}_g(\mathbf{v}) \cdot n_T dA$$

$$+ \int_{V_T} \sum_{s \neq g} \underline{I}_g^s(\mathbf{v})\, dV - \int_{V_T} \sum_{s \neq g} \underline{T}_{gr}^I dV - \int_{V_T} \underline{\epsilon}_g \nabla \cdot \underline{T}_{gg} dV - \int_{V_T} \underline{\theta}_g(\mathbf{v})\, dV = 0 \qquad (2.118)$$

Solid field

$$\int_{V_T} \frac{d}{dt} (\underline{\epsilon}_r \rho_r \underline{v}_r)\, dV + \int_{A_T} \underline{\epsilon}_r \rho_r \underline{v}_r \underline{v}_r \cdot n_T dA + \int_{A_T} \underline{C}_r(\mathbf{v}) \cdot n_T dA$$

$$+ \int_{V_T} \sum_{s \neq r} \underline{I}_r^s(\mathbf{v})\, dV + \int_{V_T} \underline{T}_{gr}^I dV - \int_{V_T} \underline{\epsilon}_r \nabla \cdot \underline{T}_{gr} dV - \int_{V_T} \underline{\theta}_r(\mathbf{v})\, dV$$

$$- \int_{V_T} \sum_{s \neq r,g} \underline{T}^V_{rs} dV + \int_{A_T} \sum_{s \neq g} \underline{T}^A_{rs} \cdot n_T dA = 0 \qquad (2.119)$$

where terms are presented as follows

Term $\underline{C}_r(\mathbf{v})$, r represents here both gas and solid

$\underline{C}_r(\mathbf{v})$ is the dispersion term, which can be considered as turbulent inertial stress due to random exchange

$$\underline{C}_r(\mathbf{v}) = {}^{t,S_t}\langle \rho \tilde{\mathbf{v}}_r \tilde{\mathbf{v}}_r \rangle_r \qquad (2.120)$$

For $\underline{C}_r(\mathbf{v})$ there has often been proposed the same model as for the stress tensor of a Newtonian fluid [Jackson 1971, Roco and Shook 1985]. Applying the same assumption to present notation and assuming bulk viscosity negligible, $\underline{C}_r(\mathbf{v})$ can be written in the form

$$\underline{C}_r(\mathbf{v}) = \underline{\epsilon}_r \rho_r \varepsilon_r \nabla \cdot \underline{\mathbf{v}}_r \qquad (2.121)$$

where ε_r is turbulent diffusion coefficient

This kind of model has been used in various applications [Pritchett et al. 1978, Roco and Shook 1985, Homsy 1979]. In suspension rheology there has also been presented various forms for shear viscosity of mixture [Brady and Bossis 1985, Kulshreshtha

1985, Ishii and Chawla 1979]. At the moment it seems, however, that there exists very scanty theoretical and especially experimental knowledge on the subject of fluidized beds and thus all the models for the dispersion term are more or less based on intuition.

Two-equation k-ε-model has been proposed with large number of correlation terms [Elghobashi and Abou-Arab 1983] for two-phase time averaged flow equations. Also, to some degree, a more pragmatic approach has been used by Berker and Tulig (1986) in order to model a minimum number of turbulence correlation terms.

One way of avoiding the difficulty to model the fluctuation average term has been an assumption that the importance of the term is negligible. This assumption has been widely used for gas phase in fluidized bed model solutions. For solid phase, too, most of the models ignore the corresponding term. The assumption is supported by the results of Padhye (1985), who reported that changes in the parameter values of the term did not have appreciable effects on the calculated results of his application.

Term $\underline{I}_r^s(\mathbf{v})$

$\underline{I}_r^s(\mathbf{v})$ represents momentum transfer due to convection between different fields. Mathematical form is (equation 2.80)

$$\underline{I}_r^s(\mathbf{v}) = t_< \; A_{rs} <\rho \mathbf{v}_r (\mathbf{v}_r - \mathbf{v}_{brs})>_r a_{rs}> \qquad (2.122)$$

Assuming correlations between i_r, v_r^s and a_{rs} negligible we may write

$$\underline{I}_r^s(v) = \underline{i}_r^s \, \underline{v}_r^s \, \underline{a}_{rs} \tag{2.123}$$

where $\underline{v}_r^s$ is the velocity on the field boundary between fields r and s. If convective momentum transfer between the solid fields is assumed negligible, there is only gas-solid convective momentum exchange and for $\underline{v}_r^s$ it may be written

$$\underline{v}_r^s = \begin{cases} \underline{v}_r, \text{ if r is solid} \\ \underline{v}_s. \text{ if s is solid} \end{cases} \tag{2.124}$$

One way of modeling convective momentum transfer between the fields is to include it into gas-solid momentum drag, which is presented below. Some additional parameters and function forms are then required for consideration of mass transfer.

Term $\underline{T}_{gr}^I$

$\underline{T}_{gr}^I$ is gas-solid momentum drag term, which is due to rapidly varying stress between fields g and r.

Equation (2.85) gives

$$\underline{T}^{I}_{gr} = {}^{t}\langle {}^{A_{gr}}(\overset{\circ}{T}_{g})a_{gr}\rangle \tag{2.125}$$

or from equation (2.27), applying time averaging

$$\underline{T}^{I}_{gr} = {}^{t}\langle \int_{A_{gr}} \overset{\circ}{T}_{g} \cdot n_{R} \, dA \rangle \tag{2.126}$$

There are numerous correlations for gas-particle drag term, which may differ from each other considerably due to different experimental arrangements, conditions and measuring scales. In fluidized bed applications, care must be taken not to get confused with applying models based on homogeneous or non-homogeneous experiments. For example, for aggregate fluidized beds there could be a small length scale where flow may be considered homogeneous and respective models may be applied to model flow locally. On the other hand, macroscopic models based e.g. on reactor area averaging (1-dimensional models) would give meaningless results, if homogeneous submodels were applied to it. In this chapter it is assumed that averaging length scale is such that flow condition may be considered locally homogeneous. In chapter 3 non-homogeneous situations will be discussed.

For a single spherical particle there has often been used correlation proposed by Schiller and Naumann[1]

$$\underline{\underline{T}}^{I}_{gr} = - C_{Dr} 0.5\ \rho(v_g - v_r)|v_g - v_r| \frac{\pi\ d_{pr}^2}{4} \frac{\epsilon_r}{V_{pr}} \quad , \tag{2.127}$$

where

$$C_{Dr} = \begin{cases} \dfrac{24}{Re_p}\left(1 + 0.15 Re_p^{0.687}\right) & , Re_p < 1000 \\ 0.44 & , Re_p \geq 1000 \end{cases} \tag{2.128}$$

$$Re_p = \frac{\epsilon_g \rho_g d_p |v_g - v_r|}{\mu_g} \tag{2.129}$$

Richardson-Zaki correlation has been widely used [Arastoopour et al. 1982, Ettenhadieh 1982, Adewumi 1985, Syamlal 1985] for a group of particles, when gas void fraction has been more than 0.8.

$$\underline{\underline{T}}^{I}_{gr} = - \frac{3}{4} C_{Dr} \rho_g (v_g - v_r)|v_g - v_r| \frac{\epsilon_r}{d_{pr} \epsilon_g^{2.67} \omega_r} \quad , \epsilon_g > 0.8 \tag{2.130}$$

For porosities less than 0.8 Ergun equation is often used [Kunii and Levenspiel 1984, Ettenhadieh 1982, Syamlal 1985], which holds

---

[1] cited e.g. in [Arastoopour et al. 1982a]

for particulate fluidized beds

$$\underline{T}^{I}_{gr} = -\left[150\ \frac{(1-\epsilon_g)^2\mu_g}{\epsilon_g(d_{pr}\omega_r)^2} + 1.75\ \frac{\rho_g|v_g-v_r|(1-\epsilon_g)}{\omega_r d_{pr}}\right](v_g-v_r) \quad (2.131)$$

Ishii and Chawla (1979) have presented a model based on mixture viscosity model. Their drag coefficient may be presented as follows

$$C_{Dr} = \frac{24}{Re_{rm}}\left(1 + 0.1Re_{rm}^{0.75}\right) \quad , Re_{rm} < 1000 \quad (2.132)$$

$$C_{Dr} = 0.45\left\{\frac{1 + 17.67\,[f(\epsilon_r)]^{6/7}}{18.67\,f(\epsilon_r)}\right\}^2 \quad , Re_{rm} > 1000 \quad (2.133)$$

where

$$f(\epsilon_r) = (1-\epsilon_r)^{0.5}\left(1 - \frac{\epsilon_r}{\epsilon_{rmax}}\right)^{1.55} \quad (2.134)$$

$$Re_{rm} = \frac{\rho_g d_p|v_g - v_r|}{\mu_m} \quad (2.135)$$

ϵ_{rmax} is maximum value for solid fraction

Term $\nabla\cdot\underline{\underline{T}}_{gr}$

Term represents gas stress term, which is defined in equation (2.87)

$$\nabla\cdot\underline{\underline{T}}_{gr} = \frac{{}^{t}\langle\epsilon_r \nabla\cdot {}^{V_g}\langle T_g\rangle_g\rangle}{\underline{\epsilon}_r} \qquad (2.136)$$

or if time correlation between ϵ_r and $\nabla\cdot{}^{V_g}\langle T_g\rangle_g$ may be assumed negligible and ${}^{t}\langle\epsilon_r\rangle$ equal to $\underline{\epsilon}_r$

$$\nabla\cdot\underline{\underline{T}}_{gr} = \nabla\cdot {}^{t,V_g}\langle\underline{\underline{T}}_g\rangle \qquad (2.137)$$

A stress tensor form of a Newtonian fluid has been proposed for stress term [Jackson 1971, Anderson and Jackson 1967, Murray 1967]. However, the viscous part of the stress tensor is usually assumed small and thus ignored in the fluidized bed model applications. The only part of the stress term which is taken into consideration is the one due to pressure.

Term $\underline{\theta}_r(v)$

$\underline{\theta}_r(v)$ is momentum source term due to gravitation and for solid fields also due to momentum exchange through field limits. For gas phase

$$\underline{\theta}_g(v) = \underline{\epsilon}_g \, \rho_g \, g \tag{2.138}$$

and for solid field r

$$\underline{\theta}_r(v) = \underline{\epsilon}_r \, \rho_r \, g + \underline{J}^{+}_{ri}(v) - \underline{J}^{-}_{ri}(v) \tag{2.139}$$

Term $\underline{T}^{V}_{rs}$

$\underline{T}^{V}_{rs}$ may be interpreted as momentum interaction between solid fields r and s in volume V_T. Fields r and s may not be the same. Equation (2.88) gives

$$\underline{T}^{V}_{rs} = t_{<} \, A_{rs} \langle T_r \rangle_r a_{rs} \rangle \tag{2.140}$$

For collisional momentum transfer between particles r and particles s has been presented models by Soo (1967) and Nakamura and Capes (1976). Syamlal (1985) has derived an expression for momentum exchange in dense bed. His equation reduces into dilute case equation given by Nakamura and Capes, when solid fraction tends to zero. Syamlal's model is

$$\underset{-rs}{I^{V}} = -\frac{(1+e)\,\epsilon_r\epsilon_s\rho_r\rho_s(d_{pr}+d_{ps})^2\left[1+3\left(\frac{\epsilon^*_{rs}}{\epsilon_r+\epsilon_s}\right)^{1/3}\right]}{2(d_{pr}^3\rho_r+d_{ps}^3\rho_s)\left[\left(\frac{\epsilon^*_{rs}}{\epsilon_r+\epsilon_s}\right)^{1/3}-1\right]}\,|v_r-v_s|(v_r-v_s) \qquad (2.141)$$

where

ϵ^*_{rs} is the maximum solid volume fraction of a random close-packed structure.

The coefficient of restitution e has values from 0 to 1, if collisions between the particles are plastic or elastic, respectively.

Recently Syamlal [Syamlal 1987] has derived an expression for the particle-particle drag based on the kinetic theory of dense gases. He has also compared his model to experimental data and he found that a part of the results was predicted reasonably well, when he assumed that some disagreement was due to the absence of granular stress in the model.

Some empirical correlations for a limited experimental range have been also suggested by Arastoopour et al. 1982a and Arastoopour and Cutchin 1985.

Term $\underline{\underline{T}}^A_{rs}$

$\underline{\underline{T}}^A_{rs}$ accounts for the flux due to solid-solid interactions on particles, which are on the boundary A_T subtracted by gas interaction on respective particles. $\underline{\underline{T}}^A_{rs}$ is defined by equation

$$t_< \int_{A_{Bs}} (T_s - T_g) \cdot n_R dA > = \int_{A_T} \underline{\underline{T}}^A_{rs} \cdot n_T dA \qquad (2.142)$$

For a fixed bed of only one particle size, where all velocities are zero, solid field momentum equation reduces to

$$\int_{V_T} \underline{\epsilon}_r \, \rho_r g \, dV - \int_{A_T} \underline{\underline{T}}^A_{rs} \cdot n_T dA = 0 \qquad (2.143)$$

From equation (2.143) it is seen, that $\underline{\underline{T}}^A_{rs}$ is the only force opposing gravitational force and thus preventing particles from collapsing into too high solid fraction. In order to avoid collapsing and to make equation system well-posed [Lyczkowski et - al. 1982] an assumption has been presented that for a Newtonian solid flow a normal component stress gradient is presented with the aid of modulus of elasticity, $G(\epsilon_g)$ [Rietema and Mutsers 1973]. In one dimension the gradient for normal stress is

$$\frac{\partial T_N}{\partial y} = G(\epsilon_g) \frac{\partial \epsilon_g}{\partial y} \qquad (2.144)$$

where

$$G(\epsilon_g) = \frac{\partial T_N}{\partial \epsilon_g} \qquad (2.145)$$

Expression for $G(\epsilon_g)$ has been given by Ettenhadieh (1982) fitted to the experimental data of Rietema and Mutsers

$$G(\epsilon_g) = 10^{(-8.76\epsilon_g + 5.43)} \ , \ \frac{N}{m^2} \qquad (2.146)$$

For multiparticle case Syamlal (1985) has suggested

$$\frac{\partial T_{Nr}}{\partial y} = \epsilon_r G(\epsilon_g) \frac{\partial \epsilon_g}{\partial y} \quad , \quad \text{where} \qquad (2.147)$$

$$G(\epsilon_g) = - g_1 e^{[g_2(\epsilon^* - \epsilon_g)]} \qquad (2.148)$$

with parameter values

$$g_1 = 1.5 \cdot 10^{-3} \frac{N}{m^2}$$

$$g_2 = 500$$

$\epsilon^* \approx 0.4$

SSS-group has used solid pressure of the form [Pritchett et. al. 1978, Padhye 1985]

$$G(\epsilon_g) = G(\epsilon_{gmin}) - A^2(\epsilon_{gmin} - \epsilon_g) \ , \ \epsilon_g < \epsilon_{gmin} \qquad (2.149)$$

$$G(\epsilon_g) = 0 \qquad , \ \epsilon_g \geq \epsilon_{gmin} \qquad (2.150)$$

where A is a large number. Equation is stated necessary to avoid slumping in non-fluidized beds. Rogers and Padhye [Padhye 1985] have formulated a numerical method for calculating Newtonian normal stress tensor for solids. Their formulation is based on the molecular dynamics theory applied to solid particles.

Expressions in equations (2.146), (2.148) and (2.149) may be regarded more as mathematical terms to avoid undesirable effects rather than as real physical terms. The physical meaning of the term is illustrated e.g. by applying the model in equation (2.119) to stable fixed bed with zero gas and solid velocities leading to equality

$$- \epsilon_r \rho_r g + G(\epsilon_g) \frac{\partial \epsilon_g}{\partial y} = 0 \ , \qquad (2.151)$$

which gives very high values for the modulus of elasticity for an uniformly packed bed, when the gradient of volume fraction is small.

2.8.3 Energy balance

Fluidized bed applications may usually be assumed isobaric, when energy conservation is considered. Thus the general equations are applied to thermal energy balance assuming isobaric case, which gives in terms of enthalpy

Gas

$$\int_{V_T} \frac{d}{dt} (\underline{\epsilon}_g \rho_g \underline{h}_g)\, dV + \int_{A_T} \underline{\epsilon}_g \rho_g \underline{h}_g \underline{v}_g \cdot \mathbf{n}_T dA + \int_{A_T} \underline{C}_g(\mathbf{h}) \cdot \mathbf{n}_T dA$$

$$+ \int_{V_T} \sum_{s \neq g} \underline{I}_g^s(\mathbf{h})\, dV - \int_{V_T} \sum_{s \neq g} \underline{q}_{gr}^I dV - \int_{V_T} \underline{\epsilon}_g \nabla \cdot \underline{q}_{gg} dV - \int_{V_T} \underline{\theta}_g(\mathbf{h})\, dV = 0 \qquad (2.152)$$

Solid field

$$\int_{V_T} \frac{d}{dt} (\underline{\epsilon}_r \underline{\rho}_r \underline{h}_r)\, dV + \int_{A_T} \underline{\epsilon}_r \underline{\rho}_r \underline{h}_r \underline{v}_r \cdot n_T dA + \int_{A_T} \underline{C}_r(h) \cdot n_T dA$$

$$+ \int_{V_T} \sum_{s \neq r} \underline{I}_r^s(h)\, dV + \int_{V_T} \underline{q}_{cr}^I dV - \int_{V_T} \underline{\epsilon}_r \nabla \cdot \underline{q}_{cr} dV - \int_{V_T} \underline{\theta}_r(h)\, dV \qquad (2.153)$$

$$- \int_{V_T} \sum_{s \neq r,c} \underline{q}_{rs}^V dV + \int_{A_T} \sum_{s \neq c} \underline{q}_{rs}^A \cdot n_T dA = 0$$

The energy equation has been applied in computer simulations made by Systems, Science and Software (SSS) [Schneyer 1981, Pritchett et. al. 1978], JAYCOR [Chan et al. 1982, Klein et al. 1983] and Illinois Institute of Technology [Syamlal 1985, Syamlal and Gidaspow 1985, Gidaspow 1986]. SSS and JAYCOR used a mixture energy equation, which would then be written in differential form and with isobaric and negligible viscous terms

$$\frac{D(\sum_r \epsilon_r \rho_r h_r)}{Dt} = \nabla \cdot (\lambda_m \nabla T) + \theta(h) \qquad (2.154)$$

where λ_m is mixture conductivity

In calculations made in IIT, equations were similar to K-FIX computer code [Rivard and Torrey 1977], which may be written with previous assumptions in this chapter for gas or solid

$$\frac{D\ (\epsilon_r \rho_r h_r)}{Dt} = \nabla\cdot(\epsilon_r \lambda_r \nabla T_r) + K_v(T_s - T_r) \qquad (2.155)$$

When comparing equations (2.154) and (2.155) with (2.152) and (2.153) it is seen that the latter ones are greatly simplified forms. In equation (2.155) the two terms on the left may be interpreted as follows [Syamlal and Gidaspow 1985]

$$\underline{\nabla\cdot(\epsilon_r \lambda_r \nabla T_r)}$$

The term represents heat transfer within a field. For particle-particle transfer it is caused by contact conductance, conduction through the thin layer of gas sticking to the particles, and radiation. For solid field there has not been found any work dealing with the constitutive relation for λ_r, and Syamlal (1985) has used effective radial thermal conductivity of solids obtained from a packed bed correlation.

$K_v(T_s - T_r)$

The term represents the interphase heat transfer term, which is primarily due to transfer through a gas film surrounding the individual particle. K_v has been calculated from the dimensionless correlation, which is applicable for fluidized bed interphase heat transfer.

According to IIT calculations, simulations with equation (2.155) led to heat transfer values in reasonably close agreement with the experiment, although their equation seems to be strongly simplified.

As can be seen from the previous discussion, there is a very small amount of work done to model the terms in energy equation and there are only few applications found, in which energy balance has been considered in multidimensional fluidized bed simulations. Thus, at the moment it does not seem possible to obtain good quantitative models for unknown terms in energy equation until there is more experimental knowledge of the subject. However, even with rough approximations, the total result may be acceptable, if hydrodynamic model is good enough. Intuitively, many of the terms in energy balance may be modeled respectively to corresponding terms in momentum equations. But because there is so scanty experimental knowledge on constitutive equations for energy

balance, the following contains only a list of the different terms in thermal energy equation with their physical interpretation.

$$\underline{C}_r(h) = {}^{t,S}_{t}\langle \rho \tilde{\mathbf{v}}_r \tilde{h}_r \rangle_r \qquad (2.156)$$

- the dispersion term for enthalpy due to local nonhomogeneities in space and time

$$\underline{I}^s_r(h) = {}^{t}_{<}{}^{A_{rs}}\langle \rho_r h_r (\mathbf{v}_r - \mathbf{v}_{brs}) \rangle_r \, a_{rs} \rangle \qquad (2.157)$$

- thermal energy transfer due to convection between different fields

$$q^I_{gs} = {}^{t}_{<}{}^{A_{gr}}(\overset{\circ}{q}_g) \, a_{gr} \rangle \qquad (2.158)$$

- gas-solid interphase heat transfer due to heat flux varying rapidly in space. Term $K_v(T_g - T_r)$ in equation (2.155) is interpreted roughly in the same way and intuitively it looks like similar models may be used for both of the terms.

$$\underline{\epsilon}_r \nabla \cdot \underline{q}_{gr} = {}^{t}\langle \epsilon_r \nabla \cdot {}^{V_r}\langle \mathbf{q}_g \rangle_g \rangle \qquad (2.159)$$

- gas heat flux term

$\underline{\theta}_r(h)$

- source term including e.g. radiation, viscous dissipation and thermal energy exchange through field limits

$$\underline{q}^V_{rs} = t_< {}^{A}_{rs} <q_r> a_{rs}> \tag{2.160}$$

- heat conduction between solid fields r and s ($r \neq s$)

$$\int_{A_T} \underline{q}^A_{rs} \cdot n_T dA = t_< \int_{A_{gr}} (q_s - q_g) \cdot n_R dA > \tag{2.161}$$

- heat flux due to solid-solid interactions on particles which are on the boundary A_T subtracted by gas phase heat flux

3. MACROSCOPIC MULTIPHASE EQUATIONS

In chapter 2 the balance equations were derived averaged in time and space. The main purpose of the averaging was to obtain continuum model from non-continuous flow written in terms of defined and measurable quantities. The usage of the resulting equations may be considered comparable to e.g. single-phase turbulent flow equations. Reduction in mathematical complexity of the equations was achieved by the aid of averaging definitions for averaging integrals. But still the solution of the equations for a flow case with continuum equations is difficult even for supercomputers available today.

Certain means have been derived in single-phase theory to make flow equations more simple, also applicable in everyday engineering. As an example, fluid flow in a pipe has been simplified by averaging over pipe cross area. In this chapter, a way to treat the continuum equations in multifield flow by macroscopic space averaging is presented and averaged equations are derived. The main purpose is to obtain a general equation structure, which is suitable for different engineering applications and is simple enough for practical calculations and which can be used as a tool in construction of different level models.

In multiphase cases macroscopic averaging has earlier been applied to liquid based two-phase cases [Hughes et al. 1976, Wallis

1969] and to porous media [Bachmat and Bear 1986a, 1986b], where some empirical data has been obtained for equation closure system. For 1-dimensional or multidimensional gas-solid fluidized bed models there has not been systematic macroscopic averaging, and experimental parameters have been evaluated mainly based on more intuitive hydrodynamic models.

In this chapter macroscopic averaging is formulated with integral balances, which as a special case reduce into macroscopic averaged differential equations. Integral formulation can be also applied, when different averaging spaces are required in the same application.

3.1 MACROSCOPIC AVERAGING FOR SPACE/TIME-AVERAGED EQUATIONS

In the following the fixed macroscopic control volume is considered, the boundaries of which are divided into different parts, which may be open or closed surfaces. In this context separate macroscopic time averaging has not been applied.

Macroscopic volume and area averages are defined as follows

$$ {}^{V_T}\langle \underline{\psi}_C \rangle = \frac{1}{V_T} \int_{V_T} \underline{\psi}_C dV \qquad (3.1) $$

$$ {}^{A_T}\langle \underline{\psi}_C \rangle = \frac{1}{A_T} \int_{A_T} \underline{\psi}_C dA \qquad (3.2) $$

Unit normal vector is assumed to be constant on each macroscopic surface and thus we can write

$$\int_{A_T} \psi \cdot \underline{n}_T dA = {}^{A_T}\langle \psi \rangle \cdot \underline{n}_T \, A_T \tag{3.3}$$

Substituting macroscopic averaging definitions into general conservation equations (2.91) and (2.92) and applying form (2.42) for the flux term in continuum equation we may write

Continuum

$$\frac{d}{dt}{}^{V_T}\langle \rho_c^{\epsilon} \underline{\psi}_c \rangle \, V_T + \sum_i {}^{A_{Ti}}\langle \rho_c^{\epsilon} \underline{\psi}_c \underline{v}_c \rangle \cdot \underline{n}_{Ti} A_{Ti} + \sum_i {}^{A_{Ti}}\langle \underline{C}_c(\psi) \rangle \cdot \underline{n}_{Ti} A_{Ti}$$

$$+ \sum_{s \neq c} {}^{V_T}\langle \underline{I}_c^s(\psi) \rangle \, V_T - \sum_{s \neq c} {}^{V_T}\langle \underline{\phi}_{cs}^I \rangle \, V_T + \sum_{s \neq c} {}^{V_T}\langle \underline{\epsilon}_s \nabla \cdot \underline{\phi}_{cs} \rangle \, V_T$$

$$- \sum_i {}^{A_{Ti}}\langle \underline{\phi}_c \rangle \cdot \underline{n}_{Ti} A_{Ti} - {}^{V_T}\langle \underline{\theta}_c(\psi) \rangle \, V_T = 0 \tag{3.4}$$

Solid field

$$\frac{d}{dt}{}^{V_T}\langle \rho_r^{\epsilon} \underline{\psi}_r \rangle \, V_T + \sum_i {}^{A_{Ti}}\langle \rho_r^{\epsilon} \underline{\psi}_r \underline{v}_r \rangle \cdot \underline{n}_{Ti} A_{Ti} + \sum_i {}^{A_{Ti}}\langle \underline{C}_r(\psi) \rangle \cdot \underline{n}_{Ti} A_{Ti}$$

$$+ \sum_{s\neq r} {}^{V_T}\langle \underline{I}_r^s(\psi)\rangle\, V_T + {}^{V_T}\langle \underline{\phi}_{cr}^I\rangle\, V_T - {}^{V_T}\langle \underline{\epsilon}_r \nabla\cdot\underline{\phi}_{cr}\rangle\, V_T - {}^{V_T}\langle \underline{\theta}_r(\psi)\rangle\, V_T$$

$$- \sum_{s\neq r,c} {}^{V_T}\langle \underline{\phi}_{rs}^V\rangle\, V_T + \sum_i \sum_{s\neq c} {}^{V_T}\langle \underline{\phi}_{rs}^A\rangle\cdot\underline{n}_{Ti} A_{Ti} = 0 \qquad (3.5)$$

In equation (3.4) a new definition has been applied for continuum flux term

$$\underline{\phi}_c = {}^{t}\langle {}^{V_c}\langle \phi_c\rangle_c\rangle \qquad (3.6)$$

In the above equations there is a similar problem to microscopic averaged equations (2.70) and (2.71) in section 2.6 - in the equation system there are more unknown variables than equations. Thus there is a need to replace averages of variable functions by functions of averaged variables and to obtain additional relations for macroscopic volume- and area-averaged variables. It depends much on an application how the total equation closure is reasonable to build up, and thus in this context no general equation closure is derived. The first and the second terms in equations (3.4) and (3.5) have the same function form regardless of an application and in the following section is presented what effect the averaging choices have on the modeling of them.

3.2 MACROSCOPIC SPACE, MASS AND MOMENTUM AVERAGING

Density may be averaged over space in macroscopic averaging. For a general quantity there is also other definitions possible instead of pure space averaging. In this section is studied the effect of different definitions on equation closure problem. Respective forms, which are considered here are illustrated with terms

$$\varrho_r^{\epsilon}\underline{\psi}_r \qquad \text{and} \qquad \varrho_r^{\epsilon}\underline{v}_r\underline{\psi}_r$$

These terms are essential in balance equations representing rate of change and convection terms.

Space-averaging

In space-averaging a similar definition is used for all different variables by using pure space-averaged values. It leads to different turbulent extra products for both of the terms, which are considered here.

Definitions:

$$^{S_T}\langle\underline{\psi}_r\rangle = \frac{1}{S_T}\int_{S_T}\underline{\psi}_r\cdot dS \tag{3.7}$$

$$\psi_r = {}^{S_T}\langle \psi_r \rangle + {}^{S_T}\langle \tilde{\psi}_r \rangle \qquad (3.8)$$

Terms:

$$S_T\langle \rho_r^{\epsilon} \psi_r \rangle = S_T\langle \rho_r^{\epsilon} \rangle \; S_T\langle \psi_r \rangle + S_T\langle \; S_T\langle \tilde{\rho}_r^{\epsilon} \rangle \; S_T\langle \tilde{\psi}_r \rangle \rangle \qquad (3.9)$$

$$S_T\langle \rho_r^{\epsilon} \psi_r \underline{v}_r \rangle = S_T\langle \rho_r^{\epsilon} \rangle \; S_T\langle \psi_r \rangle \; S_T\langle \underline{v}_r \rangle + S_T\langle \rho_r^{\epsilon} \; S_T\langle \tilde{\psi}_r \rangle \; S_T\langle \tilde{\underline{v}}_r \rangle \rangle$$

$$+ S_T\langle \psi_r \rangle \; S_T\langle \; S_T\langle \tilde{\rho}_r^{\epsilon} \rangle \; S_T\langle \tilde{\underline{v}}_r \rangle \rangle + S_T\langle \underline{v}_r \rangle \; S_T\langle \; S_T\langle \tilde{\rho}_r^{\epsilon} \rangle \; S_T\langle \tilde{\psi}_r \rangle \rangle \qquad (3.10)$$

Mass averaging

The mass averaging is defined in order to make the turbulent product term disappear in density-variable product. Thus e.g. a mass flow rate can be presented by simple product of density and velocity. This kind of averaging has also been used in microscopic gas phase turbulence theory for time-averaged equations as discussed in section 2.3.2 (Favre-averaging).

Definitions:

$$S_{T<\varrho_r^{\epsilon}\underline{\psi}_r>} = S_{T<\varrho_r^{\epsilon}>}{}^{\rho,}S_{T<\underline{\psi}_r>} \tag{3.11}$$

$$\underline{\psi}_r = {}^{\rho,}S_{T<\underline{\psi}_r>} + {}^{\rho,}S_{T<\tilde{\underline{\psi}}_r>} \tag{3.12}$$

Terms:

$$S_{T<\varrho_r^{\epsilon}\underline{\psi}_r>} = S_{T<\varrho_r^{\epsilon}>}{}^{\rho,}S_{T<\underline{\psi}_r>} \tag{3.13}$$

$$S_{T<\varrho_r^{\epsilon}\underline{\psi}_r\underline{v}_r>} = S_{T<\varrho_r^{\epsilon}>}{}^{\rho,}S_{T<\underline{\psi}_r>}{}^{\rho,}S_{T<\underline{v}_r>} + S_{T<\varrho_r^{\epsilon}}{}^{\rho,}S_{T<\tilde{\underline{\psi}}_r>}{}^{\rho,}S_{T<\tilde{\underline{v}}_r>>} \tag{3.14}$$

Momentum averaging

The reason for momentum averaging is similar to mass averaging above, but convection term is used as an averaging basis.

Definitions:

$$S_{T<\varrho_r^{\epsilon}\underline{\psi}_r\underline{v}_r>} = S_{T<\varrho_r^{\epsilon}>}{}^{v,}S_{T<\underline{\psi}_r>}{}^{v,}S_{T<\underline{v}_r>} \tag{3.15}$$

$$\underline{\psi}_r = {}^{v,S_T}\langle \underline{\psi}_r \rangle + {}^{v,S_T}\langle \tilde{\underline{\psi}}_r \rangle \tag{3.16}$$

Terms:

$$S_t\langle \varrho_r^{\epsilon} \underline{\psi}_r \rangle = {}^{S_T}\langle \varrho_r^{\epsilon} \rangle \, {}^{v,S_T}\langle \underline{\psi}_r \rangle + {}^{S_T}\langle \varrho_r^{\epsilon} \, {}^{v,S_T}\langle \tilde{\underline{\psi}}_r \rangle \rangle \tag{3.17}$$

$$S_T\langle \varrho_r^{\epsilon} \underline{\psi}_r \underline{v}_r \rangle = {}^{S_T}\langle \varrho_r^{\epsilon} \rangle \, {}^{v,S_T}\langle \underline{\psi}_r \rangle \, {}^{v,S_T}\langle \underline{v}_r \rangle \tag{3.18}$$

The above terms are obtained in the same way as the terms in section 2.6 for microscopic averages. Relations between different velocities may be obtained from equations (3.9), (3.13) and (3.17) by substituting velocity instead of general quantity, which gives

$${}^{\rho,S_T}\langle \underline{v}_r \rangle = {}^{S_T}\langle \underline{v}_r \rangle + \frac{{}^{S_T}\langle \, {}^{S_T}\langle \tilde{\varrho}_r^{\epsilon} \rangle \, {}^{S_T}\langle \tilde{\underline{v}}_r \rangle \rangle}{{}^{S_T}\langle \varrho_r^{\epsilon} \rangle} \tag{3.19}$$

$${}^{v,S_T}\langle \underline{v}_r \rangle = {}^{S_T}\langle \underline{v}_r \rangle + \frac{1}{{}^{S_T}\langle \varrho_r^{\epsilon} \rangle} \left({}^{S_T}\langle \, {}^{S_T}\langle \tilde{\varrho}_r^{\epsilon} \rangle \, {}^{S_T}\langle \tilde{\underline{v}}_r \rangle \rangle - {}^{S_T}\langle \varrho_r^{\epsilon} \, {}^{v,S_T}\langle \tilde{\underline{v}}_r \rangle \rangle \right) \tag{3.20}$$

$${}^{v,S_T}\langle \underline{v}_r \rangle = {}^{\rho,S_T}\langle \underline{v}_r \rangle - \frac{{}^{S_T}\langle \varrho_r^{\epsilon} \, {}^{v,S_T}\langle \tilde{\underline{v}}_r \rangle \rangle}{{}^{S_T}\langle \varrho_r^{\epsilon} \rangle} \tag{3.21}$$

The choice between different definitions depends on a flow application and measurement arrangements. The objective of a choice is to obtain as few extra terms as possible in addition to products of averaged variables and also to have extra terms, which can be expressed as functions of averaged variables. As an example we may compare effects of different definitions for a 1-dimensional application, in which mass balance, momentum balance and one additional general balance are required.

Rate of change and convection terms in equations have the following forms

	rate of change	convection
mass	$V_T<\rho_r^{\epsilon}>$	$A_T<\rho_r \underline{v}_r>$
momentum	$V_T<\rho_r^{\epsilon} \underline{v}_r>$	$A_T<\rho_r^{\epsilon} \underline{v}_r \underline{v}_r>$
general	$V_T<\rho_r^{\epsilon} \psi_r>$	$A_T<\rho_r^{\epsilon} \psi_r \underline{v}_r>$

Applying equations (3.9), (3.10), (3.13), (3.14), (3.17) and (3.18) the number of extra terms in the above terms may be obtained for convection and rate of change terms. These numbers are presented in Table 3.1 for mass, momentum and one general quantity conservation equations.

Table 3.1 The amount of extra terms in mass, momentum and general quantity balance equations

averaging basis	MASS		MOMENTUM		GENERAL	
	change	convect.	change	convect.	change	convect.
space	0	1	1	3	1	3
mass	0	0	0	1	0	1
momentum	0	1	1	0	1	0

Total amount of extra terms for space-, mass- and momentum-averaged variables for one field are 9, 2 and 3 respectively thus mass-averaging leading to the smallest amount. For steady flow case the rate of change terms are negligible and the amount of extra terms is 7, 2 and 1. So, whether the case is steady or unsteady, different averaging procedure leads to a smaller amount of extra terms. In addition to the amount of extra terms, there are also other things to be considered. For example, momentum averaged velocity is not usually as well documented in literature as mass averaged velocity, and finding experimental data to respective equation model is difficult.

Mass, momentum and general balances are presented as an example of using averaged variables. Equations are written for continuum and one solid field applying mass averaged variables. Substitution

of mass averaged definitions into equations (3.4) and (3.5) gives

General balance

Continuum

$$\frac{d}{dt}{}^{V_T}\langle \underline{\rho}_c^{\epsilon} \rangle^{\rho,V_T}\langle \underline{\psi}_c \rangle V_T + \sum_i \left({}^{A_{Ti}}\langle \underline{\rho}_c^{\epsilon} \rangle^{\rho,A_T}\langle \underline{\psi}_c \rangle^{\rho,A_T}\langle \underline{v}_c \rangle \right) \cdot \underline{n}_{Ti} A_{Ti}$$

$$+ \sum_i {}^{A_{Ti}}\langle \underline{C}_c(\psi) \rangle \cdot \underline{n}_{Ti} A_{Ti} + \sum_i {}^{A_{Ti}}\langle \underline{C}_c^T(\psi) \rangle \cdot \underline{n}_{Ti} A_{Ti}$$

$$+ \sum_{s \neq c} {}^{V_T}\langle \underline{I}_c^s(\psi) \rangle V_T - \sum_{s \neq c} {}^{V_T}\langle \underline{\phi}_{cs}^I \rangle V_T + \sum_{s \neq c} {}^{V_T}\langle \underline{\epsilon}_s \nabla \cdot \underline{\phi}_{cs} \rangle V_T \qquad (3.22)$$

$$- \sum_i {}^{A_{Ti}}\langle \underline{\phi}_c \rangle \cdot \underline{n}_{Ti} A_{Ti} - {}^{V_T}\langle \underline{\theta}_c(\psi) \rangle V_T = 0$$

Solid field

$$\frac{d}{dt}{}^{V_T}\langle \underline{\rho}_r^{\epsilon} \rangle^{\rho,V_T}\langle \underline{\psi}_r \rangle V_T + \sum_i \left({}^{A_{Ti}}\langle \underline{\rho}_r^{\epsilon} \rangle^{\rho,A_T}\langle \underline{\psi}_r \rangle^{\rho,A_T}\langle \underline{v}_r \rangle \right) \cdot \underline{n}_{Ti} A_{Ti}$$

$$+ \sum_i {}^{A_{Ti}}\langle \underline{C}_r(\psi) \rangle \cdot \underline{n}_{Ti} A_{Ti} + \sum_i {}^{A_{Ti}}\langle \underline{C}_r^T(\psi) \rangle \cdot \underline{n}_{Ti} A_{Ti} \qquad (3.23)$$

$$+ \sum_{s \neq r} {}^{V_T}\langle \underline{I}_r^s(\psi) \rangle V_T + {}^{V_T}\langle \underline{\phi}_{cr}^I \rangle V_T - {}^{V_T}\langle \underline{\epsilon}_r \nabla \cdot \underline{\phi}_{cr} \rangle V_T$$

$$- {}^{V_T}\langle \underline{\theta}_r(\psi) \rangle V_T - \sum_{s \neq r,c} {}^{V_T}\langle \underline{\phi}^V_{rs} \rangle V_T + \sum_i \sum_{s \neq c} {}^{V_T}\langle \underline{\phi}^A_{rs} \rangle \cdot \underline{n}_{Ti} A_{Ti} = 0$$

Mass and momentum balances may be derived from general balances by substituting respective variables instead of general quantities, which gives following equations

Mass balance

Continuum

$$\frac{d}{dt} {}^{V_T}\langle \underline{\rho}^{\epsilon}_c \rangle V_T + \sum_i {}^{A_{Ti}}\langle \underline{\rho}^{\epsilon}_c \rangle^{\rho, A_{Ti}} \langle \underline{v}_c \rangle \cdot \underline{n}_{Ti} A_{Ti} + \sum_{s \neq c} {}^{V_T}\langle \underline{I}^s_c(1) \rangle V_T = 0 \qquad (3.24)$$

Solid field

$$\frac{d}{dt} {}^{V_T}\langle \underline{\rho}^{\epsilon}_r \rangle V_T + \sum_i {}^{A_{Ti}}\langle \underline{\rho}^{\epsilon}_r \rangle^{\rho, A_{Ti}} \langle \underline{v}_r \rangle \cdot \underline{n}_{Ti} A_{Ti} + \sum_{s \neq c} {}^{V_T}\langle \underline{I}^s_r(1) \rangle V_T$$

$$- \left[{}^{V_T}\langle \underline{J}^+_{ri}(1) \rangle - {}^{V_T}\langle \underline{J}^-_{ri}(1) \rangle \right] V_T = 0 \qquad (3.25)$$

Momentum balance

Continuum

$$\frac{d}{dt}\,{}^{V_T}\langle \underline{\rho}_c^{\epsilon}\rangle^{\rho,V_T}\langle \underline{v}_c\rangle\, V_T + \sum_i \left({}^{A_{Ti}}\langle \underline{\rho}_c^{\epsilon}\rangle^{\rho,A_T}\langle \underline{v}_c\rangle^{\rho,A_T}\langle \underline{v}_c\rangle\right)\cdot \underline{n}_{Ti} A_{Ti}$$

$$+ \sum_i {}^{A_{Ti}}\langle \underline{C}_c(v)\rangle \cdot \underline{n}_{Ti} A_{Ti} \quad + \sum_i {}^{A_{Ti}}\langle \underline{C}_c^T(v)\rangle \cdot \underline{n}_{Ti} A_{Ti}$$

$$+ \sum_{s\neq c} {}^{V_T}\langle \underline{I}_c^s(v)\rangle\, V_T - \sum_{s\neq c} {}^{V_T}\langle \underline{T}_{cr}^I\rangle\, V_T + \sum_{s\neq c} {}^{V_T}\langle \underline{\epsilon}_s \nabla\cdot \underline{T}_{cs}\rangle\, V_T \qquad (3.26)$$

$$- \sum_i {}^{A_{Ti}}\langle \underline{T}_c\rangle \cdot \underline{n}_{Ti} A_{Ti} - {}^{V_T}\langle \underline{\rho}_c^{\epsilon}\rangle\, \underline{g}\, V_T = 0$$

Solid field

$$\frac{d}{dt}\,{}^{V_T}\langle \underline{\rho}_r^{\epsilon}\rangle^{\rho,V_T}\langle \underline{v}_r\rangle\, V_T + \sum_i \left({}^{A_{Ti}}\langle \underline{\rho}_r^{\epsilon}\rangle^{\rho,A_T}\langle \underline{v}_r\rangle^{\rho,A_T}\langle \underline{v}_r\rangle\right)\cdot \underline{n}_{Ti} A_{Ti}$$

$$+ \sum_i {}^{A_{Ti}}\langle \underline{C}_r(v)\rangle \cdot \underline{n}_{Ti} A_{Ti} \quad + \sum_i {}^{A_{Ti}}\langle \underline{C}_r^T(v)\rangle \cdot \underline{n}_{Ti} A_{Ti}$$

$$+ \sum_{s\neq r} {}^{V_T}\langle \underline{I}_r^s(v)\rangle\, V_T + {}^{V_T}\langle \underline{T}_{cr}^I\rangle\, V_T - {}^{V_T}\langle \underline{\epsilon}_r \nabla\cdot \underline{T}_{cr}\rangle\, V_T \qquad (3.27)$$

$$- {}^{V_T}\langle \underline{\rho}_r^{\epsilon}\rangle \underline{g}\, V_T + \left[{}^{V_T}\langle \underline{J}_{ri}^{+}(v)\rangle - {}^{V_T}\langle \underline{J}_{ri}^{-}(v)\rangle\right] V_T - \sum_{s\neq r,c} {}^{V_T}\langle \underline{T}_{rs}^V\rangle\, V_T$$

$$+ \sum_i \sum_{s\neq c} {}^{V_T}\langle \underline{T}_{rs}^A\rangle \cdot \underline{n}_{Ti} A_{Ti} = 0$$

Macroscopic term $\underline{C}_r^T(\psi)$ is defined as follows

$$\underline{C}_r^T(\psi) = {}^{S_T}\langle \varrho_r^{\epsilon} \rangle^{\rho,S_T}\langle \tilde{\psi}_r \rangle^{\rho,S_T}\langle \tilde{\underline{v}}_r \rangle \rangle \qquad (3.28)$$

In equations (3.22)-(3.27) only few terms are written as functions of averaged variables. The rest of the terms must be presented as functions of primary averaged variables in order to close the equation system. Because the form of different terms varies in different applications, it is not reasonable to try to close the system in general level in this connection. In the following section the equations are formulated for a certain application instead of a general case.

3.3 APPLICATION: 1-DIMENSIONAL, NON-REACTIVE FLOW

In this section we apply macroscopic equations to 1-dimensional continuum-solid particles flow case, in which we assume the following:

- cross sectional area of flow geometry is constant
- microscopic dispersion terms $C_g(\psi)$ and $C_r(\psi)$ are negligible and also macroscopic dispersion term $C_g^T(\psi)$ for gas phase is negligible

- there is no mass transfer between the phases or fields
- gas phase viscous terms are negligible excluding the gas-particle drag term
- only vertical direction of flow is considered, gravitation g = -9.81 m/s = g
- gas phase acceleration in momentum balance is negligible
- particle-wall non-convective momentum flux is small
- macroscopic area- and volume-averaged variables are equal
- only steady flow is considered
- material densities for gas and solid are constant
- solid-solid stress term is negligible

For this case only mass and momentum balances are considered.

3.3.1 Mass-averaged form

In 1-dimensional model we apply notation presented in Figure 3.1. Indexes 1 and 2 represent bottom and top surfaces respectively and w means all other walls for control volume.

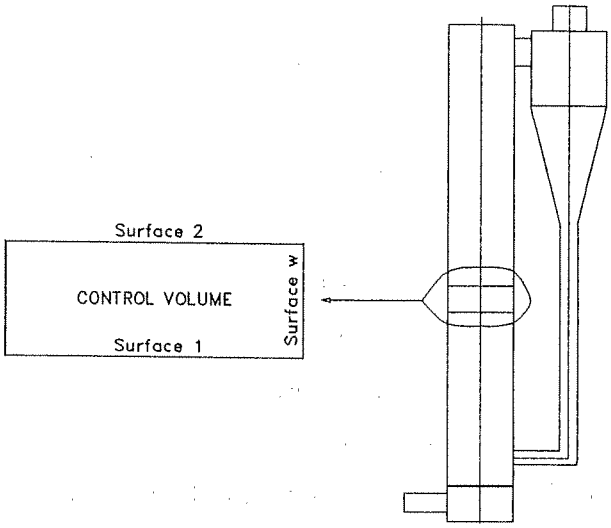

Figure 3.1 Control volume for 1-dimensional application

When the above-mentioned assumptions and macroscopic mass average definitions are applied to mass and momentum balances (3.24) - (3.27), the following equations are obtained

Mass balance

Continuum

$$\sum_{i=1,2} {}^{A_{Ti}}\langle \rho_{ci}^{\epsilon} \rangle^{\rho, A_{Ti}} \langle \underline{v}_{ci} \rangle \cdot \underline{n}_{Ti} A_{Ti} + \underline{I}_{c}^{w}(1)\, V_T = 0 \qquad (3.29)$$

Solid field

$$\sum_{i=1,2} {}^{A_{Ti}}\langle \underline{\rho}_{ri}^{\epsilon} \rangle^{\rho, A_{Ti}}\langle \underline{v}_{ri} \rangle \cdot \underline{n}_{Ti} A_{Ti} + \underline{I}_r^w(1)\, V_T = 0 \qquad (3.30)$$

Momentum balance

Continuum

$$- \sum_{s \neq c} {}^{V_T}\langle \underline{T}_{cs}^I \rangle\, V_T - \sum_{s \neq c} {}^{V_T}\langle \underline{\epsilon}_s \frac{d\underline{p}}{dx} \rangle\, V_T$$

$$+ \sum_{i=1,2} {}^{A_{Ti}}\langle \underline{p}_{ci} \rangle \cdot \underline{n}_{Ti} A_{Ti} - {}^{V_T}\langle \underline{\rho}_c^{\epsilon} \rangle\, g\, V_T = 0 \qquad (3.31)$$

Solid field

$$\sum_{i=1,2} \left({}^{A_{Ti}}\langle \underline{\rho}_{ri}^{\epsilon} \rangle^{\rho, A_T}\langle \underline{v}_{ri} \rangle - {}^{\rho, A_T}\langle \underline{v}_{ri} \rangle \right) \cdot \underline{n}_{Ti} A_{Ti} + \sum_{i=1,2} {}^{A_{Ti}}\langle \underline{C}_{ri}^T(v) \rangle \cdot \underline{n}_{Ti} A_{Ti}$$

$$+ {}^{V_T}\langle \underline{T}_{cr}^I \rangle\, V_T + {}^{V_T}\langle \underline{\epsilon}_r \frac{d\underline{p}}{dx} \rangle\, V_T - {}^{V_T}\langle \underline{\rho}_r^{\epsilon} \rangle g\, V_T - \sum_{s \neq r,c} {}^{V_T}\langle \underline{T}_{rs}^V \rangle\, V_T$$

$$+ \underline{I}_r^w(v)\, V_T = 0 \qquad (3.32)$$

where the following definition has been used for convection through the walls

$$I_r^w(\psi) = {}^{A_{Tw}}\langle \rho_{rw}^{\epsilon} \underline{v}_{rw} \psi_{rw} \rangle \cdot n_{Tw} A_{Tw} \frac{1}{V_T} \tag{3.33}$$

where r is either continuum or solid field and ψ means either velocity (momentum balance) or unit value 1 (mass balance).

In order to simplify notation in equations (3.29)-(3.32) the following definitions are introduced

For macroscopic space average

$$\underline{\psi} = {}^{S_T}\langle \underline{\psi} \rangle \tag{3.34}$$

except for velocity, for which is written

$$\underline{v} = {}^{\rho, S_T}\langle \underline{v} \rangle \tag{3.35}$$

Substitution of definitions (3.34) and (3.35) into equations (3.29)-(3.32) gives

Mass balance

Continuum

$$(\rho_{c2}^{\epsilon} \underline{v}_{c2} - \rho_{c1}^{\epsilon} \underline{v}_{c1}) A_T + \underline{I}_c^w(1) V_T = 0 \tag{3.36}$$

Solid field

$$(\underline{\rho}^{\epsilon}_{r2}\ \underline{v}_{r2} - \underline{\rho}^{\epsilon}_{r1}\ \underline{v}_{r1})\ A_T + \underline{I}^{w}_{r}(1)\ V_T = 0 \qquad (3.37)$$

Momentum balance

Continuum

$$-\sum_{s\neq c}\underline{T}^{I}_{cs}\ V_T - \sum_{s\neq c}\underline{\epsilon}_s \frac{dp}{dx} V_T + (p_2 - p_1)\ A_T - \underline{\rho}^{\epsilon}_{c}\ g\ V_T = 0 \qquad (3.38)$$

Solid field

$$(\underline{\rho}^{\epsilon}_{r2}\ \underline{v}^{2}_{r2} - \underline{\rho}^{\epsilon}_{r1}\ \underline{v}^{2}_{r1})\ A_T + [\underline{C}^{T}_{r2}(v) - \underline{C}^{T}_{r1}(v)]\ A_T + \underline{T}^{I}_{cr}\ V_T$$

$$+ \underline{\epsilon}_r \frac{dp}{dx} V_T - \underline{\rho}^{\epsilon}_{r}\ g\ V_T - \sum_{s\neq r,c}\underline{T}^{V}_{rs}\ V_T + I^{w}_{r}(v)\ V_T = 0 \qquad (3.39)$$

In equations (3.38) and (3.39) it has been assumed that the correlation between fluctuating values of volume fractions and pressure gradient is small, i.e.

$$V_T \langle \underline{\epsilon}_s \frac{dp}{dx} \rangle = V_T \langle \underline{\epsilon}_s \rangle V_T \langle \frac{dp}{dx} \rangle$$

Equations may also be written for differential length to give differential equations

Mass balance

Continuum

$$\frac{d(\underline{\rho}_c^{\epsilon}\ \underline{v}_c)}{dx} + \underline{I}_c^w(1) = 0 \qquad (3.40)$$

Solid field

$$\frac{d(\underline{\rho}_r^{\epsilon}\ \underline{v}_r)}{dx} + \underline{I}_r^w(1) = 0 \qquad (3.41)$$

Momentum balance

Continuum

$$-\sum_{s\neq c} \underline{T}_{cr}^I + \underline{\epsilon}_c \frac{dp}{dx} - \underline{\rho}_c^{\epsilon}\ g = 0 \qquad (3.42)$$

Solid field

$$+\frac{d(\underline{\rho}_r^{\epsilon}\ \underline{v}_r^2)}{dx} + \frac{d\underline{C}_r^T(v)}{dx} + \underline{T}_{cr}^I + \underline{\epsilon}_r \frac{dp}{dx} - \underline{\rho}_r^{\epsilon}\ g - \sum_{s\neq r,c} \underline{T}_{rs}^V - I_r^w(v) = 0 \qquad (3.43)$$

In addition to equations (3.40)-(3.43) we may write

$$\sum_s \underline{\epsilon}_s = 1 \tag{3.44}$$

$$\underline{\rho}_c^{\epsilon} = \underline{\epsilon}_c \, \rho_c \tag{3.45}$$

$$\underline{\rho}_r^{\epsilon} = \underline{\epsilon}_r \, \rho_r \tag{3.46}$$

In the equation system primary variables are

$$\underline{\rho}_c^{\epsilon}, \ \underline{\epsilon}_c, \ \underline{\rho}_r^{\epsilon}, \ \underline{\epsilon}_r, \ \underline{v}_c, \ \underline{v}_r \text{ and } \underline{p}$$

and for each primary variable there is also a corresponding equation among equations (3.40-3.46).

There are still left three additional terms, which must be presented as functions of primary variables in order to close the equation system. These terms are

$$\underline{T}_{cr}^{I}, \ \underline{C}_r^{T}(v) \text{ and } \underline{T}_{rs}^{V}$$

One way of closing the system is to assume the macroscopic average term to be a direct function of macroscopic averaged variables and to try to find an optimal experimental function for it. It will then require experimental data fitting into the

equation system. The macroscopic drag term may be defined e.g. respectively to microscopic Stokes drag term by equation

$$\underline{T}^{I}_{cr} = - \underline{\beta}_{cr} \rho^{\epsilon}_{r} (\underline{v}_{c} - \underline{v}_{r}) \qquad (3.47)$$

In this connection it must be stated, that the choice for the drag submodel above is intuitive and quite arbitrary. Functional forms have been presented scantily in literature for macroscopic drag.

In equation (3.47) the macroscopic drag coefficient may be determined either by using local drag coefficient and stochastic values of local variables (as presented later in this chapter) or it may be determined directly from macroscopic experimental data.

Next we will assume that there is only one homogeneous solid field and we consider region in flow, where there is not flow through walls. So there remains two terms in equation closure, which have to be expressed by primary variables; gas-particle drag and dispersion average term. Balance equations reduce thus into the following form

Mass balance

Continuum

$$\frac{d(\underline{\rho}_c^{\epsilon}\ \underline{v}_c)}{dx} = 0 \qquad (3.48)$$

Solid field

$$\frac{d(\underline{\rho}_r^{\epsilon}\ \underline{v}_r)}{dx} = 0 \qquad (3.49)$$

Momentum balance

Continuum

$$-\ \underline{T}_{cr}^{I} + \underline{\epsilon}_c \frac{dp}{dx} - \underline{\rho}_c^{\epsilon}\ g = 0 \qquad (3.50)$$

Solid field

$$+\ \frac{d(\underline{\rho}_r^{\epsilon}\ \underline{v}_r^2)}{dx} + \frac{d\underline{C}_r^{T}(v)}{dx} + \underline{T}_{cr}^{I} + \underline{\epsilon}_r \frac{dp}{dx} - \underline{\rho}_r^{\epsilon}\ g = 0 \qquad (3.51)$$

Pressure term may be eliminated by substituting the equation (3.50) for the pressure derivative to the equation (3.51)

$$+\ \frac{d(\underline{\rho}_r^{\epsilon}\ \underline{v}_r^2)}{dx} + \frac{d\underline{C}_r^{T}(v)}{dx} + \left(1 + \frac{\epsilon_r}{\epsilon_c}\right) \underline{T}_{cr}^{I} - \left(\underline{\rho}_r^{\epsilon} - \frac{\epsilon_r}{\epsilon_c}\ \underline{\rho}_c\right) g = 0 \qquad (3.52)$$

If experimental data is going to be used to determine the value of functions, at least two of the primary variables must be measured.

In the following formulation pressure and solid density profiles are assumed to be known as well as gas and solid mass flow rates as boundary conditions.

From solid density profile it is possible to determine continuum density profile and continuum and solid fractions from relations (3.44), (3.45) and (3.46). Continuum and solid velocities may then be calculated from mass balances. For determination of macroscopic drag term the continuum momentum balance (3.50) can be represented in the following form

$$\underline{T}_{cr}^{I} = \underline{\epsilon}_c \frac{dp}{dx} - \underline{\rho}_c^{\epsilon} g \qquad (3.53)$$

It is possible to calculate the derivative of macroscopic dispersion term e.g. from total momentum balance, which is obtained by adding continuum and solid field momentum equations together. Thus it can be written

$$\frac{d\underline{C}_r^T(v)}{dx} = - \frac{d(\underline{\rho}_r^{\epsilon} \underline{v}_r^2)}{dx} - \frac{dp}{dx} + (\underline{\rho}_c^{\epsilon} + \underline{\rho}_r^{\epsilon}) g \qquad (3.54)$$

From the above equation it can also be concluded, what is the relationship between pressure drop and solid density under

assumptions in this chapter. One large term is the dispersion term, which seems to get quite high values according to the measurements presented in chapter 4. and also by Hartge et al. (1988).

Another possibility to determine macroscopic fluctuating average term is to determine it from stochastic experimental data according to the equation (3.28)

$$\underline{C}_r^T(v) = {}^{A_T<\underline{\rho}_r^{\epsilon}}{}^{\rho,A_T<\tilde{\underline{v}}_r>^2>} \qquad (3.55)$$

3.3.2 Momentum-averaged form

Applying momentum averaged forms instead of mass averaged forms in equations (3.29)-(3.32) mass and momentum balances may be written

Mass balance

Continuum

$$\sum_{i=1,2} {}^{A_{Ti}<\underline{\rho}_{ci}^{\epsilon}>}{}^{v,A_{Ti}<\underline{v}_{ci}>}\cdot\underline{n}_{Ti}A_{Ti} + \sum_{i=1,2} {}^{A_{Ti}<\underline{\rho}_c^{\epsilon}}{}^{v,A_{Ti}<\tilde{\underline{v}}_c>>}\cdot\underline{n}_{Ti}A_{Ti}$$

$$+ \underline{I}_c^w(1)\, V_T = 0 \qquad (3.56)$$

Solid field

$$\sum_{i=1,2} {}^{A_{Ti}}\langle \varrho_{ri}^{\epsilon} {}^{v,A_{Ti}}\langle \underline{v}_{ri}\rangle \cdot \underline{n}_{ri} A_{Ti} + \sum_{i=1,2} {}^{A_{Ti}}\langle \varrho_r^{\epsilon} {}^{v,A_{Ti}}\langle \tilde{\underline{v}}_r\rangle\rangle \cdot \underline{n}_{Ti} A_{Ti}$$

$$+ \underline{I}_r^w(1)\, V_T = 0 \qquad (3.57)$$

Momentum balance

Continuum

$$- \sum_{s\neq c} {}^{V_T}\langle \underline{T}_{cr}^I\rangle\, V_T - \sum_{s\neq c} {}^{V_T}\langle \underline{\epsilon}_s \frac{dp}{dx}\rangle\, V_T$$

$$+ \sum_{i=1,2} {}^{A_{Ti}}\langle p_{ci}\rangle \cdot \underline{n}_{Ti} dA - {}^{V_T}\langle \varrho_c^{\epsilon}\rangle\, g\, V_T = 0 \qquad (3.58)$$

Solid field

$$\sum_{i=1,2} ({}^{A_{Ti}}\langle \varrho_{ri}^{\epsilon} {}^{v,A_T}\langle \underline{v}_{ri}\rangle {}^{v,A_T}\langle \underline{v}_{ri}\rangle) \cdot \underline{n}_{Ti} A_{Ti} + {}^{V_T}\langle \underline{T}_{cr}^I\rangle\, V_T$$

$$+ {}^{V_T}\langle \underline{\epsilon}_r \frac{dp}{dx}\rangle\, V_T - {}^{V_T}\langle \varrho_r^{\epsilon}\rangle g\, V_T - \sum_{s\neq r,c} {}^{V_T}\langle \underline{T}_{rs}^V\rangle\, V_T + I_r^w(v)\, V_T = 0 \qquad (3.59)$$

If definition (3.34) is now applied in addition to new definitions (3.60) and (3.61)

$$\underline{\underline{v}} = {}^{v,S_T}\langle \underline{v} \rangle \quad , \tag{3.60}$$

$$\underline{C}_r^T(1) = {}^{A_T}\langle \rho_r^\epsilon \, {}^{v,A_T}\langle \tilde{\underline{v}}_r \rangle \rangle \tag{3.61}$$

we may write differential equations respective to equations (3.40)-(3.43)

Mass balance

Continuum

$$\frac{d(\rho_c^\epsilon \, \underline{\underline{v}}_c)}{dx} + \frac{d}{dx} \underline{C}_c^T(1) + \underline{I}_c^w(1) = 0 \tag{3.62}$$

Solid field

$$\frac{d(\rho_r^\epsilon \, \underline{\underline{v}}_r)}{dx} + \frac{d}{dx} \underline{C}_c^T(1) + \underline{I}_c^w(1) = 0 \tag{3.63}$$

Momentum balance

Continuum

$$- \sum_{s \neq c} \underline{T}^{I}_{cr} + \sum_{s \neq c} \underline{\epsilon}_c \frac{dp}{dx} - \underline{\rho}^{\epsilon}_c g = 0 \qquad (3.64)$$

Solid field

$$+ \frac{d(\underline{\rho}^{\epsilon}_r \underline{v}^2_r)}{dx} + \underline{T}^{I}_{cr} + \underline{\epsilon}_r \frac{dp}{dx} - \underline{\rho}^{\epsilon}_r g - \sum_{s \neq r,c} \underline{T}^{V}_{rs} - I^{w}_{r}(v) = 0 \qquad (3.65)$$

When considering additional equations (3.44)-(3.46) we obtain an equation system where the number of equations is equal to the number of primary variables. Additionally, there are again extra terms, which have to be presented as functions of primary variables in order to close the equation system. There are now altogether four extra terms, which are

$\underline{T}^{I}_{cr}$, $\underline{T}^{V}_{rs}$, $\underline{C}^{T}_{c}(1)$ and $\underline{C}^{T}_{r}(1)$

Next we will assume similar flow application as for mass averaged form in order to evaluate extra terms experimentally. In addition, the gas dispersion term in gas mass balance is assumed negligible. So, there are only two extra terms to be determined from experimental data

$\underline{T}^{I}_{cr}$, $\underline{C}^{T}_{r}(1)$

and respective equations are

Mass balance

Continuum

$$\frac{d(\rho^{\epsilon}_{c}\ \underline{v}_{c})}{dx} = 0 \qquad (3.66)$$

Solid field

$$\frac{d(\rho^{\epsilon}_{r}\ \underline{v}_{r})}{dx} + \frac{d}{dx}\ \underline{C}^{T}_{r}(1) = 0 \qquad (3.67)$$

Momentum balance

Continuum

$$- \underline{T}^{I}_{cr} + \underline{\epsilon}_{c}\ \frac{dp}{dx} - \rho^{\epsilon}_{c}\ g = 0 \qquad (3.68)$$

Solid field

$$+ \frac{d(\rho^{\epsilon}_{r}\ \underline{v}^{2}_{r})}{dx} + \underline{T}^{I}_{cr} + \underline{\epsilon}_{r}\ \frac{dp}{dx} - \rho^{\epsilon}_{r}\ g = 0 \qquad (3.69)$$

Experimental determination of the two extra terms may be done respectively to mass average form equations (3.48)-(3.51) by applying equations (3.66)-(3.69), but they are not determined in this work.

3.3.3 Two-region form

Area averaging of the rate of change or convection terms leads to stochastic average terms like e.g. in equations (3.7-3.18). If homogeneous constitutive models are applied into non-homogeneous field, similar stochastic terms arise also e.g. for gas-particle drag as will be presented in section 3.4.1. These terms are due to differences between local values and average values and thus the more homogeneous the flow structure is, the smaller are the stochastic average terms. One way of reducing values of the terms is to divide flow into more homogeneous subfields, for which balance equations are written separately.

In fast fluidized beds there has been reported flow structures in which solid flow is divided into dilute phase and into more dense phase (terms like clusters, strands etc.) [Yerushalmi et al. 1976, Li et al. 1980]. Dilute phase is mainly going up in the reactor and dense phase has lower velocity or is going down especially near the walls of the reactor. Thus in fast fluidized bed more homogeneous fields are obtained, if non-homogeneous solid

field is divided into two or more uniform regions according to total solid density.

In the following we will divide solid field into two different regions according to the critical solid density value, then apply mass averaged variables under assumptions presented at the beginning of the section 3.3 and define macroscopic averaging space to be that of the dilute or the dense region respectively. In addition to one region equations, interactions between dense and dilute regions must be considered. The conservation equations are written below for two-region model

Mass balance

Continuum

$$(\underline{\rho}^{\epsilon}_{c,d}\ \underline{v}_{c,d}\ f_d\ A_T)_2 - (\underline{\rho}^{\epsilon}_{c,d}\ \underline{v}_{c,d}\ f_d\ A_T)_1 + \underline{I}^{w}_{c,d}(1)\ V_T f_d$$

$$+ \underline{I}^{c,e}_{c,d}(1)\ V_T f_d - \underline{I}^{c,d}_{c,e}(1)\ V_T f_e = 0 \qquad (3.70)$$

$$(\underline{\rho}^{\epsilon}_{c,e}\ \underline{v}_{c,e}\ f_e\ A_T)_2 - (\underline{\rho}^{\epsilon}_{c,e}\ \underline{v}_{c,e}\ f_e\ A_T)_1 + \underline{I}^{w}_{c,e}(1)\ V_T f_e$$

$$+ \underline{I}^{c,d}_{c,e}(1)\ V_T f_e - \underline{I}^{c,e}_{c,d}(1)\ V_T f_d = 0 \qquad (3.71)$$

Solid field

$$(\underline{\rho}^{\epsilon}_{r,d}\ \underline{v}_{r,d}\ f_d\ A_T)_2 - (\underline{\rho}^{\epsilon}_{r,d}\ \underline{v}_{r,d}\ f_d\ A_T)_1 + \underline{I}^{w}_{r,d}(1)\ V_T f_d$$

$$+ \underline{I}^{r,e}_{r,d}(1)\ V_T f_d - \underline{I}^{r,d}_{r,e}(1)\ V_T f_e = 0 \qquad (3.72)$$

$$(\underline{\rho}^{\epsilon}_{r,e}\ \underline{v}_{r,e}\ f_e\ A_T)_2 - (\underline{\rho}^{\epsilon}_{r,e}\ \underline{v}_{r,e}\ f_e\ A_T)_1 + \underline{I}^{w}_{r,e}(1)\ V_T f_e$$

$$+ \underline{I}^{r,d}_{r,e}(1)\ V_T f_e - \underline{I}^{r,e}_{r,d}(1)\ V_T f_d = 0 \qquad (3.73)$$

where

$\underline{I}^{i,k}_{i,j}(1)$ is mass transfer of field i from region j to region k

$\underline{I}^{w}_{i,j}(1)$ is mass transfer of field i through walls of the reactor, respectively to equation (3.33)

Momentum balance

Continuum

$$-\sum_{s\neq c} \underline{T}^{I}_{cr,d}\ V_T\ f_d - \sum_{s\neq c} \underline{\epsilon}_{s,d}\ \frac{dp}{dx}\ V_T\ f_d - \quad p\ [f_{d2} - f_{d1}]\ A_T$$

$$+ [(\underline{p}\ f_d)_2 - (\underline{p}\ f_d)_1]\ A_T - \underline{\rho}^{\epsilon}_{c,d}\ g\ V_T\ f_d$$

$$+ \underline{T}^{c,e}_{c,d}\ V_T\ f_d + \underline{I}^{w}_{c,d}(v)\ V_T\ f_d + \underline{I}^{c,e}_{c,d}(1)\ \underline{v}^{*}_{c,d}\ V_T f_d$$

$$- \underline{I}^{c,d}_{c,e}(1)\ \underline{v}^{*}_{c,e}\ V_T f_e = 0 \qquad (3.74)$$

$$-\sum_{s\neq c}\ \underline{T}^{I}_{cr,e}\ V_T\ f_e - \sum_{s\neq c}\ \underline{\epsilon}_{s,e}\ \frac{d\underline{p}}{dx}\ V_T\ f_e - \underline{p}\ [f_{e2} - f_{e1}]\ A_T$$

$$+ [(\underline{p}\ f_e)_2 - (\underline{p}\ f_e)_1]\ A_T - \underline{\rho}^{\epsilon}_{c,e}\ g\ V_T\ f_e$$

$$+ \underline{T}^{c,d}_{c,e}\ V_T\ f_e + \underline{I}^{w}_{c,e}(v)\ V_T\ f_e + \underline{I}^{c,d}_{c,e}(1)\ \underline{v}^{*}_{c,e}\ V_T f_e$$

$$- \underline{I}^{c,e}_{c,d}(1)\ \underline{v}^{*}_{c,d}\ V_T f_d = 0 \qquad (3.75)$$

Solid field

$$[(\underline{\rho}^{\epsilon}_{r,d}\ \underline{v}^{2}_{r,d}\ f_d)_2 - (\underline{\rho}^{\epsilon}_{r,d}\ \underline{v}^{2}_{r,d}\ f_d)_1]\ A_T + \{[\underline{C}^{T}_{r,d}(v)\ f_d]_2$$

$$- [\underline{C}^{T}_{r,d}(v)\ f_d]_1\ \}\ A_T + \underline{T}^{I}_{cr,d}\ f_d\ V_T + \underline{\epsilon}_{r,d}\ \frac{d\underline{p}}{dx}\ V_T\ f_d - \underline{\rho}^{\epsilon}_{r,d}\ g\ V_T\ f_d$$

$$- [\sum_{s\neq r,c}\ \underline{T}^{V}_{rs,d} - \sum_{s}\ \underline{T}^{s,d}_{r,d} - \underline{I}^{w}_{r,d}(v)]\ V_T\ f_d$$

$$+ \underline{I}^{r,e}_{r,d}(1)\ \underline{v}^{*}_{r,d}\ V_T f_d - \underline{I}^{r,d}_{r,e}(1)\ \underline{v}^{*}_{r,e}\ V_T f_e = 0 \qquad (3.76)$$

$$[(\rho^{\epsilon}_{r,e}\ \underline{v}^{2}_{r,e}\ f_e)_2 - (\rho^{\epsilon}_{r,e}\ \underline{v}^{2}_{r,e}\ f_e)_1]\ A_T + \{[\underline{C}^{T}_{r,e}(v)\ f_e]_2$$

$$- [\underline{C}^{T}_{r,e}(v)\ f_e]_1\ \}\ A_T + \underline{T}^{I}_{cr,e}\ f_e\ V_T + \underline{\epsilon}_{r,e}\ \frac{dp}{dx}\ V_T\ f_e - \rho^{\epsilon}_{r,e}\ g\ V_T\ f_e$$

$$- [\sum_{s\neq r,c}\ \underline{T}^{V}_{rs,e} - \sum_{s}\ \underline{T}^{s,d}_{r,e} - \underline{I}^{w}_{r,e}(v)]\ \ V_T\ f_e$$

$$+ \underline{I}^{r,d}_{r,e}(1)\ \underline{v}^{*}_{r,e}\ V_T f_e - \underline{I}^{r,e}_{r,d}(1)\ \underline{v}^{*}_{r,d}\ V_T f_d = 0 \qquad (3.77)$$

where

$\underline{T}^{s,e}_{r,d}$ is momentum flux from field r in region d into field s in region e.

$v^{*}_{i,j}$ is average velocity for momentum transfer from field i in region j to another region.

$\underline{I}^{w}_{i,j}$ (v) is momentum transfer of field i in region j through the walls of the reactor, respectively to equation (3.33)

Field fractions f_d and f_e can be defined according to critical solid density as follows

$$f_d = \frac{1}{A_T} \int_{A_T} \gamma_d\ dA \qquad (3.78)$$

$$f_e = \frac{1}{A_T} \int_{A_T} \gamma_e \, dA \tag{3.79}$$

where γ_d and γ_e are region functions for dilute and dense fields, respectively. Dilute region function is 1, when solid density is less than critical value and 0, when more than critical value. Between region functions there is relation $\gamma_d + \gamma_e = 1$ and thus it may be written

$$f_d = 1 - f_e \tag{3.80}$$

Respective equations to mass averaged form equations (3.48-3.51) and momentum-averaged form equations (3.66-3.69) are obtained, if we assume total cross sectional area constant, particles of similar size and convective flux through walls negligible. In addition non-convective momentum flux between different regions is assumed small and macroscopic fluctuating term negligible because of more uniform fields.

Mass balance

Continuum

$$\frac{d(\underline{\rho}^{\epsilon}_{c,d}\ \underline{v}_{c,d}\ f_d)}{dx} + \underline{I}^{c,e}_{c,d}(1)\ f_d - \underline{I}^{c,d}_{c,e}(1)\ f_e = 0 \qquad (3.81)$$

$$\frac{d(\underline{\rho}^{\epsilon}_{c,e}\ \underline{v}_{c,e}\ f_e)}{dx} + \underline{I}^{c,d}_{c,e}(1)\ f_e - \underline{I}^{c,e}_{c,d}(1)\ f_d = 0 \qquad (3.82)$$

Solid field

$$\frac{d(\underline{\rho}^{\epsilon}_{r,d}\ \underline{v}_{r,d}\ f_d)}{dx} + \underline{I}^{r,e}_{r,d}(1)\ f_d - \underline{I}^{r,d}_{r,e}(1)\ f_e = 0 \qquad (3.83)$$

$$\frac{d(\underline{\rho}^{\epsilon}_{r,e}\ \underline{v}_{r,e}\ f_e)}{dx} + \underline{I}^{r,d}_{r,e}(1)\ f_e - \underline{I}^{r,e}_{r,d}(1)\ f_d = 0 \qquad (3.84)$$

Momentum balance

Continuum

$$- \underline{T}^{I}_{cr,d}\ f_d + \underline{\epsilon}_{c,d}\ \frac{dp}{dx}\ f_d - \underline{\rho}^{\epsilon}_{c,d}\ g\ f_d$$

$$+ \underline{I}^{c,e}_{c,d}\ (1)\ \underline{v}^{*}_{c,d}\ f_d - \underline{I}^{c,d}_{c,e}(1)\ \underline{v}^{*}_{c,e}\ f_e = 0 \qquad (3.85)$$

$$- \underline{T}^{I}_{cr,e} f_e + \underline{\epsilon}_{c,e} \frac{dp}{dx} f_e - \underline{\rho}^{\epsilon}_{c,e} g f_e +$$

$$+ \underline{I}^{c,d}_{c,e}(1) \underline{v}^{*}_{c,e} f_e - \underline{I}^{c,e}_{c,d}(1) \underline{v}^{*}_{c,d} f_d = 0 \qquad (3.86)$$

Solid field

$$\frac{d(\underline{\rho}^{\epsilon}_{r,d} \underline{v}^{2}_{r,d} f_d)}{dx} + \underline{T}^{I}_{cr,d} f_d + \underline{\epsilon}_{r,d} \frac{dp}{dx} f_d - \underline{\rho}^{\epsilon}_{r,d} g f_d$$

$$- \underline{I}^{r,e}_{r,d}(1) \underline{v}^{*}_{r,d} f_d + \underline{I}^{r,d}_{r,e}(1) \underline{v}^{*}_{r,e} f_e = 0 \qquad (3.87)$$

$$\frac{d(\underline{\rho}^{\epsilon}_{r,e} \underline{v}^{2}_{r,e} f_e)}{dx} + \underline{T}^{I}_{cr,e} f_e + \underline{\epsilon}_{r,e} \frac{dp}{dx} f_e - \underline{\rho}^{\epsilon}_{r,e} g f_e$$

$$- \underline{I}^{r,d}_{r,e}(1) \underline{v}^{*}_{r,e} f_e + \underline{I}^{r,e}_{r,d}(1) \underline{v}^{*}_{r,d} f_d = 0 \qquad (3.88)$$

In the equation system there are altogether 8 balance equations. Primary variables are

$$\underline{\rho}^{\epsilon}_{c,d},\ \underline{\rho}^{\epsilon}_{c,e},\ \underline{\rho}^{\epsilon}_{r,d},\ \underline{\rho}^{\epsilon}_{r,e},\ \underline{v}_{c,d},\ \underline{v}_{c,e},\ \underline{v}_{r,d},\ \underline{v}_{r,e},\ \underline{p}$$

and additional unknown terms are

$$\underline{I}^{c,e}_{c,d}(1),\ \underline{I}^{c,d}_{c,e}(1),\ \underline{I}^{r,e}_{r,d}(1),\ \underline{I}^{r,d}_{r,e}(1),\ f_d,\ f_e,\ \underline{T}^{I}_{cr,d},\ \underline{T}^{I}_{cr,e},\ \underline{\epsilon}_{r,d},$$

$\underline{\epsilon}_{r,e}$, $v^*_{c,d}$, $v^*_{c,e}$, $v^*_{r,d}$, $v^*_{r,e}$

Six variables out of four solid densities and four volume fractions may be eliminated by applying equations (3.89)-(3.94)

$$\sum_s \underline{\epsilon}_{s,d} = 1 \tag{3.89}$$

$$\sum_s \underline{\epsilon}_{s,e} = 1 \tag{3.90}$$

$$\underline{\rho}^{\epsilon}_{c,d} = \underline{\epsilon}_{c,d}\, \rho_{c,d} \tag{3.91}$$

$$\underline{\rho}^{\epsilon}_{c,e} = \underline{\epsilon}_{c,e}\, \rho_{c,e} \tag{3.92}$$

$$\underline{\rho}^{\epsilon}_{r,d} = \underline{\epsilon}_{r,d}\, \rho_{r,d} \tag{3.93}$$

$$\underline{\rho}^{\epsilon}_{r,e} = \underline{\epsilon}_{r,e}\, \rho_{r,e} \tag{3.94}$$

Equation (3.80) holds between the field fractions and pressure field is assumed constant in horizontal direction (this assumption will be discussed in section 3.4.1). Thus there are seven variables and 9 independent unknown terms. Drag term is here assumed to be known as a function of primary variables, because fields are assumed more uniform than in one solid field case and thus

fluctuating values are assumed small. At least 8 variables have to be determined from experiments in order to calculate unknown terms from equations (3.81) - (3.88). In addition some value for critical density is required for defining the field boundary between dilute and dense regions.

If momentum transfer between continuum fields is assumed negligible and continuum mass balances are added together, the amount of equations reduces by one and four extra terms are eliminated giving the following equation system

Mass balance

Continuum

$$\frac{d(\rho^{\epsilon}_{c,d}\ \underline{v}_{c,d}\ f_d)}{dx} + \frac{d(\rho^{\epsilon}_{c,e}\ \underline{v}_{c,e}\ f_e)}{dx} = 0 \qquad (3.95)$$

Solid field

$$\frac{d(\rho^{\epsilon}_{r,d}\ \underline{v}_{r,d}\ f_d)}{dx} + \underline{I}^{r,e}_{r,d}(1)\ f_d - \underline{I}^{r,d}_{r,e}(1)\ f_e = 0 \qquad (3.96)$$

$$\frac{d(\rho^{\epsilon}_{r,e}\ \underline{v}_{r,e}\ f_e)}{dx} + \underline{I}^{r,d}_{r,e}(1)\ f_e - \underline{I}^{r,e}_{r,d}(1)\ f_d = 0 \qquad (3.97)$$

Momentum balance

Continuum

$$- \underline{T}^{I}_{cr,d} f_d + \underline{\epsilon}_{c,d} \frac{dp}{dx} f_d - \underline{\rho}^{\epsilon}_{c,d} g f_d = 0 \qquad (3.98)$$

$$- \underline{T}^{I}_{cr,e} f_e - \underline{\epsilon}_{c,e} \frac{dp}{dx} f_e - \underline{\rho}^{\epsilon}_{c,e} g f_e = 0 \qquad (3.99)$$

Solid field

$$\frac{d\,(\underline{\rho}^{\epsilon}_{r,d}\, \underline{v}^{2}_{r,d}\, f_d)}{dx} + \underline{T}^{I}_{cr,d} f_d + \underline{\epsilon}_{r,d} \frac{dp}{dx} f_d - \underline{\rho}^{\epsilon}_{r,d} g f_d$$

$$- \underline{I}^{r,e}_{r,d}(1)\, \underline{v}^{*}_{r,d} f_d + \underline{I}^{r,d}_{r,e}(1)\, \underline{v}^{*}_{r,e} f_e = 0 \qquad (3.87)$$

$$\frac{d\,(\underline{\rho}^{\epsilon}_{r,e}\, \underline{v}^{2}_{r,e}\, f_e)}{dx} + \underline{T}^{I}_{cr,e} f_e + \underline{\epsilon}_{r,e} \frac{dp}{dx} f_e - \underline{\rho}^{\epsilon}_{r,e} g f_e$$

$$- \underline{I}^{r,d}_{r,e}(1)\, \underline{v}^{*}_{r,e} f_e + \underline{I}^{r,e}_{r,d}(1)\, \underline{v}^{*}_{r,d} f_d = 0 \qquad (3.88)$$

Evaluation of equation system with six extra terms still seems to require much more detailed experimental data compared with mass and momentum averaged formulations in the previous chapter. Thus, in order to evaluate parameters for two-region model, much better experimental knowledge must be available about CFB flow behaviour and at the moment the model seems not to be reasonable in this form.

3.4 EQUATION CLOSURE FOR MACROSCOPIC MASS-AVERAGED MODEL

3.4.1 Drag

Drag coefficients for particulate gas-solid interactions were reviewed in chapter 2. In circulating fluidized beds flow is aggregate and for macroscopic averaged equations particulate flow parameters cannot be applied. However, certain relations can be written between parameters of particulate microscopic fluidization and aggregate macroscopic fluidization.

In chapter 2 some equations were presented for gas-particle and particle-particle drag in equation system, where averaging scale was 1. Below we will try to formulate the relation between the terms of scales 1 and L.

As an example macroscopic gas-particle drag term will be considered, which may be expressed as a macroscopic average of a microscopic average gas-particle drag term

$$\underline{T}^{I}_{cr} = {}^{V_T}\langle \underline{T}^{I}_{cr} \rangle \qquad (3.100)$$

For microscopic averaged value we use the following form

$$\underline{T}^{I}_{cr} = - \beta_{cr} \rho^{\epsilon}_{r} (\underline{v}_c - \underline{v}_r) \ , \qquad (3.101)$$

where β_{cr} is function of primary variables

If form (3.101) is substituted into macroscopic term equation (3.100), we may write

$$\underline{T}^{I}_{cr} = \underline{V}_T \langle \beta_{cr} \, \varrho_r^{\epsilon} \, (\underline{v}_c - \underline{v}_r) \rangle \qquad (3.102)$$

This form again is an averaged value of a function, which depends on local values of primary variables. In order to change it into form which is function of averaged primary variables, additional correlation terms have to be introduced, which again leads to difficulties in closing the system.

Next we will consider a case, in which the gas gravitation is negligible in gas momentum balance. Thus, we may write for some point of cross sectional area

$$\varrho_r^{\epsilon} \, \beta_{cr} \, (\underline{v}_c - \underline{v}_r) = - \underline{\epsilon}_c \, \frac{\partial \underline{p}}{\partial x} \qquad (3.103)$$

For continuum mass flow holds

$$\dot{m}_c = \int_A \varrho_c \, \underline{\epsilon}_c \, \underline{v}_c \, dA \qquad (3.104)$$

From the continuum momentum equation (3.26) we can derive equation for pressure gradient in horizontal direction. According to the equation (3.50) pressure gradient term will be equal to drag term for horizontal direction, which is proportional to the velocity difference between solid and continuum velocity. Because the flow is assumed to be vertical, pressure gradient in horizontal direction is thus assumed to be negligible compared with vertical direction (similar assumption to single-phase nearly parallel boundary layer flows [Arpaci and Larsen 1984]).

If velocity is substituted from equation (3.103) into equation (3.104) and if we assume that pressure is constant on cross sectional area, continuum mass flow rate can be written

$$\dot{m}_c = \int_A - \frac{\underline{\epsilon}_c^2}{(1-\underline{\epsilon}_c)\beta_{cr}} \, dA \, \frac{\rho_c}{\rho_r} \, \frac{\partial \underline{p}_c}{\partial x} + \int_A \underline{\rho}_c \, \underline{\epsilon}_c \, \underline{v}_r \, dA \qquad (3.105)$$

For mass flow rate we may write with macroscopic variables

$$\dot{m}_c = \rho_c \, \underline{\epsilon}_c \, \underline{v}_c \, A \qquad (3.106)$$

Elimination of mass flow rate from equations (3.105) and (3.106) and applying macroscopic gas momentum balance (3.50) and macroscopic drag definition (3.47) gives

$$\underline{\beta} = - \frac{\underline{\epsilon}_g \left(\underline{\epsilon}_g \underline{v}_g A - \int \epsilon_g v_s dA \right)}{(1-\underline{\epsilon}_g)(\underline{v}_g - \underline{v}_r) \int \frac{\epsilon_g^2}{(1-\epsilon_g)} \frac{1}{\beta} dA} \qquad (3.107)$$

If we now assume, that solid velocity is negligible and local drag coefficient is constant, equation (3.107) reduces into form

$$\underline{\beta}_{cr} = \frac{\frac{(1 - \underline{\epsilon}_r)^2}{\underline{\epsilon}_r}}{\frac{1}{A}\int_A \frac{(1 - \underline{\epsilon}_r)^2}{\underline{\epsilon}_r} dA} \beta_{cr} \qquad (3.108)$$

Equation (3.108) shows in this simple case that ratio factor between constant local and macroscopic drag coefficients can be determined, if stochastic values of local solid fraction are known. The above equations (3.107) and (3.108) have been obtained for vertical flow case, i.e. terms in momentum equation are assumed negligible in horizontal direction. Better accuracy for drag coefficient should be obtained, if the above equations would be written multidimensionally. However, local flow values are not yet known so well in practice that such a procedure would be realistic.

Drag coefficient has been determined experimentally for fast beds [Kwauk et al. 1985, Sankar et al. 1986, Matsen 1982] which indicates, that drag coefficient factor is less than one for non-

homogeneous solid flow. It will get greater values for more homogeneous flow regions i.e. for dilute cases or for very dense cases. In pneumatic transport, drag effect is taken into consideration by using slip velocity values. If solid momentum equation (3.52) and macroscopic drag coefficient definition (3.47) are combined, we may write relationship between averaged drag coefficient and slip velocity for a case, where there is negligible vertical change in flow structure

$$\left(1+ \frac{\epsilon_r}{\epsilon_c} \right) \underline{\beta}_{cr} \underline{\rho}_r \underline{v}_{sl} - \left(\underline{\rho}_r^{\epsilon} - \frac{\epsilon_r}{\epsilon_c} \underline{\rho}_c\right) g = 0 \qquad (3.109)$$

Matsen (1982) has stated, that slip velocities should increase with solid concentration in dilute region of pneumatic transport systems, which is considered controversial to many other investigators. For example Richardson-Zaki correlation gives decreasing slip velocity for decreasing void fraction. Matsen's qualitative conclusion has been verified in many recent experimental studies [Yerushalmi 1976, Avidan et al. 1981, Sankar et al. 1986, Klinzing and Mathur 1984, Kojima et al. 1986, Kwauk et al. 1985, Bingyu and Kwauk 1985, Han et al. 1985, Shao 1986]. Matsen has concluded, that explanation for this lies in the phenomenon of cluster formation. It seems, that this explanation can be presented in a general case with degree of aggregation of flow. Thus for low gas velocity and dense concentration regions high drag coefficients may again be expected, because flow is less aggregative.

Matsen presented function form for slip velocity correlation, the parameters of which were evaluated later by Sankar et al. (1986) giving the correlation of the form

$$\frac{\underline{v}_{sl}}{v_t} = 1 \quad , \quad \epsilon_s < \epsilon_{s,min} \tag{3.110}$$

$$\frac{\underline{v}_{sl}}{v_t} = a_1 \epsilon_s^{a_2} \quad , \quad \epsilon_s > \epsilon_{s,min} \tag{3.111}$$

The application of correlation (3.110) to practical fast bed cases is limited by its experimental coverage. Maximum tube diameter has been only 38.1 mm and correlations for parameters a_1 and a_2 give unreasonable slip velocities for extrapolations with larger diameters. But it shows qualitatively the form of dependence of drag term as a function of solid concentration. Matsen proposed, that his correlation is valid only to void fractions above 0.9. For lower void fractions he has presented a correlation, which depends on minimum fluidization values and the diameter of a non-slug bubble.

Kwauk et al. (1985) have used correlation of the form

$$\underline{v}_g - \underline{v}_s \left(\frac{\epsilon_g}{1 - \epsilon_g} \right) = v_t \, \epsilon_g^n \, [\, 1 + F(\epsilon_g)] \tag{3.112}$$

where $F(\epsilon_g)$ depends on the level of aggregation and its form has been presented semiempirically

$$F(\epsilon_g) = C_1 \left[(1-\epsilon_g)(\epsilon_g-\epsilon_{g,min})^{C_2}\right]^{C_3} \qquad (3.113)$$

For particulate dense flow regions Ergun equation (2.131) or one of bed expansion equations [Couderc 1985] can be used to evaluate drag coefficient by applying equation (3.109). Also various flow diagrams used for fast beds can be applied.

Avidan and Yerushalmi (1982) have presented modified bed expansion equation also for fast bed flows. Their equation is of the form

$$\frac{v_g}{v_T^*} = \epsilon^n \qquad (3.114)$$

where v_T^* is 'effective' cluster terminal velocity.

As to the presented correlations, it seems that there is only a limited range of experiments behind the correlations. Thus their application to different materials and flow conditions, e.g. for coal combustion fast bed hydrodynamics, requires too much extrapolation.

3.4.2 Dispersion

Closing the dispersion term in macroscopic momentum equations is a problem similar to the time-averaged single-phase equations, where different closure models for turbulent stresses have been derived leading from simple algebraic equations to multiequation systems [Gupta and Lilley 1985]. In section 2.8.2 it was stated, that for microscopic gas-solid fluidization equations there does not exist any rigorous model for dispersion term and it has often been assumed negligible in model applications. For macroscopic or 1-dimensional fluidized bed equations there has not been found any work at all referring to dispersion term modeling.

Concerning the importance of velocity fluctuation terms in macroscopic time-averaged two-phase equations, Trapp (1986) has demonstrated that instabilities present in mean motion equations of two-phase flow can be explained as a result of the failure to include appropriate closure models for the velocity fluctuations in the momentum equations. A similar type of situation can also be expected to exist with space averaged CFB equations. Another problem is, that the magnitude of dispersion terms may be so large compared with other terms in momentum equation, that neglecting them may give totally incorrect results.

Different kinds of turbulence closures from algebraic to two-equation models or large eddy-simulations have been derived for single phase time averaged equations. In similar ways different

models can be used in multiphase space-averaged flow equations. We will start by applying a general equation (2.94) to momentum conservation and multiplying it by solid velocity. For assumptions used in this chapter we can write

$$\underline{v}_r \frac{d}{dx}\cdot(\underline{\rho}_r^{\epsilon}\underline{v}_r\underline{v}_r) + \underline{v}_r \underline{\underline{T}}_{cr}^{I} + \underline{v}_r \underline{\epsilon}_r \frac{d}{dx}\cdot\underline{\underline{p}}_{cr} - \underline{v}_r \underline{\rho}_r^{\epsilon} g = 0 \qquad (3.115)$$

If solid velocity is divided into the average and the fluctuating value according to equation (3.12), area average of the first term in equation (3.115) can be written in the form

$$A_T< \underline{v}_r \frac{d}{dx}\cdot(\underline{\rho}_r^{\epsilon}\underline{v}_r\underline{v}_r)> = \underline{v}_r \frac{d\ (\underline{\rho}_r^{\epsilon}\underline{v}_r^2)}{dx} + \underline{v}_r A_T< \frac{d\ (\underline{\rho}_r^{\epsilon}\tilde{v}_r^2)}{dx} >$$

$$A_T< \tilde{v}_r \frac{d\ (\underline{\rho}_r^{\epsilon}\underline{v}_r^2)}{dx} > + 2 A_T< \tilde{v}_r \frac{d\ (\underline{\rho}_r^{\epsilon}\underline{v}_r\tilde{v}_r)}{dx} > + A_T< \tilde{v}_r \frac{d\ \underline{\rho}_r^{\epsilon}\tilde{v}_r^2}{dx} > \qquad (3.116)$$

The second, the third and the fourth terms in the right hand side of the equation (3.116) can be written as follows

Second term

$$\underline{v}_r A_T< \frac{d\ (\underline{\rho}_r^{\epsilon}\tilde{v}_r^2)}{dx} > = \underline{v}_r \frac{d\ C_r^T(v)}{dx} \qquad (3.117)$$

Third term

$$A_T < \tilde{v}_r \frac{d\,(\rho_r^{\epsilon} v_r^2)}{dx} > = A_T < \tilde{v}_r \frac{d\,\rho_r^{\epsilon}}{dx} > \underline{v}_r^2 \qquad (3.118)$$

Fourth term

$$2\,A_T < \tilde{v}_r \frac{d\,(\rho_r^{\epsilon} v_r \tilde{v}_r)}{dx} > = 2 \frac{d\,C_r(v)}{dx} \underline{v}_r - \underline{v}_r\, A_T < \rho_r^{\epsilon} \frac{d\,\tilde{v}_r^2}{dx} >$$

$$+ 2\, C_r^T(v) \frac{d\,\underline{v}_r}{dx} \qquad (3.119)$$

Applying equations (3.117)-(3.119) for the second, the third and the fourth term, equation (3.116) may be written

$$A_T < \underline{v}_r \frac{d}{dx} \cdot (\rho_r^{\epsilon} \underline{v}_r \underline{v}_r) > = \underline{v}_r \frac{d\,(\rho_r^{\epsilon} v_r^2)}{dx} + \underline{v}_r \frac{d\,C_r^T(v)}{dx}$$

$$+ A_T < \tilde{v}_r \frac{d\,\rho_r^{\epsilon}}{dx} > \underline{v}_r^2 + 2 \frac{d\,C_r^T(v)}{dx} \underline{v}_r - \underline{v}_r\, A_T < \rho_r^{\epsilon} \frac{d\,\tilde{v}_r^2}{dx} >$$

$$+ 2\, C_r^T(v) \frac{d\,\underline{v}_r}{dx} + A_T < \tilde{v}_r \frac{d\,\rho_r^{\epsilon} \tilde{v}_r^2}{dx} > \qquad (3.120)$$

Combining the second and the fourth term on the right hand side gives

$$A_T\langle \underline{v}_r \frac{d}{dx}\cdot(\underline{\rho}_r^{\epsilon}\underline{v}_r\underline{v}_r)\rangle = \underline{v}_r \frac{d\,(\underline{\rho}_r^{\epsilon}\underline{v}_r^2)}{dx} + 3\,\underline{v}_r \frac{d\,C_r^T(v)}{dx}$$

$$+ 2\,C_r^T(v)\,\frac{d\,\underline{v}_r}{dx} + A_T\langle \tilde{v}_r \frac{d\,\underline{\rho}_r^{\epsilon}}{dx}\rangle \underline{v}_r^2 - \underline{v}_r\, A_T\langle \underline{\rho}_r^{\epsilon} \frac{d\,\tilde{v}_r^2}{dx}\rangle$$

$$+ A_T\langle \tilde{v}_r \frac{d\,\underline{\rho}_r^{\epsilon}\tilde{v}_r^2}{dx}\rangle \qquad (3.121)$$

Below the macroscopic solid momentum equation (3.51) is multiplied by average solid velocity thus giving

$$+ \underline{v}_r \frac{d(\underline{\rho}_r^{\epsilon}\,\underline{v}_r^2)}{dx} + \underline{v}_r \frac{d\underline{C}_r^T(v)}{dx} + \underline{v}_r\,\underline{T}_{cr}^I + \underline{v}_r\,\underline{\epsilon}_r \frac{dp}{dx} - \underline{v}_r\,\underline{\rho}_r^{\epsilon}\,g = 0 \qquad (3.122)$$

If equation (3.115) is averaged over area and equations (3.12) and (3.121) are taken into consideration and then equation (3.122) is subtracted from it, we may write

$$2\,\frac{d\,[C_r^T(v)\,\underline{v}_r]}{dx} = - A_T\langle \tilde{v}_r \frac{d\,\underline{\rho}_r^{\epsilon}}{dx}\rangle \underline{v}_r^2 + \underline{v}_r\, A_T\langle \underline{\rho}_r^{\epsilon} \frac{d\,\tilde{v}_r^2}{dx}\rangle$$

$$- A_T\langle \tilde{v}_r \frac{d\,\underline{\rho}_r^{\epsilon}\tilde{v}_r^2}{dx}\rangle - A_T\langle \tilde{v}_r\,\underline{T}_{cr}^I\rangle - A_T\langle \tilde{v}_r\,\underline{\epsilon}_r \frac{d}{dx}\cdot p_{cr}\rangle$$

$$- \underline{v}_r\,[\,A_T\langle \underline{\epsilon}_r \frac{dp}{dx}\rangle - \underline{\epsilon}_r \frac{dp}{dx}\,] + A_T\langle \tilde{v}_r\,\underline{\rho}_r^{\epsilon}\,g\rangle \qquad (3.123)$$

Gravitation is a constant in equation (3.123) and if pressure gradient is assumed constant as in chapter 3.4.1, equation (3.123) reduces into

$$2\,\frac{d\,[C_r^T(v)\,\underline{v}_r]}{dx} = -\,A_T\!<\tilde{v}_r\,\frac{d\,\underline{\rho}_r^{\epsilon}}{dx}>\underline{v}_r^2 + \underline{v}_r\,A_T\!<\underline{\rho}_r^{\epsilon}\,\frac{d\,\tilde{v}_r^2}{dx}> -\,A_T\!<\tilde{v}_r\,\frac{d\,\underline{\rho}_r^{\epsilon}\tilde{v}_r^2}{dx}> - A_T\!<\tilde{v}_r\,\underline{T}_{cr}^I> \qquad (3.124)$$

Equation (3.124) is the respective form to turbulent kinetic energy balance in time-averaged equations of single phase equations of motion, in which intuitive assumptions have often been used for closing the equation system. For multiphase flow one-equation model may also be obtained by interpreting equation (3.124) e.g. as a balance for solid turbulent energy

CONVECTION + DIFFUSION + SOURCE + DISSIPATION = 0

The problem in the turbulence models is that they all contain some additional parameters, which have to be determined experimentally. The experimental knowledge of circulating fluidized beds is so scanty at the moment, that it is not realistic to try to evaluate turbulence parameters for complicated models. Thus, a simple device-dependent algebraic function form seems to be a

reasonable way to model dispersion term in macroscopic momentum equation. If experimental knowledge increases, more complicated models can be evaluated later.

The magnitude for the dispersion term can be calculated according to the equation (3.28) and thus it can be compared with other terms in momentum equation. As a rough example, a value for dispersion term is determined from experimental solid velocity and density profiles presented by Hartge et al. (1988). Profiles in cross-sectional area are presented in Figure 3.2. These profiles are already averaged in time and the profiles may give too small dispersion. As a result dispersion term divided by solid density has value 120 m^2/s^2 compared with the value of 20 m^2/s^2 of respective momentum term calculated with averaged values. The result shows, that dispersion term is significant in momentum equation at least when compared with acceleration term.

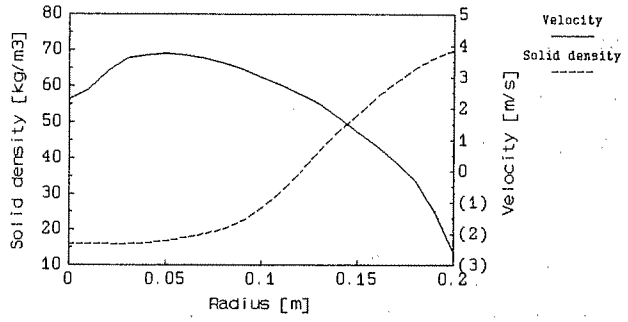

Figure 3.2 Solid density and velocity profiles in dispersion term calculation [Hartge et al. (1988)]

4. EXPERIMENTS ON CFB COLD MODEL

In the 1970's the term "fast fluidization" was introduced to illustrate fluidization mode, where dense clusters and strands of solid particles are flowing in the reactor fluidized by high gas flow rate [Yerushalmi et al. 1976]. At that time experimental investigations of fast fluidization were started in the City College of New York [Avidan et al. 1981, 1982, 1985, Yerushalmi et al. 1976, 1977, 1979, 1985]. Even earlier, Reh (1971) studied circulating fluid bed reactors in connection with endothermic and exothermic commercial processes. Significant work has also been started in the late 70's in China. [Li and Kwauk 1980]. Additionally, similar process has been studied under the subject of vertical pneumatic conveying [Leung 1980, Klinzing et al. 1987, Konrad 1986].

Most of the experiments have been performed in order to obtain some macroscopic, average values, such as average slip velocity, pressure drop, solid density and gas or solid mixing data. Solid density has often been calculated from equality of gravitation and pressure drop, which relationship has been subject in some works [Arena et al. 1985, Kato et al. 1986, Reiying et al. 1985]. The results have often been presented in the form of various fast bed diagrams [Reh 1971, Matsen 1982, Yerushalmi and Avidan 1985, Kwauk 1985, Wirth 1988]

Local flow variables in circulating fluidized beds have not been

measured until recently. Suitable measurement techniques have been developed in the research of bubbling bed as reviewed by Cheremisinoff (1986) and Atkinson and Clark (1986). In circulating fluid beds main methods have been optic fibers [Hartge et al. 1985, 1986, 1988, Horio et al. 1988, Morooka et al. 1984], capacitance probes [Brereton and Strömberg 1985], sampling probes [Monceaux et al. 1986] and reactive tracer [Dry 1986]. Experimental data has, however, been quite scanty, e.g. local solid velocities have been presented only recently in few papers [Horio et al. 1988, Hartge et al. 1988].

Most of the experimental works have concentrated on certain measurements. Usually no comprehensive experimental studies have been published, in which all the main properties would be measured, i.e. axial pressure profile, axial solid density, mass recirculation rate, gas flow rate and local solid densities and velocities. Thus the main objective of the experimental work presented here is to obtain values for different properties for the same experimental unit and for the same flow conditions. This data is needed in order to evaluate the magnitudes of different terms and parameters in fast bed flow model. It is realized, that the present knowledge of measurement techniques is deficient. Thus the experimental part is aimed to provide more qualitative data and better quantitative data can be obtained when experimental techniques, available for circulating fluid beds, have been developed to a more accurate level.

Axial mixing in circulating fluidized beds has also been a

subject which has been studied very little. Main experimental work has been accomplished in the City College of New York. Yerushalmi and Avidan (1985) have provided a summary of the published work in the area, which has only five investigators for solid mixing. Understanding solid mixing is most essential at the moment in the development of fast bed coal combustors, because scale-up into larger utility size units is one of the main questions of the technique. Thus in this study axial solid mixing was also studied.

4.1 EXPERIMENTAL SET-UP

The experimental unit shown in Figure 4.1 is 7.3 m high and its cross-sectional area is 0.25*1.00 m^2. Narrow wall is made of steel and wide walls are made of plexiglass in order to make visual observations about flow structure. In the recirculation loop, the particles are separated from gas in cyclone and then fed back to the bottom of the reactor at the level 0.7 m. Air is fed mainly through the grate in the bottom of the reactor and in addition there are two secondary air ports at two levels, 1.6 m and 3.0 m. Solid material is fed manually from solids feed hopper which is in the upper part of the reactor.

Pressure is measured at levels 0.25 m, 0.8 m, 2.1 m, 4.1 m and 7.1 m using standard pressure transducers. Air flow is measured with venturi flow meters separately for primary and secondary air.

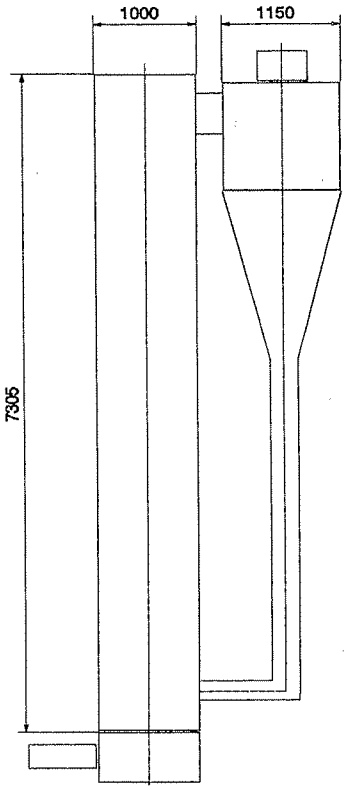

Figure 4.1 CFB cold model

Sand with average particle size of 270 μm is used as solid material. Sieve analysis of the used material is presented in table 4.1.

Table 4.1 Sieve analysis of sand

Sieve μm	500	250	177	125	90	45	0
On sieve %	1.4	56.3	19.3	15.4	5.0	2.4	0.1

4.2 MASS RECIRCULATION RATE

Two different methods were used to measure mass recirculation rate of solids. In both methods the rate was determined by measuring time of a certain amount of material coming down from the cyclone. The other one was based on three-way valve in recirculation loop and in the other one the rise of solid material surface was followed after closing the valve in the recirculation loop.

During the first experiments the return pipe of the unit was equipped with a three-way valve in order to determine mass recirculation rate. The valve was switched into such a position, that solid material was flowing into the separate vessel and after a proper time the valve was again switched into normal position, in which solid was fed into the reactor. Material in the vessel was then weighed and mass recirculation rate was calculated from weight

and time values.

Variables, which were changed during the experiments, were total air flow rate, secondary air flow rate (level 1.6 m) and total solid inventory in the reactor. Air flow rate was between 0.65 - 1.20 kg/s, secondary air 0.0 - 0.30 kg/s and total solid inventory 77 - 169 kg.

In the other measuring method, a steel return pipe was replaced by a transparent plexiglass pipe. In recirculation loop a valve was then closed and solid surface began to rise in the transparent return pipe. Time was measured as solid surface was rising from lower level to upper one. Mass of solids between the two levels was calibrated and thus flow rate was obtained by dividing the mass by the rising time. These experiments were performed with different solid inventories and different gas flow rates. Also pressure, solid concentration and velocity profiles were measured under the same conditions. Deviation of solid material flow was much smaller than during first mass flow rate experiments and it seemed that natural instability of the process was the main reason for the deviations.

The data from experiments were analyzed with regression analysis using a few different functional forms for variables. As a result, proper function was obtained for mass recirculation rate, and that functional form was then used for the rate in the evaluation of parameters in mathematical models. The mass recirculation rate

according to correlation function form is presented in Figure 2. In figure 2 a solid inventory is as a parameter in the system and in figure 2 b is seen the effect of secondary air.

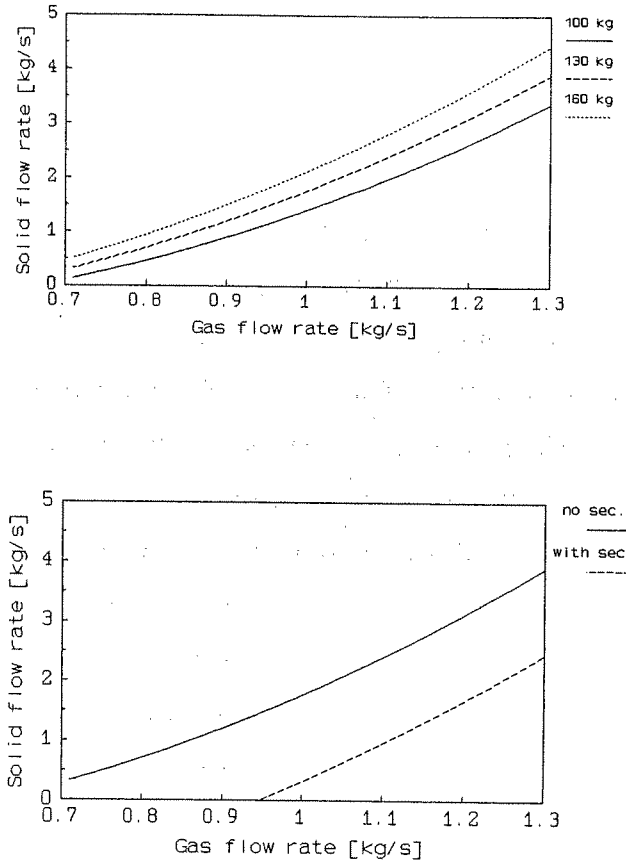

Figure 4.2. Recirculation mass flow rates
a) solid inventory as a parameter
b) secondary air as a parameter

4.3 DENSITY MEASUREMENTS

Macroscopic average value of solid density was measured by radioactive tracer technique, radioactive transmission and according to pressure data. As presented in chapter 3, pressure drop is only a rough way of estimating solid concentrations, but because it has been used so often as a solid concentration measurement, it is presented here in connection with other solid concentration measurements. Local solid densities were measured with optic fibers.

4.3.1 Pressure

Pressure values were measured on five levels of the reactor. Pressure data was then analyzed by regression analysis in order to get functional form for pressure dependence as a function of height. Functional form of regression analysis was obtained by assuming solid density form presented by Brereton and Strömberg (1985).

$$\rho_r^{\epsilon} = a\ x^b \text{ , where} \qquad (4.1)$$

a, b are parameters

Solid density function was then transformed into pressure difference function according to equation

$$\frac{dp}{dx} = \rho_r^{\epsilon} g \quad , \text{ where g is gravitation constant} \qquad (4.2)$$

Pressure value is obtained by integrating pressure difference equation (4.2) over height

$$p = \int_0^h \frac{dp}{dx} dx = \int_0^h \rho_r^{\epsilon} g \, dx = \int_0^h a \, x^b \, dx = a' \, h^{b'} + c' \qquad (4.3)$$

Measured pressure data is then fitted according to equation (4.3) and parameter values are optimized by regression analysis. After that pressure difference or solid density profiles can be calculated from pressure profile function according to equations (4.2) and (4.1).

Pressure data was obtained by using solid inventories between 75 kg and 136 kg and different gas flow rates from 0.68 kg/s to 1.15 kg/s. Experimental pressure data is compared with regression analysis result in Figure 4.3. Example values for solid densities determined according to the above procedure are presented in Figure 4.8.

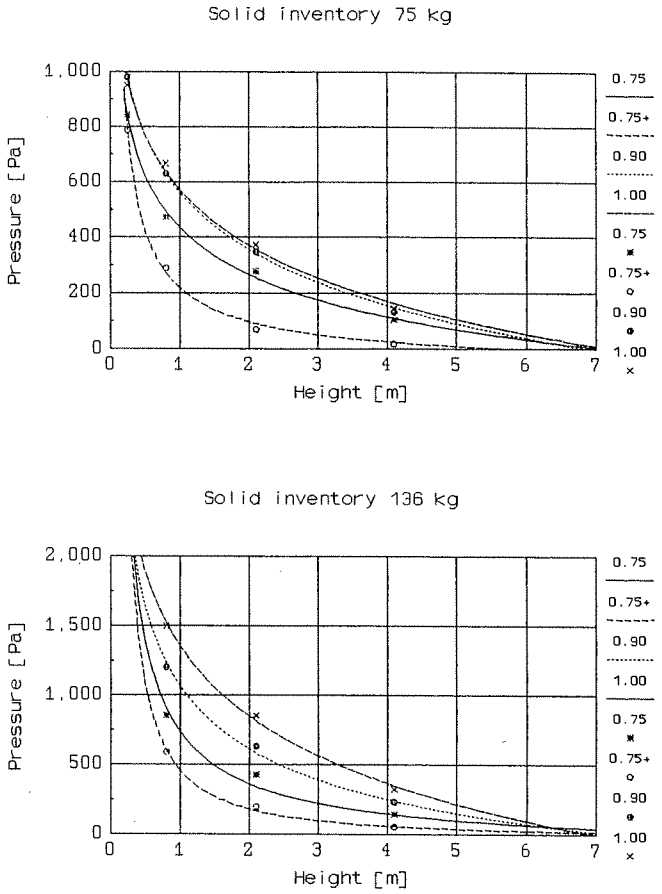

Figure 4.3 Pressure profiles, gas flow rate as a parameter (kg/s). Values with legend 0.75+ mean that secondary air has also been used with total gas flow rate 0.75 kg/s.

4.3.2 Radioactive tracer

Radioactive tracer measurements for solid density profile were accomplished by using Na-24 isotope, half-life of which is 15.0 h. Process material sample was activated in order to ensure, that tracer material would be representative. A sample was then fed into the reactor and after a transient time period radioactivity was measured from different levels of the reactor (1.2 m, 2.62 m, 4.23 m and 6.5 m above grate). Gas flow rate was used as an operational parameter in these experiments. The uncalibrated results of radiation intensity are presented in Figure 4.4.

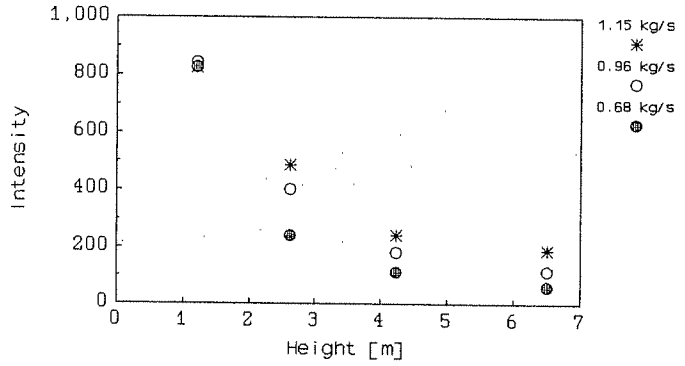

Figure 4.4 Detector signals from radioactive tracer tests

There is a functional relationship between the intensity of detecting device and solid density thus enabling the determination

of the solid density profile. One parameter value of relationship was calibrated from the pressure data. A gamma-ray NaI crystal scintillation probe was used for detecting the activity. It had a diameter of 7.5 cm and was covered by leaden collimator of opening angle 90 °.

The amount of radiation which hits the detector may be calculated when locally homogeneous solid density is assumed and attenuation coefficient of the material is known. If radiation balance is formulated, equation for intensity as a function of solid density for small cone collimator may be written, if radiation source as a linear function of solid density and attenuation are taken into consideration

$$I = ß\ (1-e^{-k\rho_s l})\ , \qquad (4.4)$$

where ß is function of activity of material and l is length of the measured zone.

The value given for glass beads, k=0.00744 m^2/kg [Seo 1985], is substituted for attenuation coefficient. Equation (4.4) shows, that for higher solid densities deviation from linear dependence between intensity of radiation and solid density increases. When calibrating the results, form of equation (4.4) was used. Thus number of unknown parameters in calibration function was only one.

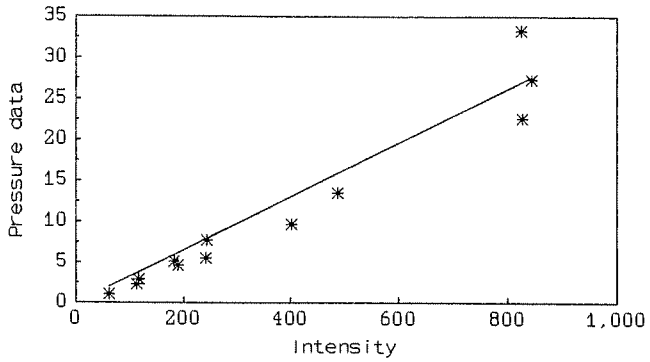

Figure 4.5 Calibration of radioactive tracer signals

Calibration of radiation intensity is illustrated in Figure 4.5. Calibration line has been assumed to go through origin, because the limit value of radioactive signal must be zero for zero solid density. Calibration coefficient can be obtained as a slope of regression analysis of intensity and pressure data. Solution of equation (4.4) gives then for the solid density

$$\rho_r^{\epsilon} = - \frac{\ln \left(1 - \frac{I}{\beta}\right)}{kl} \qquad (4.5)$$

According to equation (4.5) radioactive intensities may be transformed to solid density values, which are plotted in Figure 4.6 together with solid densities obtained from pressure profile. Solid density values in the upper part of the reactor are higher and in the bottom mainly lower for tracer-based densities.

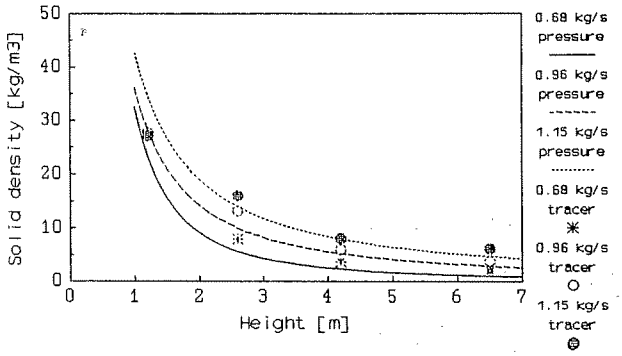

Figure 4.6 Solid densities determined from pressure data and from radioactive tracer

4.3.3 Radioactive transmission

Seo (1985) applied a gamma-ray absorption technique for solid density measurements in fluidized bed. He had a Cs-137 isotope radioactive source on one side of the reactor and a NaI scintillation detector was used on the other side to analyze transmitted radiation. Although analyzed intensity can be described by Beer's law, Seo calibrated the system by using a known material amount between source and detector.

A similar measuring and calibration method was used also in this study. It was found that the intensity analyzed by a detector was strongly dependent on the detector's position in plane perpendicular to the line between source and detector. In practice, it

was difficult to mount the detector and the source exactly to the same axis. Thus measuring analysis was modified so that during experiments radiation on each measuring point was first measured with an empty reactor in order to get a base value. Then during the operation, the detector values were compared with the base value and solid concentration was calculated according to this proportional ratio, which was also calibrated. In this way, the measuring system was not sensitive to detector position.

Measurements were made with two different solid inventories and with different gas flow rates. At each measuring level only one measuring point was used, which was in the middle of 1 m side of the reactor. Thus the results do not represent area average values and they must be interpreted as line average values of solid densities in the center of the reactor.

The measured solid density values are presented in Figure 4.7 for two different solid inventories with gas flow rates as parameters. Comparison of smaller solid inventory axial profiles with larger ones show clearly different shape. With smaller inventory there are minimum values of solid densities in the middle of the reactor, whereas with larger solid mass, densities are decreasing, when the height of the reactor is increasing. The highest point is in the region of exit conduit, in which flow is partly divided into certain flow patterns and thus line average values may deviate considerably from area averaged values. Lines in Figure 4.7 show the results of regression analysis with polynomials. These curves have been used later in chapter 5, when continuous functions of

solid density are needed for evaluation of model parameters.

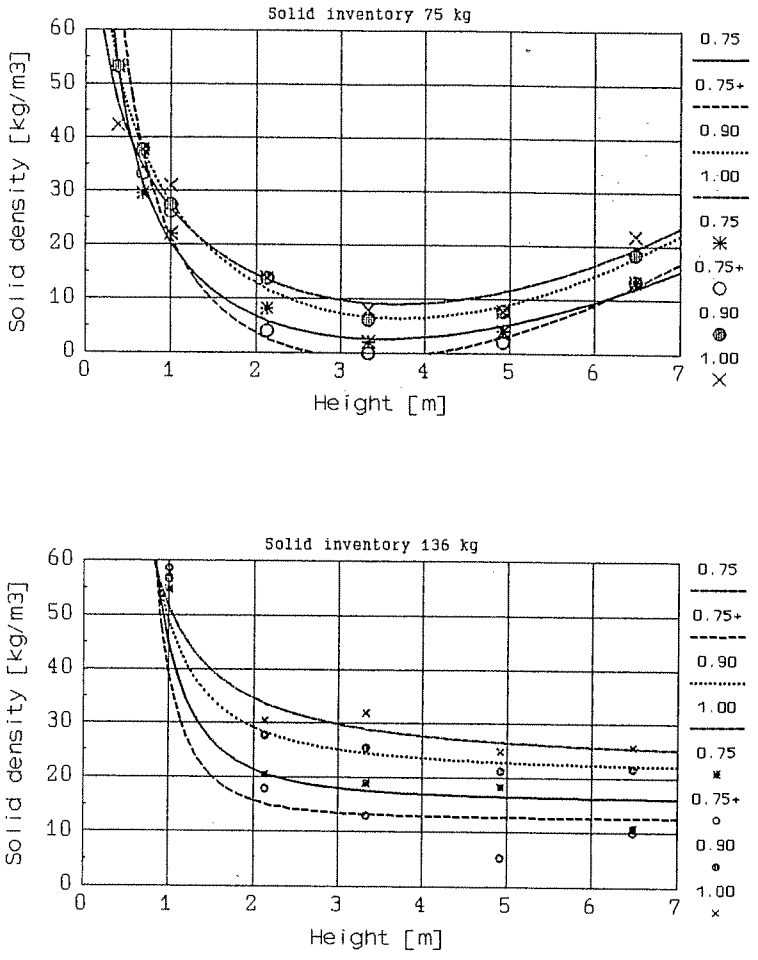

Figure 4.7 Solid density profiles from radioactive transmission measurements

In Figure 4.8 measured line-averaged solid density values are compared with solid densities obtained from pressure gradients. For both solid inventories and all gas flow rates pressure based

values are lower at the top of the reactor. A similar effect was also found in section 4.3.2 for tracer measurements.

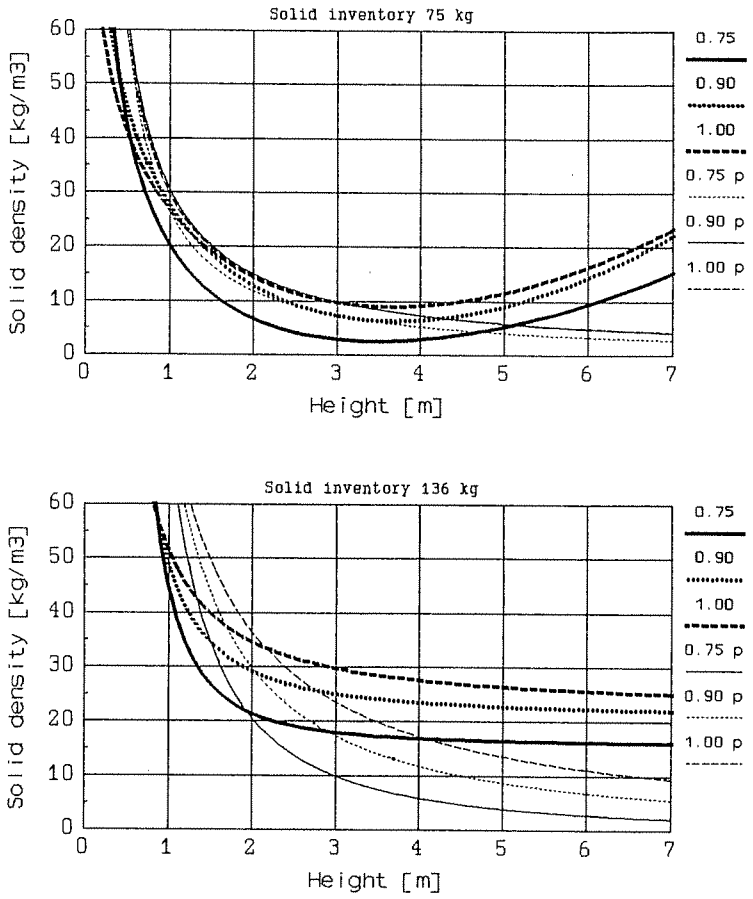

Figure 4.8 Solid density profiles from radioactive transmission and pressure data, p in the legend refers to pressure data

4.3.4 Optic fibers

Light scattering or transmission and fiber optical methods have been applied successfully to studies in bubbling fluidized beds and in dilute gas-solid flow applications [Hatano and Ishida 1983, Matsumoto et al. 1986, Matsuno et al. 1983, Morikawa et al. 1986, Oki et al. 1980]. Two main methods have been either based on light transmission from one probe into another or based on light reflection from particles back to light source probe. Depending on probe size, there has been measurements over different volumes thus giving a signal from one particle or swarm of particles. Single particle detecting gives particle number within time interval and thus particle velocities are required, if concentration of particles is needed. Detecting swarms of particles gives a signal, which is function of particle concentration. Thus probe data must be calibrated in order to find functional dependence.

After testing both the transmission and reflection principles with probe types presented in Figures 4.9 and 4.10 the latter was selected for this study. Probe diameter is 3 mm and it consists of fibers of diameter 70 μm, which are homogeneously divided into light source and receiver fibers. Modulated IR-light was used as a light source, which light was detected by photodiode and amplified according to light intensity.

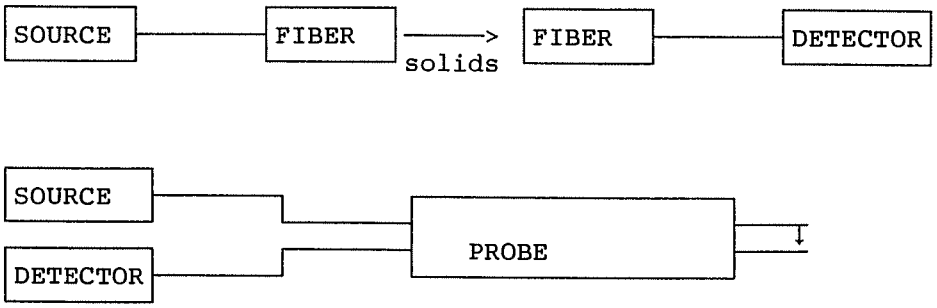

Figure 4.9 Transmission probe principle

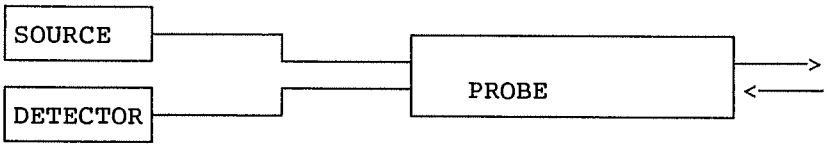

Figure 4.10 Reflection probe principle

Two different test run programs were carried out for measuring local solid densities with optic fibers. Functional dependence between solid density and output signal was first calibrated according to pressure profile data and then also a separate calibration device was used. During the latter measurements, velocity and solid density values were measured simultaneously, which allowed some qualitative conclusions about the dispersion

term in 1-dimensional solid momentum equation (3.51).

First optic fiber measurements were accomplished on three vertical levels 2.5 m, 4.4 m and 6.3 m. On each level there were eight measuring points as presented in Figure 4.11. Gas flow rate was used as a process variable. From each point measuring time was 20 s, providing time average values for solid densities. For calibration of optic fiber data, values on each level were integrated to give area averaged value. Solid density on a level was obtained from pressure data according to procedure presented in section 4.3.1. Correlation between optical values and solid density values calculated from pressure data is presented in Figure 4.12 having correlation factor 20.24 kg/m^3.

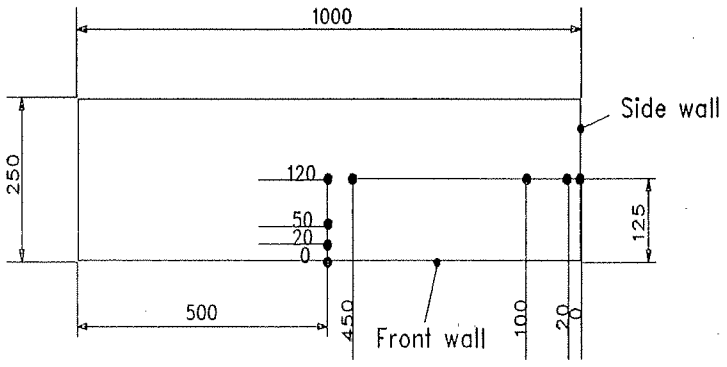

Figure 4.11 Optic fiber measuring points

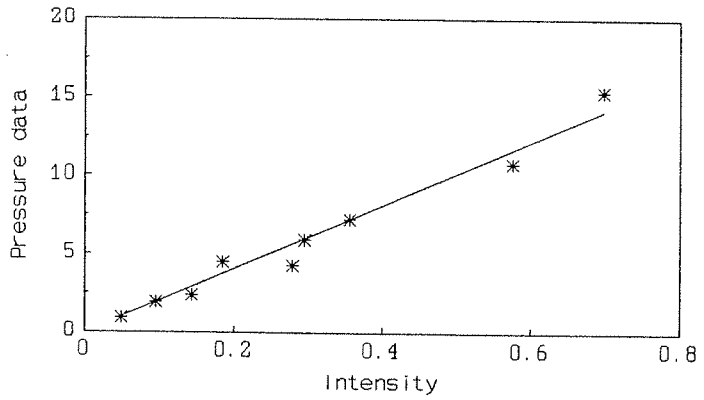

Figure 4.12 Calibration of optic fiber results with pressure data

Solid density profiles from optic fiber measurements are presented for each three levels and for three different gas flow rates in Figure 4.13. For each level there are two figures; one for wide side measurements and the other for the narrow side. For radial profiles figures show similar structure to qualitative results presented in earlier studies. The more dilute part is in the core of the reactor and there is quite a dense region within a few centimeters from the wall.

Because of the uncertainty of the previous calibration system, another method was used. A calibration device was constructed which produced falling solid flow due to gravitation. Mass flow rate divided by area was measured by weighing solid material in a vessel below the calibration point. Solid velocity was obtained with optic fibers by the aid of the method, which is presented in the next

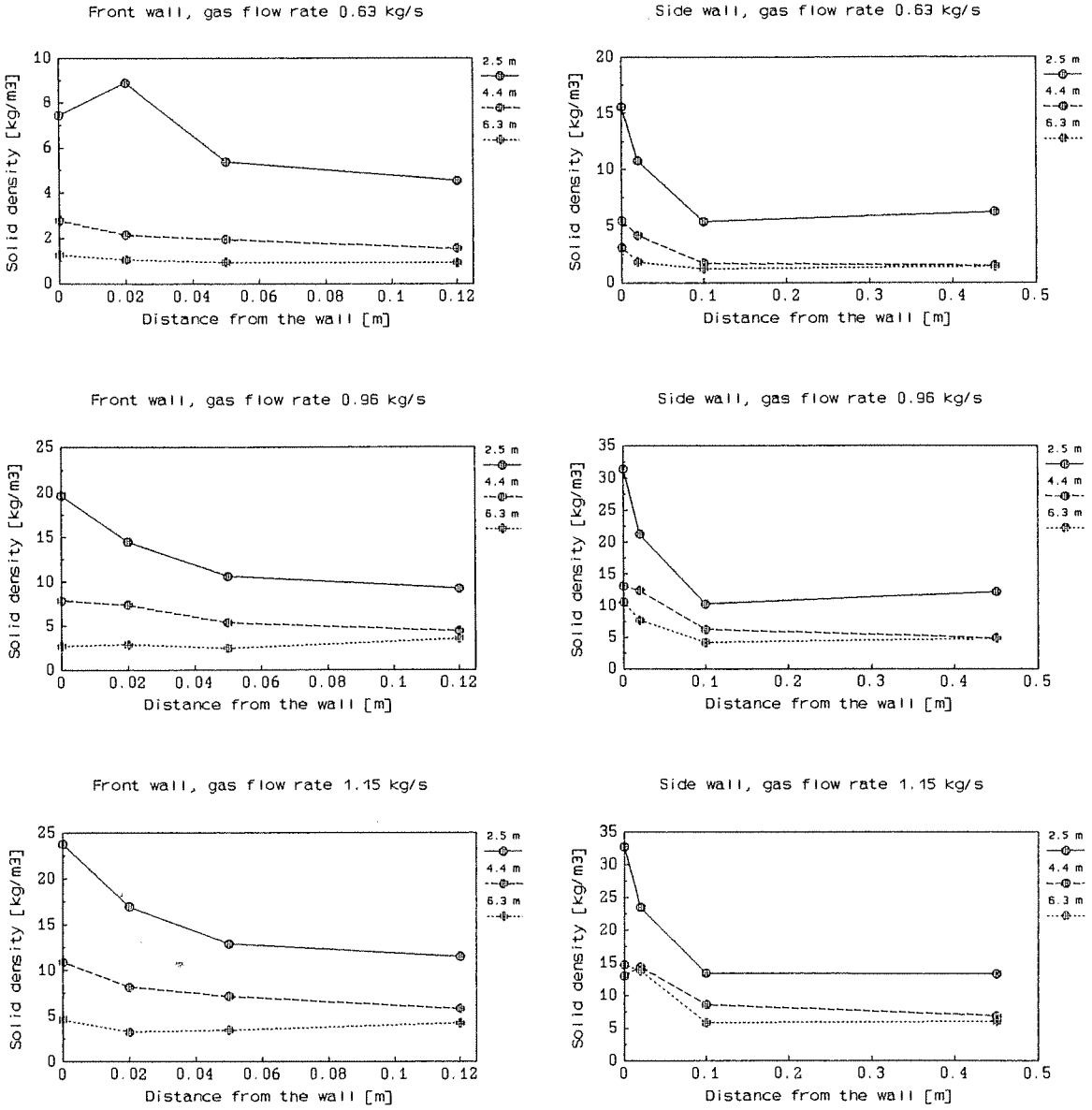

Figure 4.13 Horizontal solid density profiles, height as a parameter

section. Thus it was possible to calculate density at a certain point of flow. Intensity determined with optic fibers was also measured and that data was used in the calibration.

Using the latter method local densities were measured with two solid inventories 75 kg and 136 kg for gas flow rate 1.00 kg/s. The levels in the reactor were 1.0 m, 2.5 m, 4.4 m and 6.3 m and the points in cross-section were located as presented in Figure 4.14.

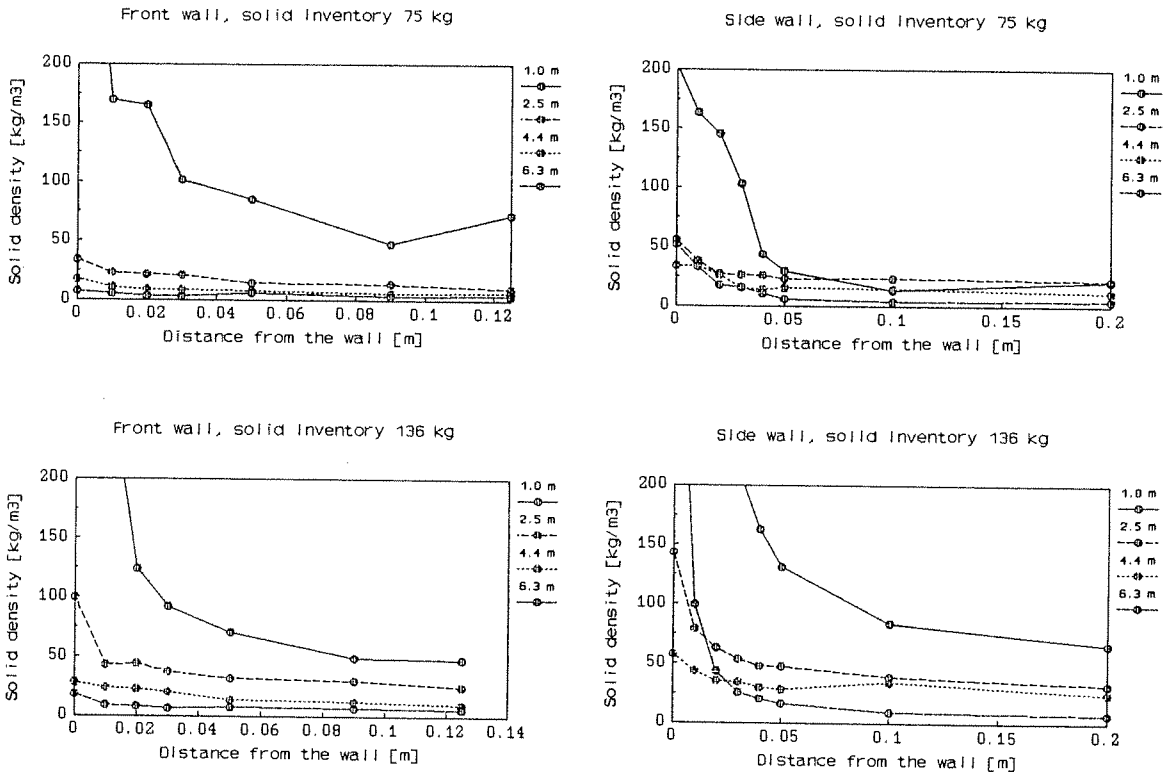

Figure 4.14 Horizontal solid density profiles, height as a parameter

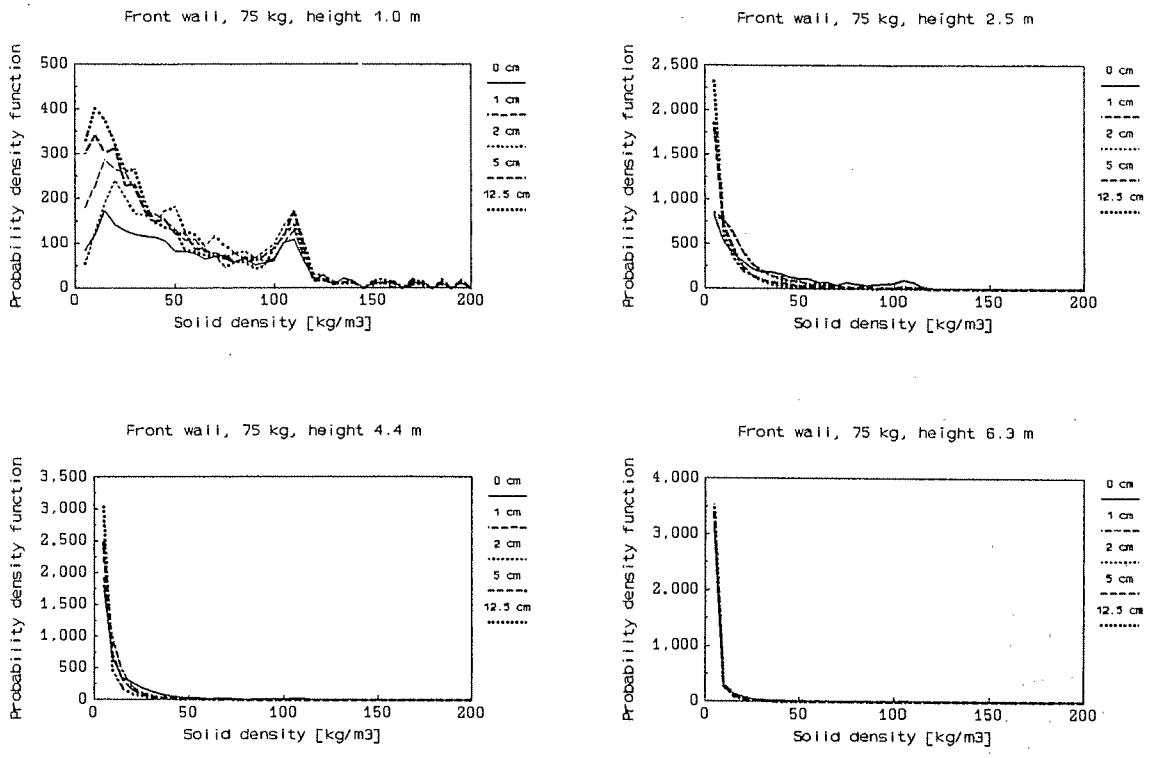

Figure 4.15 Probability density functions for solid inventory 75 kg and gas flow rate 1.00 kg/s, distance from the wall as a parameter

Probability density functions were also determined from different points of the reactor, which illustrates the stochastic nature of solid flow. Especially in lower parts of the reactor solid density values are changing a lot in one location, as can be seen in Figures 4.15 and 4.16. Horizontal location has also a clear effect on the form of the functions, so that near the wall different solid densities can be found, but in the middle of the

reactor mainly smaller solid densities.

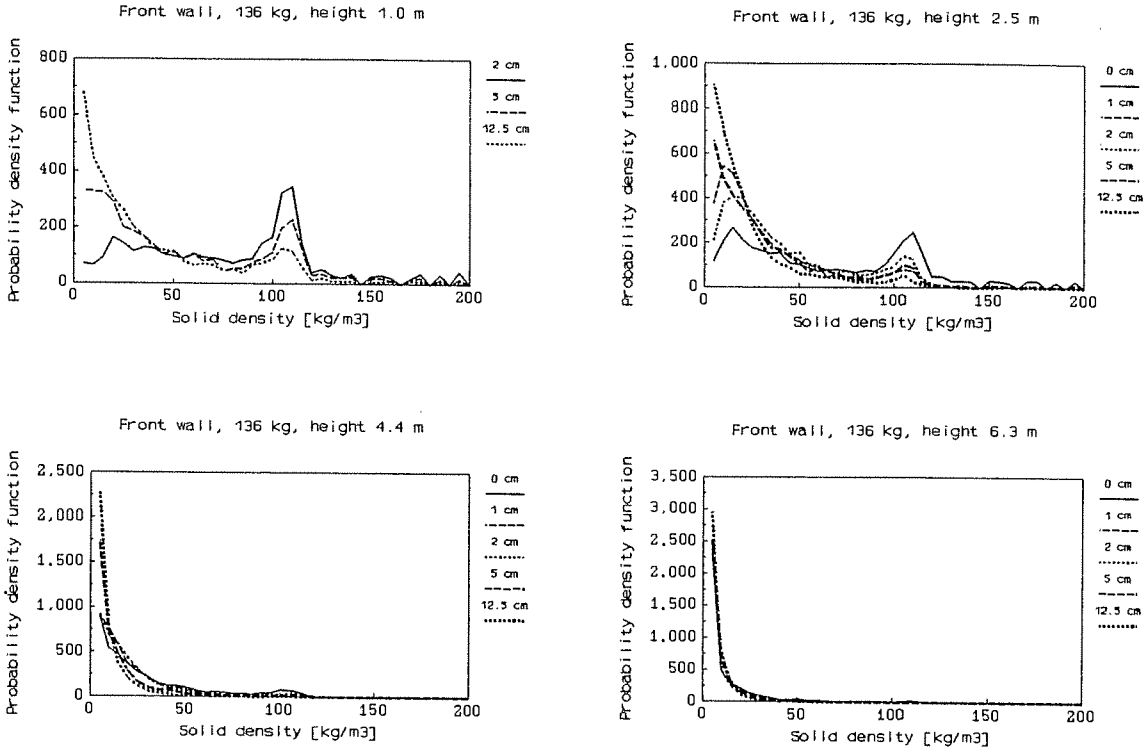

Figure 4.16 Probability density functions for solid inventory 136 kg and gas flow rate 1.00 kg/s, distance from the wall as a parameter

4.4 LOCAL SOLID VELOCITIES

Vertical components of particle velocities were measured by applying the same optical probe facility which was used to measure local solid densities. The principle was to measure fluctuating signals of two optical probes which were at certain distance l_v from each other. Solid material time delay from one point to another was then obtained by applying cross-correlation function

$$R_{xy}(\tau) = \int_{-\infty}^{\infty} x(t)y(t-\tau)dt \qquad (4.6)$$

where $x(t)$ and $y(t-\tau)$ are signals from two probes at time t and t-τ respectively. Cross-correlation function has maximum at average time delay τ_a and solid velocity may be calculated from the simple equation

$$v_r = \frac{l_v}{\tau_a} \qquad (4.7)$$

Experiments were accomplished with different gas flow rates 0.63 - 1.14 kg/s on levels 1.0 m, 2.5 m, 4.4 m and 6.3 m. Local values were measured from different points of cross-section respectively to solid density measurements. Time-averaged velocity profiles are presented in Figure 4.17 with experimental material, which is not stochastically representative having only 5-9 values for each point. For the smallest gas flow rate solid densities in the upper part of the reactor had so small fluctuation, that no clear time

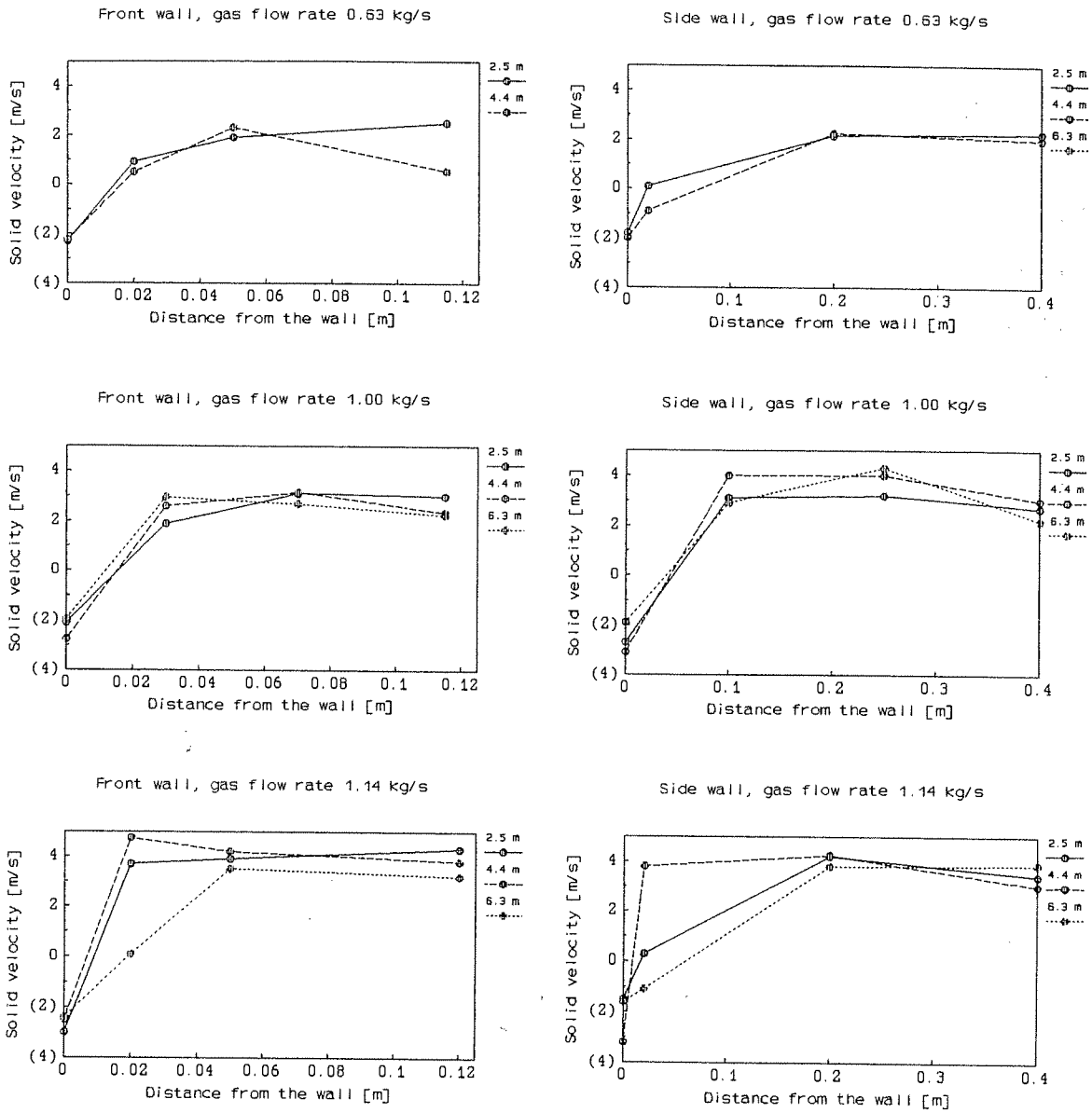

Figure 4.17 Horizontal solid velocity profiles, height as a parameter

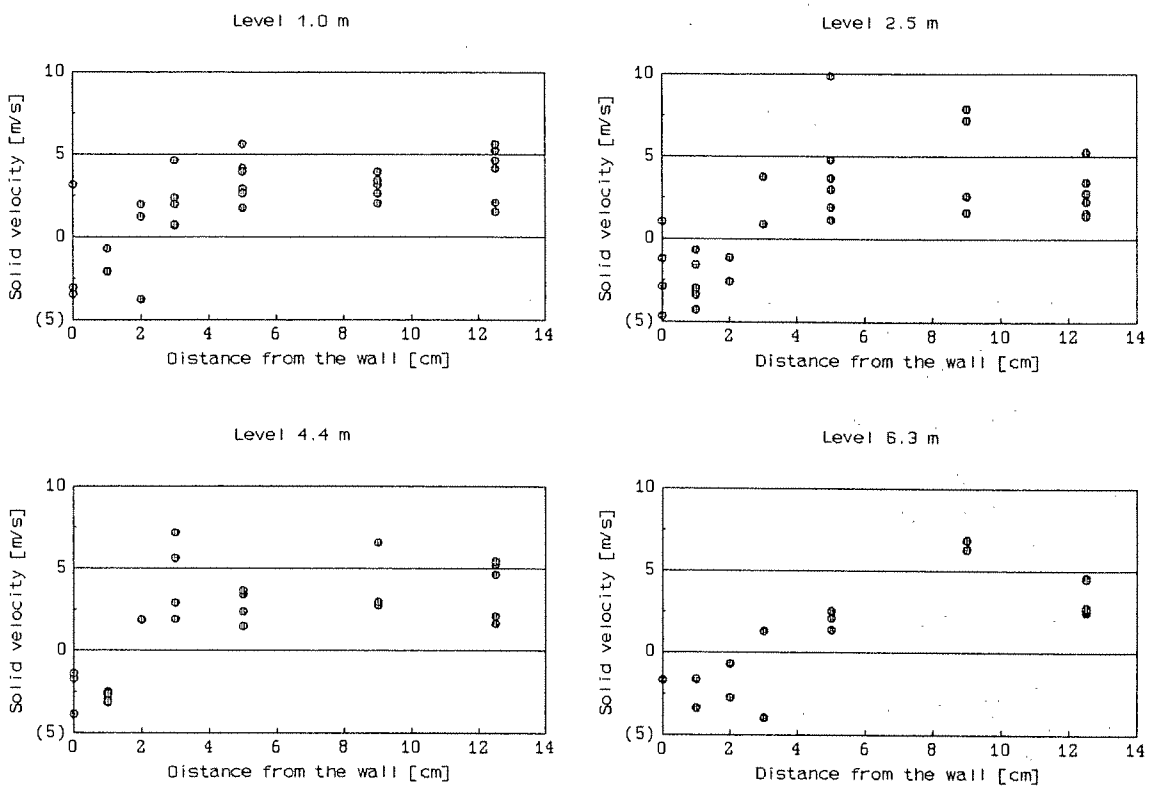

Figure 4.18 Local solid velocity values

delays were obtained with experimental facilities. Velocity values were fluctuating in each measuring point, especially a few centimeters out of the reactor wall, where large positive and negative values were found. Similar behavior has been presented recently also by Hartge et al. (1988), who reported that in their application, they detected both positive and negative velocity values in each measuring point. Solid velocities were found to be in some cases much higher than average gas velocity, which is an

indication of strongly nonuniform velocity profile also for gas. Figure 4.18 illustrates with one test run, how different the velocities are, even at the same measuring point.

Solid velocity values in Figure 4.17 are time average ones and they should not be interpreted as mass averaged values. For solid flow rate we may write

$$\dot{m}_r = \int_A \frac{1}{t} \int_t \varrho_r^{\epsilon} \underline{v}_r \, dt \, dA \tag{4.8}$$

If flow rate is presented with time averaged values

$$\dot{m}_r = \int_A \bar{\varrho}_r^{\epsilon} \underline{\bar{v}}_r \, dA + \int_A \frac{1}{t} \int_t \tilde{\varrho}_r^{\epsilon} \underline{\tilde{v}}_r dt \, dA \tag{4.9}$$

In equation (4.9) the latter term is fluctuating average term similar to single phase turbulent flow. From measurements it is possible to obtain values for total mass flow rate, time averaged density and velocity, and thus the last term is possible to determine from experimental data. Density profiles presented in section 4.3.4 are assumed to represent density profiles corresponding to velocity experiments. The results are presented in Table 4.2.

Table 4.2 Solid flow rates
f1 is the first term in r.h.s. of equation (4.9)
f2 is the second term in r.h.s. of equation (4.9)

gas flow rate kg/s	sol. flow rate kg/s	height m	f1 kg/s	f2 kg/s
1.14	2.45	2.5	10.10	-7.65
"	"	4.4	10.00	-7.55
"	"	6.3	3.37	-0.92
1.00	1.50	2.5	3.81	-2.31
"	"	4.4	3.31	-1.81
"	"	6.3	0.87	+0.63
0.63	0.30	2.5	2.25	-1.95
"	"	4.4	1.19	-0.89

Of the values of the second term it may be concluded, that fluctuation is extremely high and correlation is mainly negative indicating that high velocity values correspond mainly to low solid density values.

4.5 AXIAL SOLID MIXING

4.5.1 Equipment, arrangements

Mixing studies were accomplished by applying a radioactive tracer technique for solid material. The detectors used were described in section 4.3.2. A solid material sample was treated with radioactive material. Altogether there were ten detecting points for six detectors and five feeding points for samples. The feeding points in the reactor were located at the axial levels 1.0 m, 2.5 m, 4.4 m and 6.3 m. In addition there was one feeding point in the loop seal. Detector points were located in the reactor at the levels 1.20 m, 2.62 m, 4.23 m and 6.50 m , three points in the loop seal and one point after the cyclone, Figure 4.19. The position of six detectors were changed in different experiments according to position of feeding points.

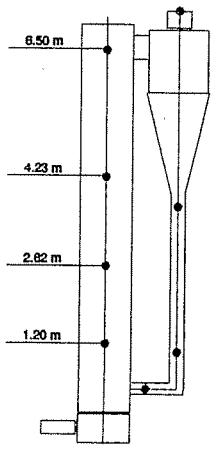

Figure 4.19 Location of radiation detectors

The same sand which was in the reactor as fluidized material was used as a solid tracer sample material. Tracer sample was fed into the reactor with probe system presented in Figure 4.20. Tracer was first fed into the probe from valve 3. Then the valve 3 was shut and compressed air was flowing to probe space through valve 2. Valve 2 was closed and a tracer sample was blown into the reactor by opening and closing the valve 1. The starting time of the tracer input was recorded with a detector, which was placed near the feeding point and concentration was recorded at five other points.

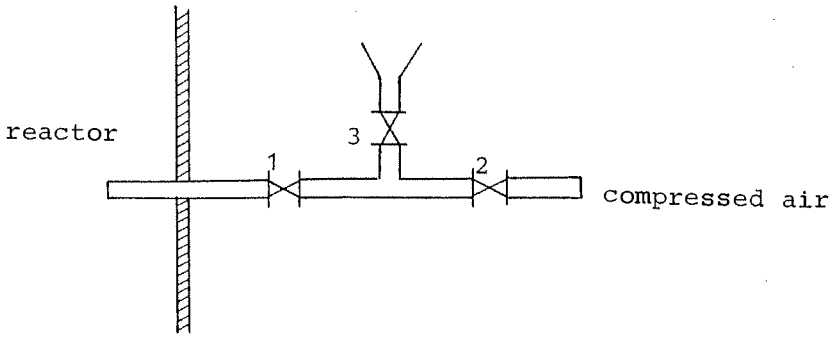

Figure 4.20 Tracer feeding probe

The particle size effect was also studied by feeding particles of three different size range divided by particle diameters 0.125 mm and 0.250 mm (less, middle, above ranges). These samples were fed into the reactor from the level 2.5 m. According to particulate solid flow theories, these samples should have quite a different behavior, which was to be tested with this experiment.

4.5.2 Results

Air flow in these experiments was 1.1 kg/s and total solid material amount in the system was 111 kg. In this connection only axial mixing data is reported.

Points 1, 4, 9 and 13 in the results correspond to reactor levels 1.2 m, 2.6 m, 4.2 m and 6.5 m for detectors and 1.0 m, 2.5 m, 4.4 m and 6.3 m for feeding points, respectively. Detector signal for point 1 is calibrated to have a much smaller coefficient for dependence between intensity and density than other detectors and thus direct quantitative comparisons for intensities may not be done. All detector signals are presented within an initial time period of 0-4 seconds, during which the material did not have time to recirculate back to the reactor, which was also confirmed by the detector in the loop seal.

Results showed that there was not a large variation between experiments, where the same feeding point had been used. In Figures 4.21 and 4.22 all the results from the same feeding point experiments have been combined to give average results for the feeding point. For each feeding point three similar tracer tests were done. Different test results are analyzed quantitatively in chapter 5, where dispersive mixing coefficients are determined.

The feeding of different particle sizes from feed point 4 did not show clear separation in behavior. Only slight differences may be seen in signals. Especially the starting time of the signal rise

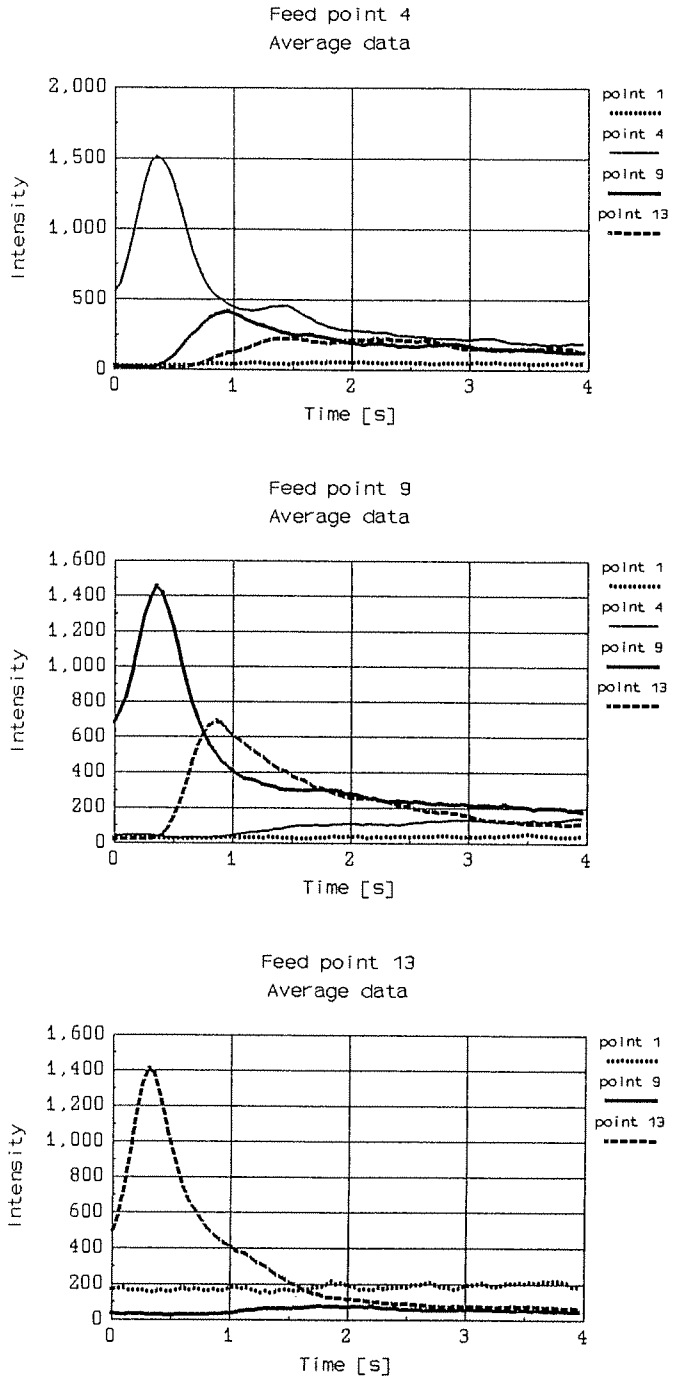

Figure 4.21 Experimental mixing curves for different feeding points

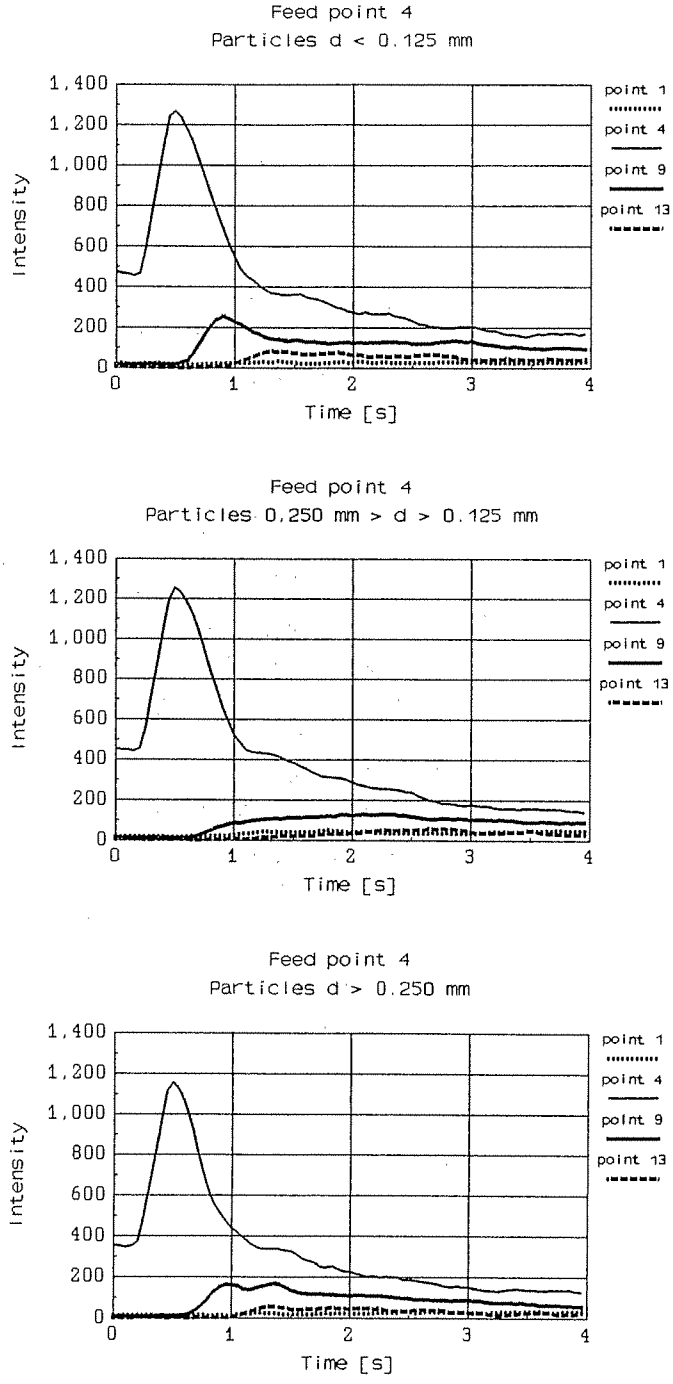

Figure 4.22 Experimental mixing curves for different particle sizes

on the respective levels is the same. The smallest particles seem to give more clear signal in the highest detector point (13), but in one of the experiments with largest particles the same effect was seen.

4.6 DISCUSSION ON EXPERIMENTS

In this chapter some promising measurement techniques have been tested and used for evaluation of overall and local variables of CFB cold model flow. Determination of accuracy of different methods is quite difficult, because there are no proven reliable ways of making comparable measurements. CFB process is very stochastic in nature and thus long measuring times are required especially for local variables in order to obtain enough information for a determination of necessary data. In addition to time-averaged values it seems that also different stochastic and correlation terms are needed to describe the process adequately.

Local values have been measured in this work by optical methods with optic fiber probes. Optical signals produce data with very high frequency, which can be utilized when different stochastic values are required. Solid density values have been measured applying the light reflection principle, which is easy to use in the evaluation of solid density values in different locations of the flow field. One of its main drawbacks seems to be difficulty

in calibrating the signals, especially for higher solid densities. In addition, calibration data is dependent on calibration material and conditions. Another problem is disturbances in the flow field due to measuring probes, the effect of which could not be reliably determined. A similar measuring principle can be utilized also in hot conditions, but then special heat resistant fiber materials are necessary.

Velocity values of solid material were determined by calculating cross correlation for two solid density signals. Thus each velocity value requires certain time for solid density data acquisition and signal analysis. In this work solid velocities were calculated separately after longer period of data acquisition. It was found that good correlation function was not always achieved. It seems however, that correlation can be improved by decreasing the distance between the probes and thus also automatic on-line measurements can be made for determination of solid velocity. That will require high data acquisition frequency, some 10 - 20 kHz for the conditions used in this work. For multidimensional solid velocity analysis more fibers are required for single velocity vector and signal analysis will become more complicated and slower. Also the problem of disturbance of the fibers will be worse.

Radioactive technique seems to be a useful method for the determination of macroscopic solid flow and especially mixing. The same equipment is viable also in hot conditions and large units. In the small cold model only axial mixing was studied, but especially in larger units also horizontal mixing can be deter-

mined. In order to measure average solid densities radioactive methods can be used to some degree. Calibration of signals may be difficult especially in large and hot units.

5. 1-DIMENSIONAL MODEL EVALUATION

5.1 LITERATURE REVIEW

Compared with multidimensional models one-dimensional models can be considered simple. That simplicity may be considered in some respect disadvantageous, but it has also many benefits. One-dimensional models have less parameters, which can more easily be obtained from experiments. It is not easy to obtain enough data for different model parameter evaluation, especially at this stage of knowledge about circulating fluid beds. One-dimensional models also require much less computing time allowing thus wide comprehensive model calculations. On the other hand they cannot straight calculate radial mixing or effects, which depend on radial profiles, at least without special modifications. So it must be approved that one-dimensional models are not optimal for all kinds of applications and purposes.

The most widely known one-dimensional flow model for circulating fluid beds is Kwauk's model [Li and Kwauk 1980, Kwauk et al. 1985]. The model is based on strongly intuitive equality of solid diffusion and buoyancy fluxes, which gives functional dependence between void fraction and height of the reactor. The function has four parameters, which are determined from experimental data. Thus Kwauk's model can, on the other hand, be considered as a suitable

functional form for experimental data fitting. A similar kind of functional form has also been presented elsewhere (Kato et al. 1988). Kwauk's model has also been used in CFB comprehensive combustion model by Weiss (1987).

Until now there has been only some attempts to model axial solid density and velocity profiles by using mass and momentum balance equations for gas and solids. One problem seems to have been, that there is found two separate balance flow states for one set of boundary conditions [Matsen 1988, Li et al. 1988] and a model for transition from more dense state to more dilute state has not been presented.

For pneumatic transport some one-dimensional model calculations have been presented based on hydrodynamic multiphase flow equations [Nakamura and Capes 1976, Arastoopour et al. 1982a, Adewumi 1985, de Souza and Santana 1986]. These models are not taking into consideration any dispersion term and they are mainly using particulate flow drag functions for gas-solid momentum interaction. Lian and Chen (1985) have used in their model changeable average drag coefficient, which has been evaluated according to experimental results. But they have not taken into consideration any dispersion terms due to aggregate flow profiles.

Mixing theories in one-phase flow are largely based on Taylor dispersion model [Taylor 1921, 1932, 1935], which have been presented e.g. in reference [Tennekes and Lumley 1987]. Combination of Taylor and mixing length theories gives correlation between turbulence variables and diffusivity for time-averaged one-phase

flow equations [Hintze 1975, Sato and Yamamoto 1987]. For space-averaged two-phase equations dispersive transport has been considered in porous media applications [Slattery 1981, Chang and Slattery 1987, Plumb and Whitaker 1987]. Different terms in averaged equations have been studied and it has been found that dispersive transport needs not always be Fickian.

Solid mixing modeling in CFB has not been studied much. More work has in the past been pointed to bubbling or turbulent fluidized beds. The first of the efforts were more concentrated on one-phase models, e.g. such as dispersion model and later on two-phase models [Potter 1971, van Deemter 1985]. For circulating fluidized bed experiments Avidan et al. (1982) tested a two-phase model presented by van Deemter, but the approach described his results only at the lowest superficial gas velocity. He also used a modified turbulent dispersion model similar to Taylor dispersion. He applied a steady state density fluctuation method described by Todes et al. (1972) to yield dispersion coefficient in the low gas velocity regimes.

5.2 MASS-AVERAGED MODEL

5.2.1 Parameter evaluation

The experimental data presented in chapter 4 has been used in the evaluation of mass averaged model of chapter 3 according to

equations (3.48)-(3.51) and (3.44)-(3.46). Known experimental values have been gas and solid mass flow rates, pressure profile and solid concentration, which have been obtained from experiments presented in chapter 4. Solid mass flow rate has been obtained from solid surface rise method and solid concentration according to radiative transmission results.

The order of the calculation procedure has been as follows:

1) solid fraction, eq. (3.46)

2) gas void fraction, eq. (3.44)

3) average gas density, eq. (3.45)

4) solid velocity, eq. (3.49)

5) gas velocity, eq. (3.48)

6) drag term, eq. (3.50) or (3.53)

7) turbulence term derivative, eq. (3.51) or (3.54)

Integration over height is needed for evaluating values for dispersion term. In order to get absolute values for the term, its level must be fixed at one point of reactor. Derivative values indicate, that the dispersion term divided by solid density has

maximum somewhere in the reactor and becomes smaller towards the bottom and top. In this connection the dispersion value was assumed fixed to zero at the top of the reactor.

In the upper parts of the reactor, flow conditions are not adequately described by 1-dimensional equations (3.53)-(3.56), because mass flow rates for gas and solid are not constant due to exit channel. If changes in convection and mass are taken into account, equations (3.40)-(3.43) may be written in the form

Mass balance

Continuum

$$\frac{d(\underline{\rho}_c^{\epsilon}\ \underline{v}_c)}{dx} + \underline{I}_c^w(1) = 0 \qquad (5.1)$$

Solid field

$$\frac{d(\underline{\rho}_r^{\epsilon}\ \underline{v}_r)}{dx} + \underline{I}_r^w(1) = 0 \qquad (5.2)$$

Momentum balance

Continuum

$$\frac{d(\underline{\rho}_c^{\epsilon} \underline{v}_c^2)}{dx} - \underline{T}_{cr}^{I} + \underline{\epsilon}_c \frac{dp}{dx} - \underline{\rho}_c^{\epsilon} g = 0 \qquad (5.3)$$

Solid field

$$+ \frac{d(\underline{\rho}_r^{\epsilon} \underline{v}_r^2)}{dx} + \frac{d\underline{C}_r^{T}(v)}{dx} + \underline{T}_{cr}^{I} + \underline{\epsilon}_r \frac{dp}{dx} - \underline{\rho}_r^{\epsilon} g - I_r^{w}(v) = 0 \qquad (5.4)$$

Pressure taps in the upper part of the reactor were located at the levels 4.1 m and 7.1 m. So, pressure profiles near the exit channel were smoothed when pressure data was fitted according to regression analysis. Because of the possibility of having varying gradients in pressure near exit channel, pressure profile was not used as a primary measurement value in parameter evaluation in the upper part of the reactor. Instead, drag coefficient variation was assumed linear between levels 4.1 m and 7.1 m and its value at the top was reiterated so that pressure at the top was the same as measured value.

As an example of the calculation procedure which was presented in the beginning of this section, calculated dispersion term and drag coefficient profiles are presented in Figures 5.1 and 5.2 for

solid inventory 136 kg and air flow rate 1.0 kg/s. Drag coefficient is calculated according to the definition in equation (3.47) and dispersion term is divided by solid density and thus its unit is m^2/s^2. Specific dispersion term seems to have low values near the bottom of the reactor, which may be due to similar phenomenon as is prevailing in single-phase turbulence. Any wall will damp velocity fluctuations near its surface and thus turbulence in single-phase flow and possibly also perpendicular solid phase dispersion as defined in this study has small values near the walls. The magnitude of the dispersion term seems to be quite high when compared with convective momentum term. It means, that if convective term is included into momentum equation, then the dispersion term should also be taken into consideration.

Drag coefficient for average-sized particle of sand is about 5 1/s according to correlation in equation (2.127). Calculation procedure has given values ranging between values 1 1/s and 4 1/s for the top and bottom of the reactor, indicating smaller values than single particle drag.

Profiles in the Figures 5.1 and 5.2 give some magnitude of the respective terms, but because at the moment accurate measurement techniques are not available for CFB hydrodynamics, the curves evaluated here cannot be considered accurate.

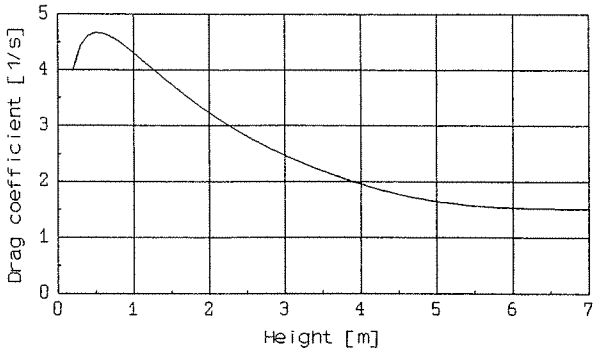

Figure 5.1 Drag coefficient as calculated from experimental data

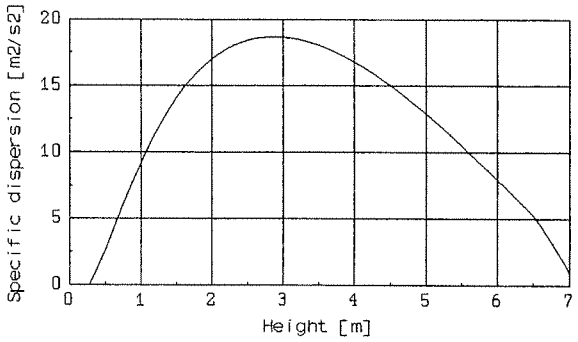

Figure 5.2 Specific dispersion as calculated from experimental data

Another method to determine dispersion term is to calculate it straight from local solid densities and velocities according to the equation (3.55). Dispersion term is next calculated according to data, the velocity values of which are presented in Figure 4.19.

Calculation results are given in Table 5.1.

Table 5.1 Calculated specific dispersion

Height [m]	Specific dispersion $[m/s]^2$
1.0	8.08
2.5	12.85
4.4	6.21
6.3	10.70

Velocity and solid density measurements of optic fibers are not fully developed at the moment and thus calculated dispersion terms give only magnitude of dispersion effect. Anyway, both of the two above methods give values of the same magnitude, which are significant when compared with convective momentum term.

Some qualitative approximation can be calculated also for drag coefficient, if equation (3.108) is used. Solid density data, which has been obtained with optic fibers has been used here as experimental data. As a result correction coefficient defined as a ratio of average and particulate drag coefficients is presented in Table 5.2.

Table 5.2 Calculated drag coefficient ratio

Height [m]	Drag coeff. ratio
1.0	0.181
2.5	0.073
4.4	0.042
6.3	0.027

The above-calculated values are based on an assumption of vertical flow only and no horizontal fluid dynamics is considered. Thus results give only some qualitative information about the variation of drag as a function of height showing that at the bottom region average drag has the highest values and at the top, smallest, which behavior is also seen in Figure 5.2. More exact average drag values could be determined according to similar 3-dimensional method, if 3-dimensional and transient solid flow profiles were known better.

5.2.2 Model calculations

For the solution of 1-dimensional flow equations, a finite difference code was developed. Stability of the calculation was reached by using staggered grid and upwind differencing for mass and momentum convection. In all calculations fixed solid inventory

in the reactor was used as a boundary condition, which is often the practice in commercial CFB combustors.

Because of the lack of experimental data a simple algebraic function model was used for dispersion term. Specific dispersion was assumed to be constant in free stream, but near the bottom it has been assumed to be damped. Correction function near the bottom has been of the form 1-exp(-x/X), where X is constant for damping distance.

Because of the limited experimental data also for drag coefficient, a model for it has been taken from correlations presented by Matsen (1982) and Sankar and Smith (1986). Extrapolation of their data to present study leads to meaningless values and thus the function form of drag correlation, which is used here, is based on 38.1 mm in diameter reactor data, where solid material has material density of 2.63 kg/m^3 and its average particle diameter is 0.173 mm.

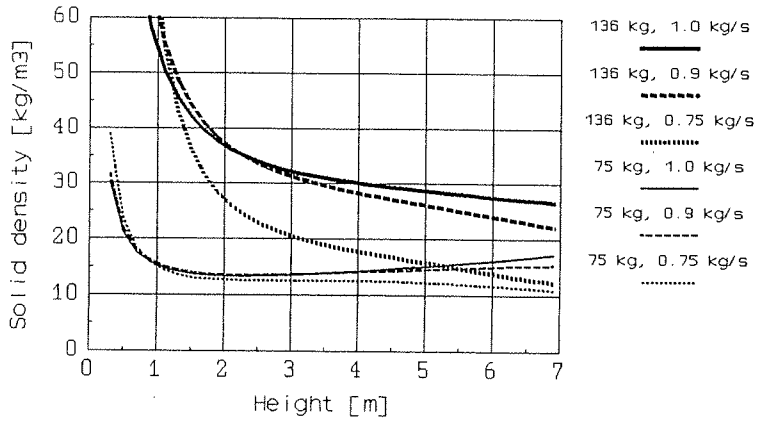

Figure 5.3 Calculated solid densities

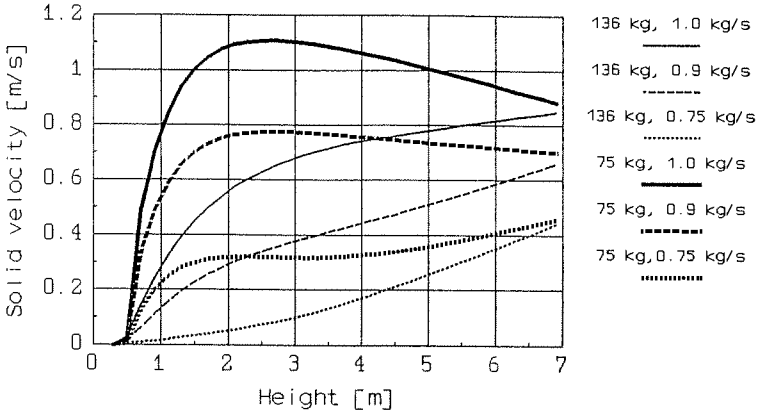

Figure 5.4 Calculated solid velocities

Some calculations have been done with the same boundary conditions as has been used in experimental work. Calculated cases have been with solid inventories of 75 kg and 136 kg and with gas flow rates of 0.75 kg/s, 0.90 kg/s and 1.00 kg/s.

Calculated solid densities and mass averaged solid velocities have been presented in Figures 5.3 and 5.4. For solid inventory 136 kg curves give similar results to experimental values. For solid inventory 75 kg solid densities near bottom drop too fast and because solid inventory has been fixed as a boundary condition, solid densities are too high in upper parts of the reactor. The difference in solid density profile can be explained with errors in drag and dispersion models. If drag term is modified so that it has smaller values, momentum balance gives smaller velocities in the bottom of the reactor. This causes solid density curves to drop in higher level and curves get closer to experimental values in the

bottom as presented in Figure 5.5. Also velocity profile changes into increasing curve as a function of height (Figure 5.6). Solid mass flow rates from calculated profiles and from experiments are presented in Figure 5.7.

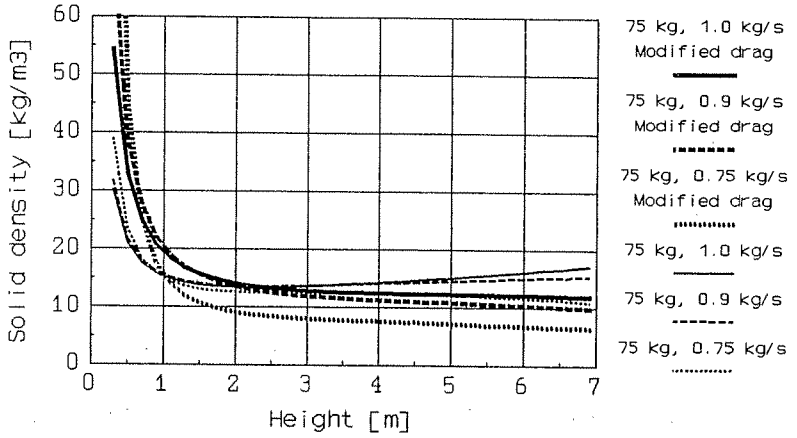

Figure 5.5 Calculated solid densities for solid inventory 75 kg, gas flow rate as a parameter

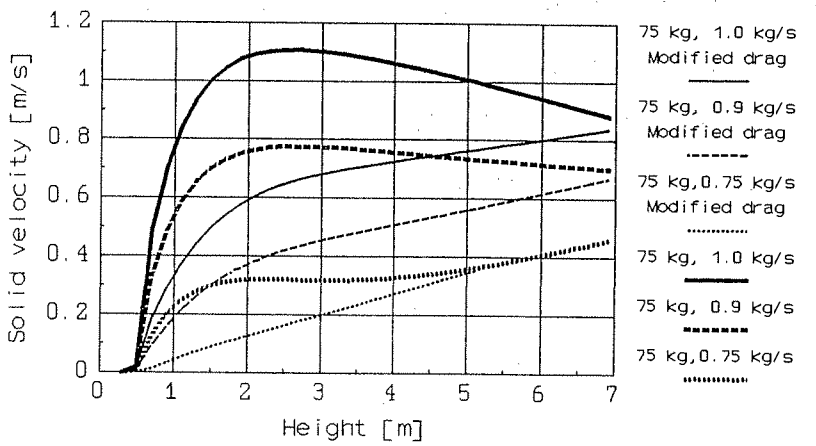

Figure 5.6 Calculated solid velocities for solid inventory 75 kg, gas flow rate as a parameter

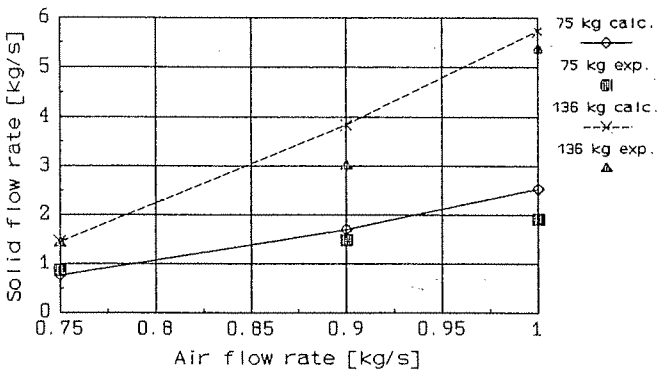

Figure 5.7 Calculated solid flow rates

A comparison of the calculated and experimental data shows, that calculated results are quite near the experimental ones. This indicates, that forms of drag term and dispersion models used in the calculations are realistic.

5.2.3 Qualitative model predictions

Flow model can be used for different kinds of parametric and sensitivity tests. Although at the moment tested submodels for average drag and dispersion are not available, some qualitative calculations can be done. In addition to using a flow model for extrapolation out of experimental range of data, drag and/or dispersion models can be matched to certain experimental profiles

in order to increase understanding of the magnitude and effect of drag and dispersion in flow dynamics.

As an example of applications of the flow model, qualitative trends of effects of solid inventory and dispersion term on flow profiles are studied in this section.

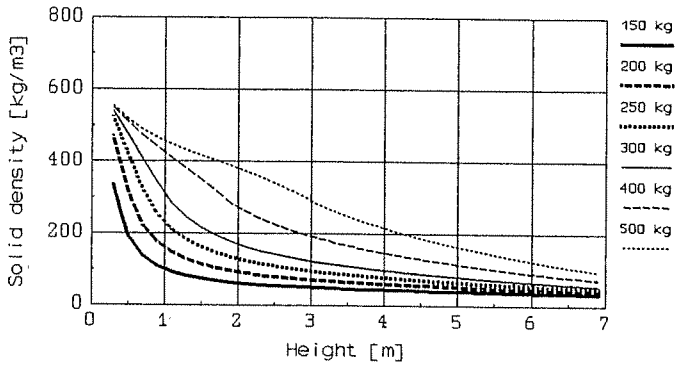

Figure 5.8 Calculated solid densities for different solid inventories

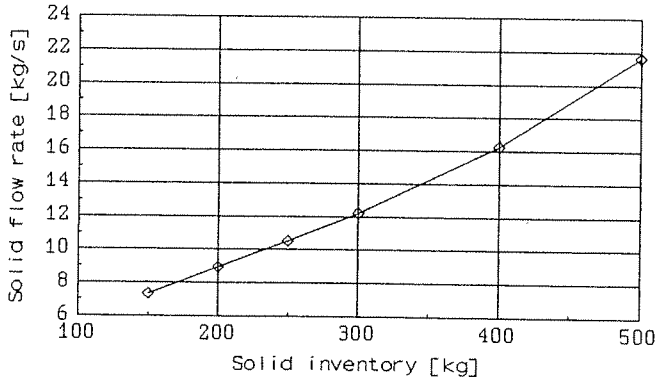

Figure 5.9 Calculated solid flow rates for different solid inventories

In Figures 5.8 and 5.9 solid density profiles and respective solid mass flow rates are presented for different solid inventories. Figure 5.10 presents the same calculation, but drag coefficient in calculation is smaller and the effect of bottom damping in the dispersion model is set to smaller value. This will increase solid density in the bottom and decrease it at the top, which leads to smaller solid flow rates. Also the inflection point for solid density can be seen in the largest solid inventory calculations, which has also been discovered experimentally in small cold models with small particles [Kwauk et al. 1985].

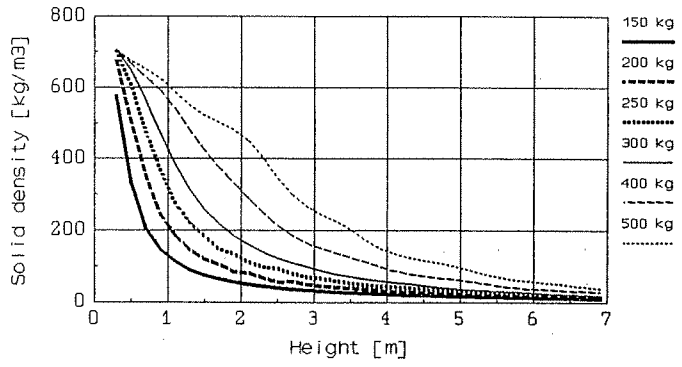

Figure 5.10 Calculated solid densities for different solid inventories applying modified drag coefficient

The effect of dispersion term magnitude is evaluated in Figure 5.11. The smaller the term, the sharper is the drop in solid density profile from dense region to dilute region. If the dispersion term reached zero, all the solids would be in dense

region and solid density profile would drop uncontinuously to value zero in upper parts of the reactor. In the smallest dispersion coefficient some unstable oscillation of solid density can be seen. It indicates that calculation method should be developed more stable, if smaller dispersion values are to be calculated.

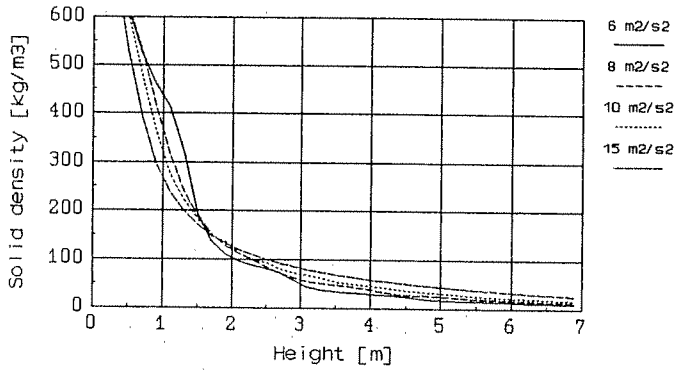

Figure 5.11 Calculated solid densities for different specific dispersion values

5.3 AXIAL SOLID MIXING

In this section the experimental mixing results of chapter 4 will be analyzed. Numerical values for mixing coefficients of certain mixing models are sought in order to quantify experimental data and also to study usefulness of mixing models.

Conservation equations for solid material and tracer material may be written

$$\int_{A_T} \rho \mathbf{v} \cdot \mathbf{n} dA = 0 \tag{5.5}$$

$$\int_{V_T} \frac{d\rho^*}{dt} dV = - \int_{A_T} \rho^* \mathbf{v}^* \cdot \mathbf{n} dA \tag{5.6}$$

As we are only interested in surfaces perpendicular to axial direction, only axial velocities are needed and velocity vectors can be replaced by scalar values.

Average values for density and velocity are defined as follows

$$\bar{\rho} = \frac{1}{A} \int \rho \, dA \quad , \quad \bar{v} = \frac{\int_A \rho \, v \, dA}{\bar{\rho} \, A} \tag{5.7), (5.8}$$

Convection flow for the tracer material may be written

$$\int_A \rho^* \mathbf{v}^* \cdot \mathbf{n} dA = \int_A \rho^* \, \bar{v} \, dA + \int_A \rho^* \, \tilde{v}^* \, dA = \bar{\rho}^* \bar{v} \, A + \int_A \rho^* \, \tilde{v}^* dA \tag{5.9}$$

where $\tilde{v}^*$ is fluctuating tracer velocity and is defined

$$\tilde{v}^* = v^* - \bar{v} \tag{5.10}$$

The first term in equation (5.9) for tracer concentration is convection caused by total mass average velocity and the latter is convection caused by tracer concentration and velocity deviation from average value. It can be considered to be due to two mass flow rates for opposite directions and that flux is often presented as a function of tracer concentration gradient according to dispersion model. In order to have zero dispersion flux, when concentration of tracer is constant, dispersion flux is expressed as

$$J_x = -D\rho \frac{d\alpha}{dx} \quad , \tag{5.11}$$

where tracer concentration is defined as follows

$$\alpha = \frac{\rho^*}{\rho}$$

and corresponding balance equation in differential form is

$$\frac{d\rho^*}{dt} = - \frac{d(\rho^* \bar{v})}{dx} + \frac{d}{dx} \left(D\rho \frac{d\alpha}{dx} \right) \tag{5.12}$$

The above equation is used to analyze experimental results presented in section 4.5. Velocity profile is obtained from experimental data by dividing solid mass flux by solid density.

The only parameter in the balance equation is the dispersion

coefficient, the value of which has been fitted by experimental data. Here we have assumed, that results may be presented and evaluated as one-dimensional, i.e. radial mixing does not effect. This may be assumed in this case, because of large height-to-width ratio and because the feeding system spreads tracer material into the cross-section of the reactor near the feeding point. Also it is assumed, that particles of this size accelerate infinitely fast (acceleration time is 0.2 s for the particles used in the experiments, if calculated for single spherical particle according to equation 2.127)

The solution of balance equation has been obtained by difference method allowing variation of velocity, density and dispersion coefficient. A solution respective to each feed point experiment has been calculated by using a constant dispersion coefficient. The matching criteria of calculated and experimental results has been the least square sum of differences between values within time period 0-3 s. Because of differences in detector calibrations, calculated values are scaled according to experimental values in such a way, that integrals of respective signals from 0 s to 3 s are the same. Thus different dispersion coefficients have been optimized for the experiments in feed point 4 by comparing calculated and measured values in points 1, 4 and 9, for feed point 9 in points 4, 9 and 13 and for feed point 13 in points 9 and 13. Results of the optimized calculations are presented in Figures 5.12-5.14.

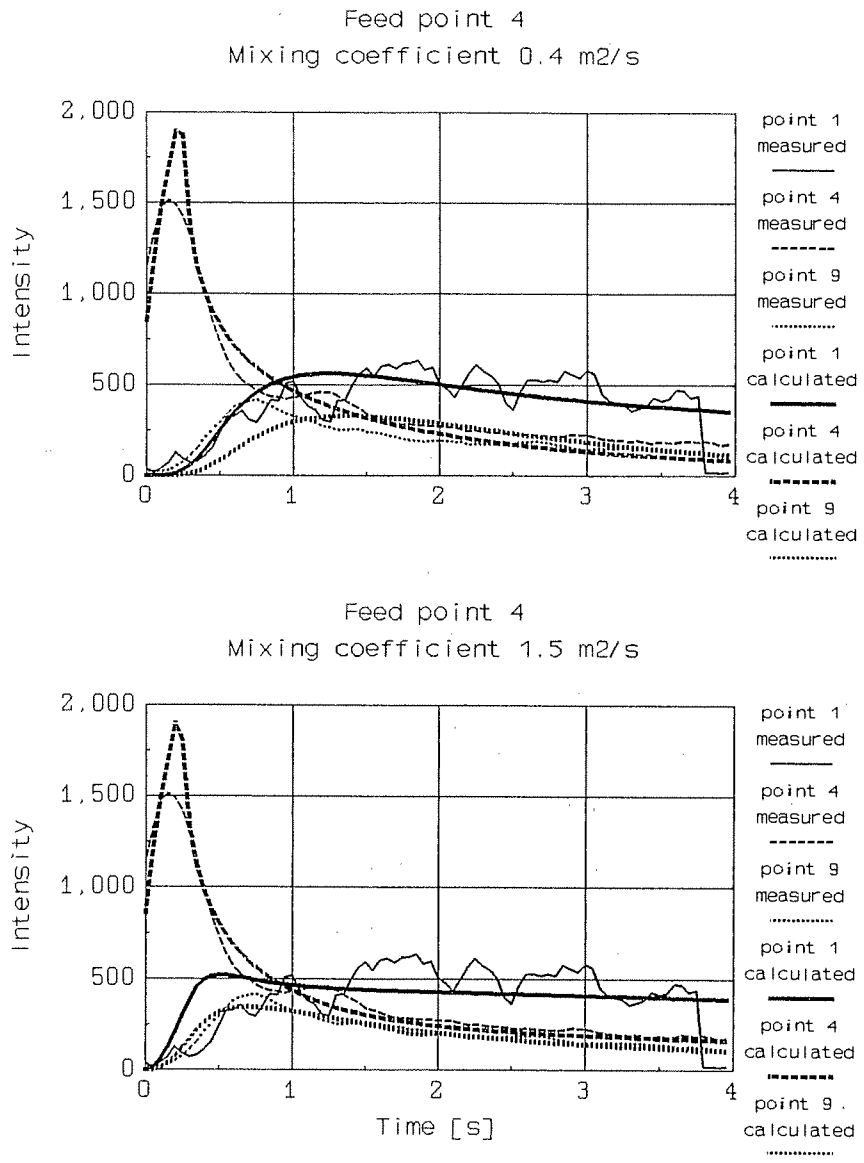

Figure 5.12 Calculated and measured mixing curves for the feeding point 4

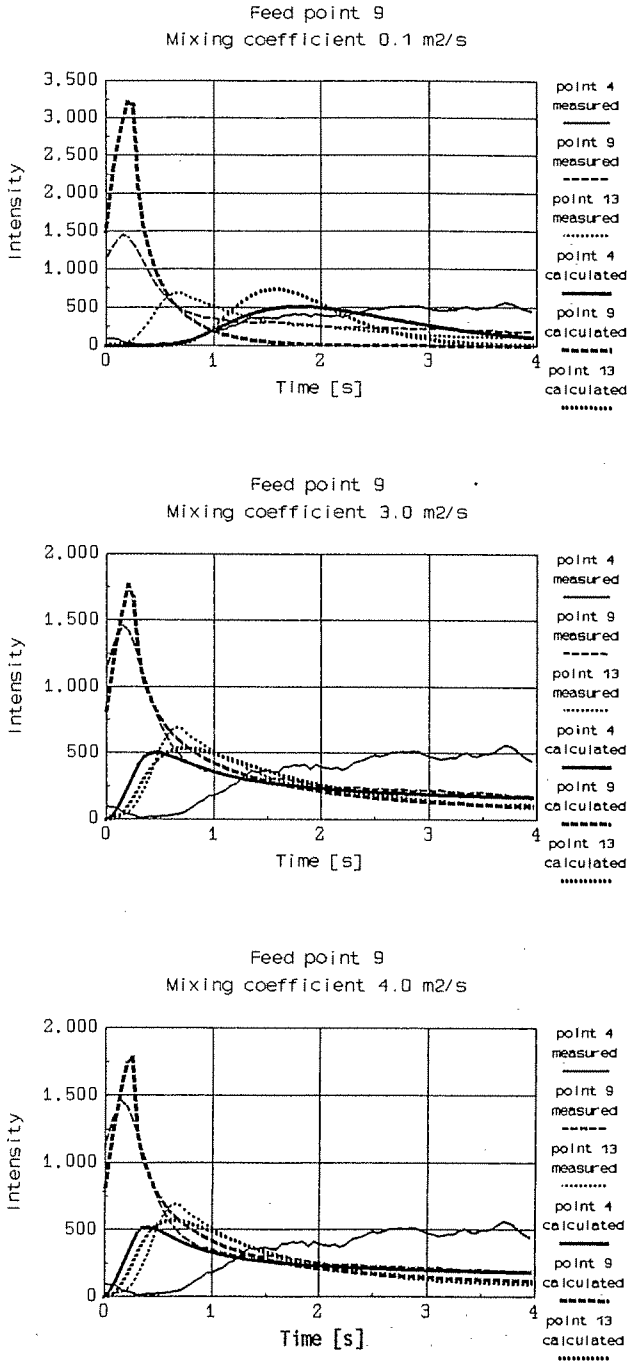

Figure 5.13 Calculated and measured mixing curves for the feeding point 9

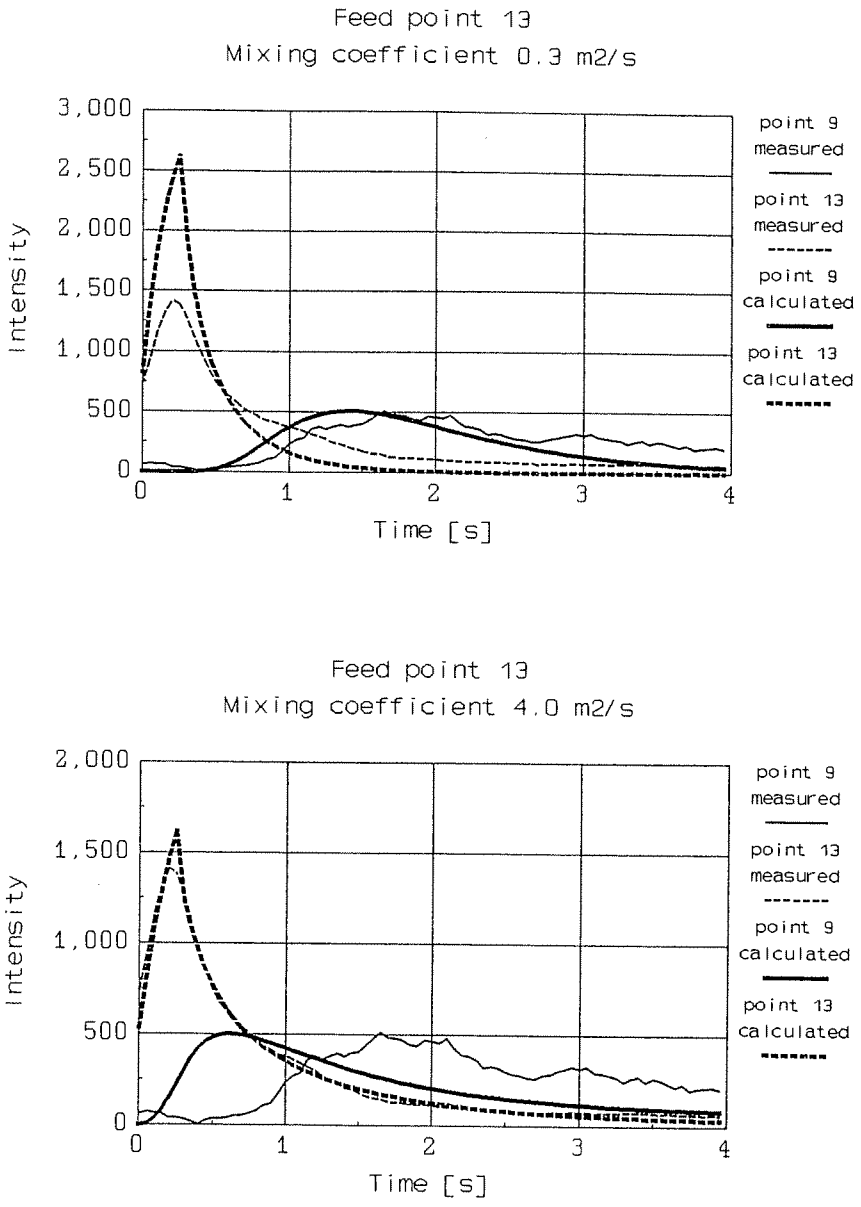

Figure 5.14 Calculated and measured mixing curves for the feeding point 13

In addition to quantitative values of dispersion coefficients, it can be seen, that dispersion coefficients for the points above the feeding point, and for the feeding point itself, are much higher than coefficients for the points below. Dispersion values of matching are presented below

$D_{4,1} = 0.4$ $D_{9,4} = 0.1$ $D_{13,9} = 0.3$

$D_{4,4} = 1.5$ $D_{9,9} = 4$ $D_{13,13} = 4$

$D_{4,9} = 1.5$ $D_{9,13} = 3$

where D_{ij} means optimal dispersion coefficient for detecting point j, when feed point has been i. Unit for the coefficients is m^2/s.

The main reason for the difference above between upward and downward mixing coefficient is due to difference between horizontal tracer concentration profile and average concentration in the reactor just after feeding moment. Although the tracer feed would homogeneously be divided into the reactor area, average velocity for the tracer would be different from reactor material velocity, because there is correlation between solid velocity and solid density. This can be illustrated by writing equations for velocities. If we assume that the tracer is homogeneously divided into the reactor area, we can write

$$\underline{v}^* = \int_A v \; dA \tag{5.13}$$

From two equations (5.8) and (5.13) may be obtained the difference between the material and tracer average velocities

$$\underline{v}^* - \bar{v} = \int_A v \; dA - \int_A \frac{\rho}{\bar{\rho}} \; v \; dA \tag{5.14}$$

According to experimental data there exists negative correlation between solid velocity and solid density. So from the above equation may be concluded, that at the start average tracer velocity is higher than average material velocity, if feeding is homogeneous. Thus dispersion model evaluation gives a result, that at the start mixing coefficient is smaller for mixing downwards and when tracer has spread out mixing is higher. This may be explained so, that at the start, the tracer average velocity is larger than the reactor material velocity and when the tracer mixes also with more dense reactor material and begins to take part into cluster flow its average velocity gets closer to material velocity. Convection is modeled with material average velocity in dispersion model and thus in order to obtain the correct result when compared with experiments, dispersion coefficient increases for upward flow and decreases for downward flow. Then when the tracer velocity begins to decrease, the artificial error in dispersion remains the

same and the difference between average material velocity and tracer velocity diminishes. Thus the model begins to give too small values for points below feeding point. This may be seen e.g. from Figure 5.13 (feed point 9), where at start (0-2 seconds) good correlation between measured and calculated value at point 4 using coefficient 0.1 m^2/s has been obtained, but then calculated value begins to decrease and measured value remains the same.

Separate tracer velocity has been used next in order to describe the mixing in a more realistic way. At the start velocity is assumed to have terminal solid particle velocity, which then linearly reaches average solid velocity value after certain initial mixing time. If particles at the start have more uniform velocity, then also mixing for the particles must be smaller. Thus also the mixing coefficient is assumed to change its value from minimum value to average value within the same time period as tracer velocity. Thus mixing coefficient and tracer velocity are both here assumed to be also time-dependent variables. The results of these model calculations are presented in Figures 5.15-5.17 using the same parameter value for all feeding points, which gives very good results when compared with measured values. Only for feeding point 9 is there more deviation between measured and calculated values. For feeding point 9 calculated intensity rises too fast for points below feeding point and too slowly for a point above it. Thus it can be concluded, that too small a tracer velocity has been assumed. It is then verified by increasing initial tracer velocity

and it shows, that curves get much nearer to experimental ones in Figure 5.18.

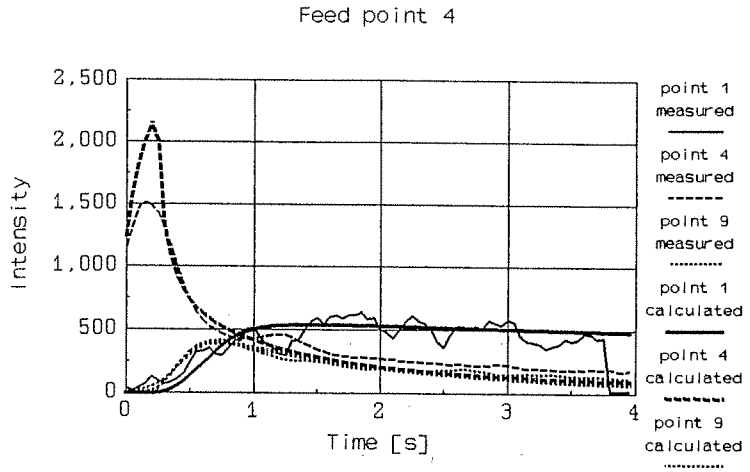

Figure 5.15 Calculated and measured mixing curves for the feeding point 4

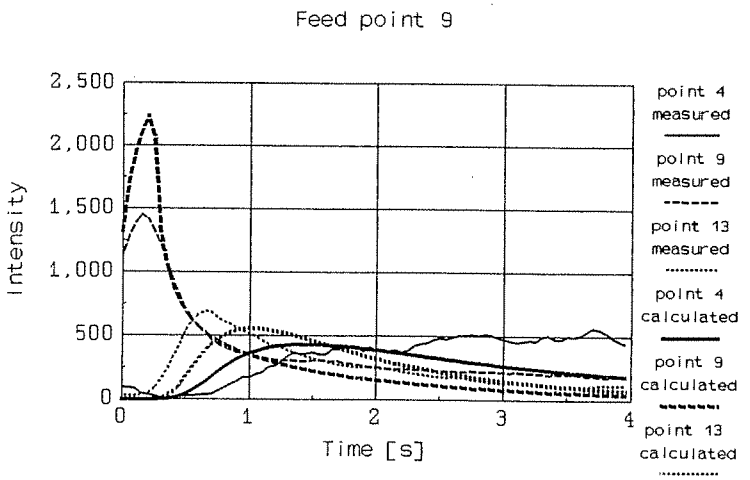

Figure 5.16 Calculated and measured mixing curves for the feeding point 9

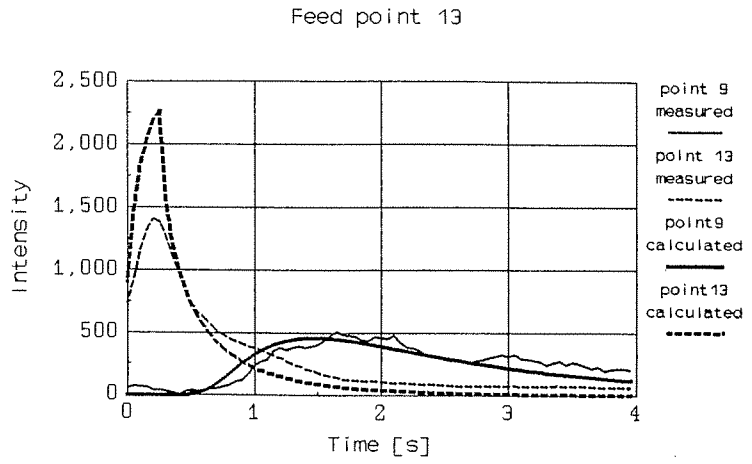

Figure 5.17 Calculated and measured mixing curves for the feeding point 13

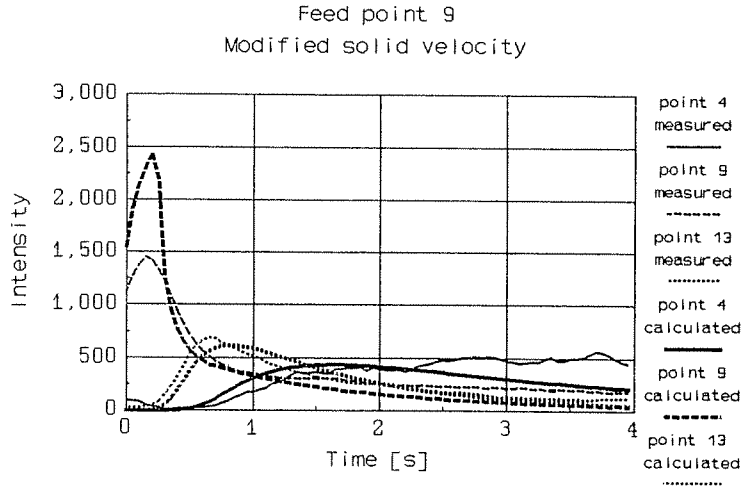

Figure 5.18 Calculated and measured mixing curves for the feeding point 9 with corrected initial tracer velocity

From the above results it can be concluded, that depending on the way, by which the tracer is fed into the reactor, it can

initially be mixed to the cross-section of reactor more or less representatively. In order to take into consideration the initial tracer flow, model parameters must be set according to tracer particles and not according to average solid values. But after a certain initial mixing time period, the tracer can be assumed to reach average solid flow conditions in the cross-sections of the reactor and then average values can be applied.

6. CONCLUSIONS

A method of formulating a theoretical equation set for multiphase gas solid flow has been presented. Applying general conservation principles with averaging definitions has lead into continuum integral and differential balance equations, which can be divided into physically reasonable and measurable terms. In addition, the usage of macroscopic averaging definitions with continuum equations has been found to be a systematic way for the construction of practical, engineering type of models for gas-solid multiphase flow. This has also been tested by applying the method to build up the model for non-reactive 1-dimensional CFB flow case. In general, also multi-dimensional macroscopic models can be derived applying similar method.

CFB cold model experimental set-up has been used to test some measuring techniques and also to evaluate behavior of gas-solid flow. Practical and useful results have been obtained both for overall and local flow quantities, but still a lot of development is needed for improving accuracy and viability of experimental methods for gas-solid flow.

1-dimensional model equations have been used to simulate experimental test runs. It has been shown that reasonable flow structure can be obtained by applying macroscopic gas-solid mass and momentum equations. The main difficulty in the modeling is the

lack of good experimental data for the parameter evaluation.

Also axial solid mixing has been modeled with mixing equation of dispersion type. Good results can be obtained, if experimental arrangements are modeled accurately. This has been shown by a comparison of model results with experimental mixing data.

The following recommendations are made for the future work in this area.

1. The development of experimental methods will be the first precondition to increase the knowledge of the CFB processes. Especially experimental techniques to measure flow values in large units and hot conditions are lacking, although they have the main industrial interest. Research groups should also be able to use larger test devices, in addition to scaling principles with dimensionless groups.

2. The solution and application of microscopic flow equations for gas-solid flow structures is under development. However, there are still barriers to that progress because of limited computer speed, unknown model terms and parameters, numerical stability and complexity of the methods. While these problems are being solved other simpler models are also needed to increase knowledge in this area. In formulation of these models, systematic handling of the general conservation principles forms the firm basis for physically realistic results and pure intuitive models should be avoided.

REFERENCES

Adewumi, M.A., 1985. Multiphase hydrodynamic modeling of vertical pneumatic conveying of solid particles., Ph.D. Thesis, Illinois Institute of Technology, Chicago, Illinois, 310 p.

Anderson, T.B. & Jackson, R., 1967. A fluid mechanical description of fluidized bed. I.&E.C. Fundamentals **6**, 4, pp. 527-539

Arastoopour, H. & Cutchin, J.H., 1985. Measurement and analysis of particle-particle interaction in a cocurrent flow of particles in a dilute gas-solid system. Chem. Engng Sci. **40**, 7, pp. 1135-1143

Arastoopour, H., Lin, S.-C. & Weil, S.A., 1982a. Analysis of vertical pneumatic conveying of solids using multiphase flow models. AIChE J. **28**, 3, pp. 467-473

Arastoopour, H., Wang, C.-H. & Weil, S.A., 1982b. Particle-particle interaction force in a dilute gas-solid system. Chem. Engng Sci. 37, 9, pp. 1379-1386

Arena, U., Cammarota, A. & Pistone, L., 1985. High velocity fluidization behavior of solids in a laboratory scale circulating bed. in Proc. 1st Int. Conf. on Circulating Fluidized Beds, Halifax, Nova Scotia, ed. Basu,P., Pergamon Press, pp. 119-125

Arpaci, V.S. and Larsen, P.S., 1984. Convection heat transfer. Prentice-Hall, New Jersey, 512 p.

Atkinson, C.M. & Clark, N.N.,1986. The analysis of fluidized bed behaviour using probes. Proc., Powder & Bulk Solids Conference, May 13-15, O'Hare Exposition Center, Rosemount, Illinois, 1986

Avidan, A.A., Weinstein, H. & Graff, R.A., 1981. Solids backmixing in high-velocity beds. DOE-Report DOE/MC/14875-1373, 205 p.

Avidan, A.A. & Yerushalmi, J., 1982. Bed Expansion in High Velocity Fluidization. Powder Tech. **32**, pp. 223-232

Avidan, A.A. & Yerushalmi, J., 1985. Solids mixing in an expanded top fluid bed. AIChE Journal, 31, 5, pp. 835-841

Bachmat, Y. & Bear, J., 1986a. Macroscopic modelling of transport phenomena in porous media. 1: The continuum approach. Transport in Porous Media, 1, pp. 213-240

Bachmat, Y. & Bear, J., 1986b. Macroscopic modelling of transport phenomena in porous media. 2: Applications to mass, momentum and energy transport. Transport in Porous Media, 1, pp. 213-240

Banerjee, S. & Chan, M.C., 1980. Analysis of the averaged and local instantaneous formulations. Int. J. Multiphase Flow 6, pp. 1-24

Bedford, A. & Drumheller, D.S., 1983. Theories of immiscible and structured mixtures. Int. J. Engng Sci. 21, 8, pp. 863-960

Berker, A. & Tulig, T.J., 1986. Hydrodynamics of gas-solid flow in a catalytic cracker riser: Implications for reactor selectivity performance. Chem. Engng Sci., 41, 4, pp. 821-827

Bingyu, C. & Kwauk, M., 1985. Generalized fluidization of nonideal systems. in Proc. 1st Int. Conf. on Circulating Fluidized Beds, Halifax, Nova Scotia, ed. Basu,P., Pergamon Press, pp. 33-62

Bouré, J.A., 1979. On the form of the pressure terms in the momentum and energy equations of two-phase flow models. Int. J. Multiphase Flow 5, pp. 159-164

Bowen, R.M.,1976. Theory of mixtures in continuum physics. ed. Eringen ,A.C., Vol.III, pp. 1-127

Brady, J.F. & Bossis, G., 1985. The rheology of concentrated suspensions of spheres in simple shear flow by numerical simulation. J. Fluid Mech. 155, pp. 105-129

Brereton, C. & Strömberg, L., 1985. Some Aspects of the Fluid Dynamic Behaviour of Fast Fluidized Beds. in Proc. 1st Int. Conf. on Circulating Fluidized Beds, Halifax, Nova Scotia, ed. Basu,P., Pergamon Press, pp. 133-144

Chan, R.K.-C., & al., 1982. Computer modeling of mixing and agglomeration in coal-conversion reactors. DOE-Report DOE/ET/10329-1211, Vols. 1, 2

Chang, S.-H. & Slattery, J.C., 1987. A new description for dispersion. in AIChE Annual Meeting, New York, NY, Nov. 15-20, 1987

Chawla, T.C. & Ishii, M., 1980. Two-fluid model of two-phase flow in a pin bundle of a nuclear reactor. Int. J. Heat Mass Transfer 23, pp. 991-1001

Cheremisinoff, N.P., 1986. Review of experimental methods for studying the hydrodynamics of gas-solid fluidized beds. Ind. Eng. Chem. Process Des. Dev. 25, pp. 329-351

Couderc, J.-P., 1985. Incipient fluidization and particulate systems. in Fluidization, Davidson, J.F., Clift, R. & Harrison, D., Eds., Academic Press, London, pp. 225-291

Crapiste, G.H., Rotstein, E. & Whitaker, S., 1986. A general closure scheme for the method of volume averaging. Chem. Engng Sci. 41, 2, 1986, pp. 227-235

Cushman, J.H., 1982. Proofs of the volume averaging theorems for multiphase flow. Adv. Water Resourc. 5, pp. 248-253

De Souza, S.G.U. & Santana, C.C., 1986. Modeling and simulation of the vertical countercurrent and cocurrent gas-solids flow. ASME FED - Vol 35, (Gas Solid Flows - 1986), pp. 157-161

Delhaye, J.M., 1977. Space-averaged equations. in Two-phase flows and heat transfer, Kakac, S., Mayinger,F. and Veziroglu, T.N., eds., Vol. 1, Hemisphere, Washington, pp. 81-90

Dobran, F., 1981. On the concistency conditions of averaging operators in 2-phase flow models and on the formulation of magnetohydrodynamic 2-phase flow. Int. J. Engng Sci. **19**, pp. 1353-1368

Dobran, F., 1984. Constitutive equations for multiphase mixtures of fluids. Int. J. Multiphase Flow **10**, 3, pp. 273-305

Dobran, F., 1985. Theory of multiphase mixtures. Int. J. Multiphase Flow 11, 1, pp. 1-30

Drew, D.A., 1971. Averaged field equations for two-phase media. Studies in Appl. Math. L, 2, pp. 133-166

Drew, D.A. & Lahey, R.T., 1979. Application of general constitutive principles to the derivation of multidimensional two-phase flow equations. Int. J. Multiphase Flow **5**, pp. 243-264

Drew, D.A. & Segel, L.A., 1971a. Averaged equations for two-phase flows. Studies in Appl. Math. L, 3, pp. 205-231

Drew, D.A. & Segel, L.A., 1971b. Analysis of fluidized beds and foams using averaged equations. Studies in Appl. Math. L, 3, pp. 233-25

Drumheller, D.S. & Bedford, A., 1980. A thermomechanical theory for reacting immiscible mixtures. Arch. Rational Mech. Anal. **73**, pp. 257-284

Dry, R.J., 1986. Radial concentration profiles in a fast fluidized bed. Powder Tech. **49**, pp. 37-44

Elghobashi, S.E. and Abou-Arab, T.W., 1983. A two-equation turbulence model for two-phase flows. Phys. Fluids, **26**, pp. 931-938, 1983

Eringen, A.C. & Ingram, J.D., 1965. A continuum theory of chemically reacting media. Int. J. Engng Sci. 3, pp. 197-212

Ettenhadieh, B., 1982. Hydrodynamic analysis of gas-solid fluidized beds. Ph.D. Thesis, Illinois Institute of Technology, Chicago, Illinois, 149 p.

Gidaspow, D., 1986. Hydrodynamics of fluidization and heat transfer:Supercomputer modeling. Appl. Mech. Rev. 39, 1, pp. 1-23

Goodman, M.A. & Cowin, S.C., 1972. A continuum theory for granular materials. Arch. Rational Mech. Anal. 44, pp. 249-266

Gray,W.G., 1975. A derivation of the equations for multi-phase transport. Chem. Engng Sci. 30, pp. 229-233

Gray, W.G., 1983. Local volume averaging of multiphase systems using a non-constant averaging volume. Int. J. Multiphase Flow 9, 6, pp. 755-761

Gray, W.G. & Lee, P.C.Y., 1977. On the theorems for local volume averaging of multiphase systems. Int. J. Multiphase Flow 3, pp. 333-340

Gupta, A.K. & Lilley, D.G., 1985. Flowfield modeling and diagnostics. Abacus Press, Kent, 414 p.

Han, G.Y., Lee, G.S & Kim, S.D., 1985. Hydrodynamic characteristics of a circulating fluidized bed. Korean J. of Chem. Eng., 2, 2, pp. 141-147

Hartge, E.-U., Li, Y. & Werther, J., 1985. Analysis of the local structure of the two phase flow in a fast fluidized bed. in Proc. 1st Int. Conf. on Circulating Fluidized Beds, Halifax, Nova Scotia, ed. Basu,P., Pergamon Press, 1985, pp. 153-160

Hartge, E.-U., Li, Y. & Werther, J., 1986. Flow Structures in Fast Fluidized Beds. in Fluidization V, Denmark, Ostergaard, K. & Sorensen, A., Eds., Engineering Foundation, 1986, pp. 345-352

Hartge, E.-U., Rensner, D. & Werther, J., 1988. Solids concentration and velocity patterns in circulating fluidized beds. Second International Conference on CFBs, Compiegne, France, 1988, March

Hassanizadeh, M. & Gray, W.G., 1979a. General conservation equations for multi-phase systems: 1. Averaging procedure. Adv. Water Resources 2, pp. 131-144

Hassanizadeh ,M. & Gray, W.G., 1979b. General conservation equations for multi-phase systems: 2. Mass, momenta, energy, and entropy equations. Adv. Water Resources 2, pp. 191-203

Hatano, H. & Ishida, M., 1983. The continuous measurement of local concentration with an optical fiber probe. Int. Chem. Engng, 23, 4, pp. 682-688

Hinze, J.O., 1975. Turbulence. McGraw-Hill, New York, 790 p.

Homsy, G.M., 1979. A discussion of some unsolved problems in the mechanics of fluidized beds. in Proceedings of the NSF Workshop on Fluidization and Fluid-Particle Systems, Rensselaer Polytechnic Institute, Troy, New York, Oct. 17-19, pp. 2-48

Horio, M., Morishita, K., Tachibana, O. & Murata, N., 1988. Solid distribution and movement in circulating fluidized beds. Second International Conference on CFBs, Compiegne, France, 1988, March

Howes, F.A. & Whitaker, S., 1985. The spatial averaging theorem revisited. Chem. Engng Sci. **40**, 8, pp. 1387-1392

Hughes, E.D., 1979. Macroscopic balance equations for two-phase flow models. Nucl. Engng Des. **54**, pp. 239-259

Hughes, E.D., Lyczkowski, R.W., McFadden, J.H. & Niederauer, G.F., 1976. An evaluation of state-of-the-art two-velocity two-phase flow models and their applicability to nuclear reactor transient analysis. EPRI-Report NP-143, Volume 2, Technical services agreement SOA 75-317, 254 p.

Ishii, M., 1975. Thermo-fluid dynamic theory of two-phase flow. Eyrolles, 248 p.

Ishii, M. & Chawla, T.C., 1979. Local drag laws in dispersed two-phase flow. Argonne National Laboratory Report ANL-79-105, 43 p.

Jackson, R., 1963. The mechanics of fluidized bed. Trans. Inst. Chem. Engrs., **41**, pp. 13

Jackson, R., 1971. Fluid mechanical theory. In Fluidization, ed. Davidson, J.F. & Harrison, D., Academic, pp. 65-119

Jiang, T.-S., Kim, M.K., Kremesec, V.J. and Slattery, J.C., 1987. The local volume-averaged equations of motion for a suspension of non-neutrally buoyant spheres. Chem. Eng. Comm., **50**, pp. 1-30

Kato, K., Ozawa, Y., Endo, H., Hiroyasu, M. & Hanzawa, T., 1988. Particles hold-up and axial pressure drop in vertical pneumatic transport reactor (riser). in Fluidization V, Denmark, Ostergaard, K. and Sorensen, A., Eds., Engineering Foundation, 1986, pp. 265-272

Klein, H.H., Dietrich, D.E., Goldman, S.R., Laird, D.H., Sharff, M.F., and Srinivas,B., 1983. Time-dependent reactive models of fluidized-bed and entrained-flow chemical reactors. In Handbook of fluids in motion, Cheremisinoff, N.P. & Gupta, R., eds., Ann Arbor Science, pp. 715-764

Klinzing, G.E. & Mathur, M.P., 1984. The behavior of the slip velocity and its relationship in pneumatic conveying. AIChE Symp. Ser. **234**, 80, pp. 24-31

Klinzing, G.E., Rohatgi, N.D., Zaltash, A. & Myler, C.A., 1987. Pneumatic Transport - a Review. Powder Tech. 51, pp. 135-149

Kojima, T., Ishihara, K., Kuramoto, M. & Furusawa, T., 1986. Behaviour of solid in a fast fluidized bed. World Congr. III Chem. Eng., Vol IV, pp. 291-294

Konrad, K., 1986. Dense-Phase Pneumatic Conveying: A Review. Powder Technology, **49**, pp. 1-35

Kulshreshtha, A.K., 1985. Suspension rheology: A theory of time-dependent particle motion in newtonian fluids and an experimental study of colloids in polymeric media. Ph. D. Thesis, Purdue University, 155 p.

Kunii, D. & Levenspiel, O., 1984. Fluidization engineering. Robert E. Krieger, Malabar, Florida, 534 p.

Kwauk, M., Ningde, W., Youchu, L., Bingyu, C. & Zhiyuan, S., 1985. Fast fluidization at ICM. in Proc. 1st Int. Conf. on Circulating Fluidized Beds, Halifax, Nova Scotia, ed. Basu,P., Pergamon Press, 1985, pp. 33-62

Leung, L.S., 1980. The ups and downs of gas-solid flow - A review. in Fluidization, Grace,J.R. and Matsen,J.M., eds., Plenum, New York, pp. 25-68

Li, Y. & Kwauk, M., 1980. The dynamics of fast fluidization. in Fluidization, Grace,J.R. and Matsen,J.M., eds., Plenum, New York, pp. 537-544

Li, J., Tung, Y. & Kwauk, M., 1988. Method of energy minmization in multi-scale modeling of particle-fluid two-phase flow. in Proc. 2nd Int. Conf. on Circulating Fluidized Beds, Compie`gne, France, Basu, P. and Large, J.F., eds., Pergamon Press, pp. 89-90

Lian, G.-S. & Chen, Y.-N., 1985. An improved numerical method for one-dimensional unsteady pneumatic transport in a turbulent horizontal flow at high loading. Part. Sci. Technol. 3, 3-4, pp. 191-204

Lyczkowski, R.W., Gidaspow, D. & Solbrig, C.W., 1982. Multiphase flow models for nuclear, fossil and biomass energy production. In Advances in Transport Processes, ed. Mujumdar, A.S. & Mashelkar, R.A., Wiley-Eastern, New York, 1982, pp. 198-351

Matsen, J.M., 1982. Mechanisms of choking and entrainment. Powder Technology, 32, pp. 21-33

Matsen, J.M., 1988. Presentation in the Second International Conference on Circulating Fluidized Beds, Compiegne, France, 1988, March

Matsumoto, S., Harakawa, H.,Suzuki, M. & Ohtani, S., 1986. Solid particle velocity in vertical gaseous suspension flows. Int. J. Multiphase Flow, 12, 3, pp. 445-458

Matsuno, Y., Yamaguchi, H., Oka, H. Kage, H. & Higashitani, K., 1983. The use of optic fiber probes for the measurement of dilute particle concentrations: Calibration and application to gas-fluidized bed carryover. Powder Tech. 36, pp. 215-221

Monceaux, L., Azzi, M., Molodtsof, Y. & Large, J.F., 1986. Particle mass flux profiles and flow regime characterization in a pilot-scale fast fluidized bed unit. in Fluidization V, Denmark, Ostergaard, K. & Sorensen, A., Eds., Engineering Foundation, 1986, pp. 337-344

Morikawa, Y., Tsuji, Y. & Tanaka, T., 1986. Measurements of horizontal air-solid two-phase flow using otical fiber probe. Bull. JSME, 29, 249, pp. 802-809

Morooka, S., Kago, T. and Kato, Y., 1984. Flow pattern of solid particles in freeboard of fluidized beds. in Fluidization, Kunii,D. & Toei,R., Eds., Engineering Foundation, pp. 291-298

Murray, J.D., 1965. On the mathematics of fluidization , Part 1. Fundamental equations and wave propagation. J. Fluid Mech. 21, 3, pp. 465-493

Muzyka, D.W., 1985. The use of probabilistic multiphase flow equations in the study of the hydrodynamics and heat transfer in gas-solids suspensions. Ph.D.Thesis, The University of Western Ontario, London, Ontario

Nakamura, K. & Capes, C.E., 1976. Vertical pneumatic conveying of binary particle mixtures. In Fluidization Technology,2,149 ed. Keairns, D.L., Hemisphere, Washington pp. 159-184

Nigmatulin, R.I., 1979. Spatial averaging in the mechanics of heterogeneous and dispersed systems. Int. J. Multiphase Flow 5, pp. 353-385

Oki, K., Ishida, M. & Shirai, T., 1980. The behaviour of jets and particles near the gas distributor grid in a three-dimensional fluidized bed. Proc., Int. Conf. on Fluidization, Henniker, New Hampshire, 1980, pp. 421-428

Padhye, A.R., 1985. Evaluation of mechanistic models for coal gasification. DOE-Report DOE/MC/19168-1832, 1985

Passman, S.L., Nunziato, J.W. & Walsh, E.K., 1983. A theory of multiphase mixtures. Sandia Report SAND-82-2261, 1983

Pauchon, C. & Banerjee, S., 1986. Interphase momentum interaction effects in the averaged multifield model-Part 1: Void propagation in bubbly flows. Int. J. Multiphase Flow 12, 4, pp. 559-573

Peters, M.H. & Nadkarni, A.R., 1983. The motions of gas and solids around a spherical void in a fluidized bed. In Fluidization IV, Kunii, D. and Toei, R., eds., Engineering Foundation, pp. 25-36

Peters, M.H. & Prybylowski, D.L., 1983. Particle motion above the surface of a fluidized bed:multiparticle effects. AIChE Symp. Ser. 222, 79, pp. 83-86

Pigford, R.L. & Baron, T., 1965. Hydrodynamic stability of fluidized beds. Ind. Eng. Chem. Fundamentals, 4, pp. 81-87

Plumb, O.A. and Slattery, S., 1987. Dispersion in heterogeneous porous media I: local volume averaging and large-scale averaging. in AIChE Annual Meeting, New York, NY, Nov. 15-20, 1987

Potter, O.E., 1971. Mixing. in Fluidization, Davidson, J.F. & Harrison, D., Eds., Academic Press, London, pp. 293-381

Pritchett, J.W., Blake, T.R. & Garg, S.K., 1978. A numerical model of gas fluidized beds. AIChE Progress Symposium Series 176, 74, pp. 134-148

Prosperetti, A. & Jones, A.V., 1984. Pressure forces in disperse two-phase flow. Int. J. Multiphase Flow 10, 4, pp. 425-440

Reh, L., 1971. Fluidized bed processing. Chem. Engng Prog., 67, 2, pp. 58-63

Reying, Z., Dabao, C. and Yang, G., 1985. Study on pressure drop of fast fluidized bed. in Fluidization'85, Kwauk, M. and Kunii, D., Eds., Science Press, Elsevier, Amsterdam, 1985, pp. 148-157

Rietema, K. & Mutsers, S.M.P., 1973. The effect of interparticle forces on expansion of a homogeneous gas-fluidized bed. Proc. Int. Symp. on Fluidization, Toulouse, France, 1973, pp. 28-40

Rietema, K. & van den Akker, H.E.A., 1983. On the momentum equations in dispersed two-phase systems. Int. J. Multiphase Flow 9, 1, pp. 21-36

Rivard, W.C. & Torrey, M.D., 1977. K-FIX: a computer program for transient two-dimensional, two fluid flow. Los Alamos, LA-NUREG-6623, 1977

Roco, M.C. & Shook, C.A., 1985. Turbulent flow of incompressible mixtures. J. Fluids Engng 107, pp. 224-231

Sankar, S.R. & Smith, T.N., 1986. Slip velocities in pneumatic transport. Powder Technology 47, pp. 167-177

Sato, Y. and Yamamoto, K., 1987. Mechanisms of mixing and diffusion in isotropic, turbulent flow based on experimental data for the Lagrangian velocity autocorrelation and for turbulent diffusion. Int. Chem. Engng, 27, 3, pp. 488-497

Schneyer, G.P., 1981. Computer modeling of coal-gasification reactors. DOE-Report DOE/ET/10242-T1, Vol.2

Schwieger, B., 1985. Fluidized-bed boilers achieve commercial status worldwide. Modern Power Systems, February 1985, pp. s·1-s·16

Seo, Y.-C., 1985. Fluidization of single and binary size particles. Ph.D., Illinois Institute of Technology, Chicago, Illinois, 194 p.

Sha, W.T., Chao, B.T. & Soo, S.L., 1983. Time averaging of volume-averaged conservation equations of multiphase flow. AIChE Symp. Series 225, 79, pp. 420-426

Sha, W.T., Chao, B.T. & Soo, S.L., 1984. Porous-media formulation for multiphase flow with heat transfer. Nucl. Engng Des. 82, pp. 93-106

Sha, W.T. & Slattery, J.C., 1980. Local volume-time averaged equations of motion for dispersed, turbulent, multiphase flows. Argonne National Laboratory Report ANL-80-51,NUREG/CR-1491, 1980

Sha, W.T. & Soo, S.L., 1979. On the effect of $P\nabla\alpha$ term in multiphase mechanics. Int. J. Multiphase Flow 5, pp. 153-158

Shao, M., 1986. Radial and axial variation in voidage in high velocity fluidized beds. Dissertation, The City University of New York, New York, 133 p.

Slattery, J.C., 1967. Flow of viscoelastic fluids through porous media. AIChE J. 13, 6, pp. 1066-1071

Slattery, J.C., 1981. Momentum, energy and mass transfer in continua. McGraw-Hill, New York, 682 p.

Soo, S.L., 1967. Fluid dynamics of multiphase systems. Blaisdell, Massachusetts

Syamlal, M., 1985. Multiphase hydrodynamics of gas-solids flow . Ph.D. Thesis, Illinois Institute of Technology, Chicago, Illinois

Syamlal, M., 1987. The particle-particle drag term in a multiparticle model for fluidization. DOE-Report DOE/MC/21353-2373

Syamlal, M. & Gidaspow, D., 1985. Hydrodynamics of fluidization: Prediction of wall to bed heat transfer coefficients. AIChE J. 31, 1, pp. 127-135

Taylor, G.I., 1921. Diffusion by continuous movements. Proc. London Math. Soc. A20, pp. 196-212

Taylor, G.I., 1932. The transport of vorticity and heat through fluids in turbulent motion. Proc. London Math. Soc. A135, pp. 685-701

Taylor, G.I., 1935. Statistical theory of turbulence. Proc. London Math. Soc. A151, pp. 421-478

Tennekes, H. & Lumley, J.L., 1987. A First Course in Turbulence. Cambridge, MA, MIT press, 300 p.

Todes, O.M., Bogomaz, E.L., Bondareva, A.K., Sheinina, L.S., Petrenko, I.I. & Skvortsov, 1972. Fluctuating method for determining the effective mixing (diffusion) coefficient of the solid phase in a fluidized bed and analogous systems. Int. Chem. Engng, 12, 2, pp. 263-270

Tosun, I. & Willis, M.S., 1980. Generalized proof of the modified averaging theorem. Chem. Engng Sci. 35, pp. 1462-1463

Tosun, I & Willis, M.S., 1981. Deviation representations for the volume averaging technique. Chem. Engng Sci. 36, pp. 781-782

Trapp, J.A., 1976. On the relationship between continuum mixture theory and integral averaged equations for immiscible fluids. Int. J. Engng Sci. 14, pp. 991-998

Trapp, J.A., 1986. The mean flow character of two-phase flow equations. Int. J. Multiphase Flow 12, 2, pp. 263-276

Truesdell, C., 1969. Rational thermodynamics. McGraw-Hill, New York

Truesdell, C. & Toupin, R.A., 1960. The classical field theories. in Handbuch der Physik , ed. Flugge,S., Vol III/1, Springer-Verlag, Berlin, 1960

Van Deemter, J.J., 1985. Mixing. in Fluidization, Davidson, J.F., Clift, R. & Harrison, D., Eds., Academic Press, London, pp. 331-355

Van Deemter, J.J. & Van der Laan, E.T., 1960. Momentum and energy balances for dispersed two-phase flow. Appl. Sci. Res. **A10**, 102

Veverka, V., 1981. Theorem for the local volume average of a gradient revised. Chem. Engng Sci. **36**, pp. 833-838

Wallis, G.B., 1969. One-dimensional two-phase flow. McGraw-Hill, New York

Weiss, V., 1987. Mathematische modellierung zirkulierender wirbelschichten für die kohleverbrennung. Dissertation, Universität-GH-Siegen, 1987

Whitaker, S., 1969. Advances in theory of fluid motion in porous motion. Ind. Engng Sci. **61**, 12, pp. 14-28

Whitaker, S., 1973. The transport equations for multi-phase systems. Chem. Engng Sci. **28**, pp. 139-147

Wirth, K.-E., 1988. Axial pressure profile in circulating fluidized beds. Chem. Eng. Technol. **11**, pp. 11-17

Yerushalmi, J. & Avidan, A., 1985. High-velocity fluidization. in Fluidization, Davidson, J.F., Clift, R. & Harrison, D., Eds., Academic Press, London, pp. 225-291

Yerushalmi, J. & Cankurt, N.T., 1979. Further studies of the regimes of fluidization. Powder Tech. **24**, pp. 187-205

Yerushalmi, J. & Squires, A.M., 1977. The phenomenon of fast fluidization. in AIChE Symposium Series **73**, 161, pp. 44-50

Yerushalmi, J., Turner, D.H. & Squires, A.M., 1976. The fast fluidized bed. Ind. Eng. Chem. Process Des. Dev. **15**, pp. 47-53